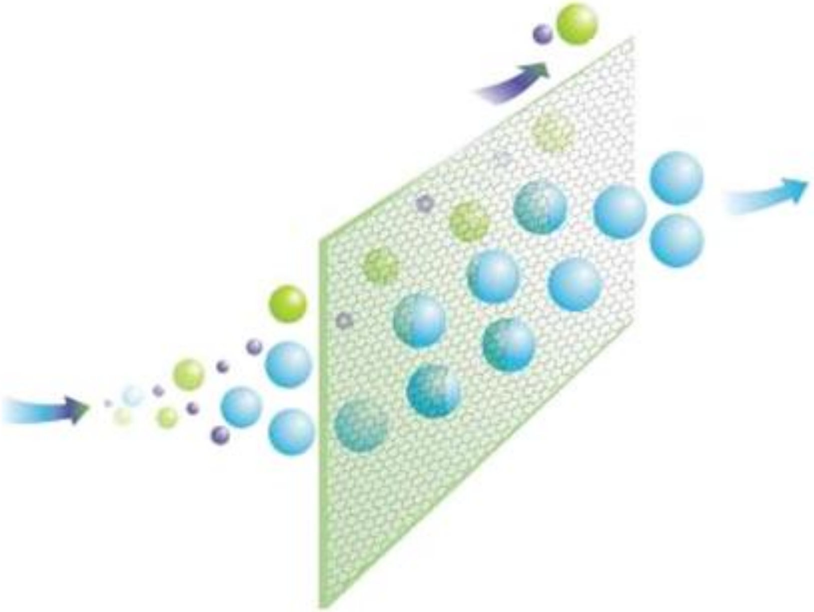

Investigation of CO_2 avoidance behaviour of membrane capture in post combustion processes

Master’s Thesis in the Master’s programme Sustainable Energy Systems

DANIEL EK WEIS

Department of Energy and Environment
Division of Energy Technology
CHALMERS UNIVERSITY OF TECHNOLOGY
Göteborg, Sweden 2011
Master’s Thesis T2011-365

MASTER'S THESIS T2011-365

Investigation of CO_2 avoidance behaviour of membrane capture in post combustion processes

Master's Thesis in the Master's programme Sustainable Energy Systems

DANIEL EK WEIS

Department of Energy and Environment
Division of Energy Technology

CHALMERS UNIVERSITY OF TECHNOLOGY
Göteborg, Sweden 2011

Investigation of CO_2 avoidance behaviour of membrane capture in post combustion processes

Master's Thesis in the Master's programme Sustainable Energy Systems
DANIEL EK WEIS

Department of Energy and Environment
Division of Energy Technology
Chalmers University of Technology
SE-412 96 Göteborg
Sweden
Telephone: + 46 (0)31-772 1000

Cover:
Flat sheet module of gas separation membrane. http://www.co2crc.com.au/research/demo_precomb_membrane.html

Chalmers Reproservice
Göteborg, Sweden 2011

Investigation of CO2 avoidance behaviour of membrane capture in post combustion processes

Master's Thesis in the Master's programme Sustainable Energy Systems
DANIEL EK WEIS
Department of Energy and Environment, Division of Energy Technology
Chalmers University of Technology

ABSTRACT

Increasing concern for the environment and taxes on carbon dioxide emissions has intensified the development of non-polluting energy supply technologies. Carbon Capture and Storage (CCS) constitute a promising option that can reduce CO_2 emissions significantly. State-of-the-art CO_2 capture techniques require very high investment costs which will lead to a substantial drop in power plant efficiency.

This thesis focuses on energetic and economical investigations of gas separation membrane systems used for post-combustion capture in coal fired power plants. The simulations were carried out with the commercial software packages PRO/II and Aspen Plus. A reference power plant termed the Reference Power Plant North Rhine-Westphalia was chosen for the analyses.

On the basis of two membrane cascades, developed by using an ideal flue gas of CO_2 and N_2, the investigation was carried out using a quasi real flue gas, composed of CO_2, N_2, O_2, H_2O and Ar. Although the water content in the flue gas leads to higher energy consumption, a positive effect can be observed: using the same membrane area as in the case with ideal flue gas, the degree of CO_2 separation is increased owing to the sweep gas effect of the water content.

A detailed heat exchanger investigation was explored for a chosen cascade. The aim was to ensure that the recovered exhaust heat generated from the compression process is sufficient to reheat the retentate in the expansion process. A modification distinguished from the ideal flue gas system was to keep the pressure ratio constant for each pressure section. This makes it possible to have a uniform intercooler design for each stage. A pressure drop of 30 mbar inside each cooler was investigated. This extensive system design results in an energy demand of 292 $\text{kWh/ton}_{\text{separated CO2}}$, a separation degree of 78% and an efficiency loss of 7.9%-points. The system has an energetic advantage in comparison with the MEA absorption method at the same degree of CO_2 separation.

On the basis of the reference power plant, a comprehensive economic analysis was made, both for CO_2 capture cost and CO_2 avoidance cost. The results manifest that the heat exchanger cost has a small influence on the total capture cost, which is dominated by the membrane cost in the process. A probable future CO_2 emission policy was considered and the CO_2 emission cost was included in the calculation. By evaluating the electricity price of the different cases (the reference power plant, the chosen cascade for CO_2 capture and the chosen cascade for CO_2 avoidance), it was found that high CO_2 permeance membranes with long life time and a cheap manufacturing price should be developed to make membrane capture systems more economically competing.

Key words: CCS, CO_2 capture, post-combustion, membrane gas separation, avoidance cost

Undersökning av CO_2-undvikande i post combustion-system med membranteknik
Examensarbete inom Sustainable Energy Systems
DANIEL EK WEIS
Institutionen för Energi och Miljö
Avdelningen för Energiteknik
Chalmers tekniska högskola

SAMMANFATTNING

Ökande oro för klimatförändringar och priser på utsläppsrättigheter för koldioxid har påskyndat utvecklingen av icke-förorenande energiomvandlingstekniker. Koldioxidinfångning är ett lovande alternativ som kan minska CO_2-utsläppen betydligt. De mest moderna teknikerna för koldioxidinfångning kräver mycket stora investeringar och leder till en väsentlig nedgång i kraftverkens verkningsgrad.

Denna avhandling utreder användandet av gasseparationsmembran i post combustion-system för kolkraftverk ur ett tekno-ekonomiskt perspektiv. Simuleringarna har genomförts med de kommersiella mjukvarorna PRO/II och Aspen Plus. Referenskraftverket Referenz Kraftwerk Nord Rhein-Westfalen valdes för analyserna.

Med två membrankaskader, som utvecklats med en ideal rökgas innehållandes CO_2 och N_2, utfördes undersökningarna med en kvasiverklig rökgas bestående av CO_2, N_2, O_2, H_2O och Ar. En energianalys visade att även om vattenhalten i rökgasen leder till högre energiförbrukning kan en positiv effekt observeras: om samma membranarea används som i fallet med ideal rökgas, ökar avskiljningsgraden av CO_2 på grund av den ”sweep”-effekt som vattnet har.

En detaljerad utredning av värmeväxlarna i systemet utfördes för ett valt kaskadsystem. Syftet var att säkerställa att värmen som genereras i kompressionsdelen av systemet kan återvinnas i expansionsprocessen. Till skillnad från simuleringar utförda med ideal rökgas modellerades alla tryckförändringsprocesser med konstant tryckförhållande. Detta gör det möjligt att ha en enhetlig design för alla mellankylare. Ett tryckfall på 30 mbar användes för varje mellankylare. Denna omfattande systemdesign resulterade i ett energibehov på 292 kWh/ton CO_2 för hela systemet, en avskiljningsgrad för CO_2 på 78% samt en förlust i verkningsgrad på 7.9%-enheter. Systemet har därmed en fördel ur energisynpunkt i jämförelse med system med MEA-absorption för denna avskiljningsgrad.

Med referenskraftverket som grund utfördes en omfattande ekonomisk analys, både för CO_2-infångning och CO_2-undvikande. Resultaten visar att kostnaden av värmeväxlarna endast har en liten betydelse för systemets totala kostnad, som domineras av membrankostnaden. En förväntad framtida utsläppspolitik antogs och kostnaden för CO_2-utsläpp togs med i beräkningarna. Genom att utvärdera elpriset för de olika fallen (referenskraftverket och de valda kaskadsystemen för CO_2-infångning och för CO_2-undvikande), kunde det konstateras att membran med hög CO_2-permeans, lång livstid och låga tillverkningskostnader bör utvecklas i syfte att göra membransystem mer ekonomiskt tilltalande.

Nyckelord: CCS, koldioxidinfångning, post combustion, membran, undvikandekostnad

Contents

Preface

The study presented in this thesis was carried out in order to fulfill the requirements for the degree Master of Science in Sustainable Energy Systems at Chalmers University of Technology, Göteborg, Sweden. The project was performed from Mars 2011 to August 2011 at the Institut für Energie- und Klimaforschung – Brennstoffzellen (IEK-3) at Forchungszentrum Jülich in Nordrhein-Westfalen, Germany. The project was supervised by Dr. Dr. Li Zhao at Forchungszentrum Jülich and by Associate Professor Tobias Mattisson at Chalmers University of Technology.

Acknowledgements

I would like to express a lot of gratitude to Dr. Dr. Li Zhao for the much appreciated collaboration and guidance throughout the time I worked at the research centre. Especially appreciated was her ability to find new ideas and approaches when computers and software stopped working.

I also want to thank Associate Professor Tobias Mattisson for believing in the thesis and for his support from the university.

Countless thanks go to Tuong-Van Nguyen for the help and support he gave me both at and outside the research centre during my time in Germany. His indirect involvement in the thesis was of great value.

I am also very grateful to Henning Weiß for being an awesome office mate throughout the six months and Thomas Heysel for his friendly attitude from the first day I arrived at the research centre. My other colleagues at IEK-3, Timo Mittag, Frederic Deschler, Christian Schuba and Carsten Krupp have also each contributed to making my time in Germany a great and memorable experience, which I am very thankful for.

Jülich, August 2011,

Daniel Ek Weis

Nomenclature

Abbreviations

ASU	Air Separation Unit
CCS	Carbon Capture and Storage
COC	Cost of Certificates
COE	Cost of Electricity
ESP	Electrostatic Precipitator
EU ETS	European Union Emissions Trading System
FGD	Flue Gas Desulphurization
IGCC	Integrated Gasification Combined Cycle
MEA	Monoethanolamine
PR	Peng-Robinson
RKW-NRW	Reference Power Plant North Rhein-Westphalia
SKR	Soave-Redlich-Kwong

Symbols

Roman upper case letters

A	Heat transfer area [m^2]
C_{cap}	Annualized capital cost [€/year]
$C_{O\&M}$	Annual operation & maintenance cost [€/year]
C_{en}	Annual energy cost [€/year]
C_{tot}	Total annual cost [€/year]
$\dot{C}_{CO_2}$	Specific CO_2 cost [€/ton]
D	Diffusion coefficient [m^2/s]
E	Energy [MWh]
F_h	Cost factor for housing, installation, etc. [-]
I	Investment cost [€]
K_{c1}	Compressor cost (for capture) [million €]
K_{c2}	Compressor cost (for compression) [million €]
K_{el}	Electricity cost [cent/kWh]
K_{ex}	Expander cost [€/W]
K_m	Membrane unit cost [€/m^2]
K_{mf}	Permanent membrane frame cost [million €]
K_{vp}	Vacuum pump cost [million €]
M	Molar mass [kg/mol]
P_c	Energy used by compressor [MW]
P_{CO_2}	CO_2 permeability [Nm^3/m^2·h·bar]
P_{ex}	Energy recovered by expanders [MW]
P_{N_2}	N_2 permeability [Nm^3/m^2·h·bar]
P_{tot}	Total energy consumption [MW]
P_{vp}	Energy used by vacuum pump [MW]
$\dot{Q}$	Heat flux [W]
S	Solubility coefficient [mol/m^3·Pa]

T	Temperature [°C]
U	Overall heat transfer coefficient [W/(m^{2}K)]

Roman lower case letters

a	Annuity factor
a_m	Annuity factor for membrane
c_p	Specific heat capacity [kJ/(kgK)]
d	Heat exchanger wall thickness [mm]
h	Heat transfer coefficient [W/(m^{2}K)]
h_d	Fouling factor [W/(m^{2}K)]
$\dot{m}$	Mass flow rate [kg/s]
p	Pressure [bar]
t_{op}	Annual operation time [h]
y	Molar fraction [-]

Greek letters

α	Selectivity [-]
Δp	Partial pressure difference [bar]
ΔT	Temperature difference between hot inlet and cold outlet stream [K]
ΔT_m	Logarithmic mean temperature difference [K]
η	Efficiency [-]
λ	Thermal conductivity [W/(mK)]

Indices

C	Carbon
c	Compressor, cold stream
cap	Capital
CCS	Power plant with CCS installations
el	Electricity
en	Energy
ex	Expander
feed	Feed gas to membrane
h	Hot stream
he	Heat exchanger
in	Input
m	Membrane
mf	Membrane frame
O&M	Operation & Maintenance
out	Output
permeate	Permeated gas
ref	Reference power plant
retentate	Retentate gas
vp	Vacuum pump
tot	Total

List of figures

List of tables

1 Introduction

This master thesis is a study about the performance and economy of carbon capture and storage with membrane technology in post-combustion systems. This chapter presents an introduction to the subject and establishes the goals of the thesis.

1.1 Background

The world is changing. The development in the last 250 years has caused the atmospheric concentration of carbon dioxide to rise to levels the race of Homo sapiens never experienced before. At the same time the global mean temperature has increased rapidly, threatening to cause irreversible damage to biological systems. Scientists all over the world state that the global warming is caused by the increased levels of atmospheric concentration of carbon dioxide and other greenhouse gases. The solution to the climate change problem is therefore to decrease the emissions of these gases to the atmosphere.

Carbon capture and storage (CCS) from high emitting fossil fuel power plants has the potential to play a major role in climate change mitigation.

1.2 Problem definition

Previous studies about gas separation membranes have mainly been based on simulations with an ideal flue gas, containing only CO_2 and N_2. The results of these studies may therefore not be completely valid, since real flue gas contains more species.

The heat exchangers in the processes have not been investigated in detail in any published papers in the subject.

Cost simulations of membrane systems have in most studies not considered that the energy requirements of CCS increase the amount of fuel input, and therefore CO_2 emissions, per unit of produced energy. In other words, the costs have been based on the amount of captured CO_2 and not on the amount of avoided CO_2.

1.3 Aim and scope

The overall aim of this thesis is to evaluate multi-stage membrane systems with respect to performance and economy. The simulations will be based on post-combustion systems in coal fired power plants and carried out using the computer programs PRO/II and Aspen Plus. The work can be categorized in the following topics:

- Simulation of multi stage membrane systems using realistic composition of flue gas
- Investigation of heat exchangers used in CO_2 capture and compression processes
- Analysis of CO_2-avoidance cost for membrane systems

2 Theory

This chapter describes the current situation of global warming and CCS, and is in many senses a literature review.

2.1 Global warming and CCS

Climate change is today on the agenda of every country and company in the European Union and in most parts of the world. It is a well known and indisputable fact that the temperature of the climate system has increased rapidly during the last 100 years [1]. A continuous increase is very likely to raise sea levels, cause changes in biological systems and increase the intensity of tropical cyclone activity.

There is a general consensus that the high temperatures are due to the increase in concentration of green house gases in the atmosphere. Since the start of the industrial revolution (around year 1750), human activity has increased the global atmospheric concentration of carbon dioxide (CO_2) from 280 ppm [1] to 391 ppm in February 2011 [2], which exceeds the levels of hundreds of thousands years [3]. Global concentrations of the green house gases methane (CH_4), nitrous oxide (N_2O) and halocarbons have also increased significantly since the levels before the industrial age [1], owing to human activities. CO_2 has a lower global warming potential than some of the other green house gases, which means that one kg of e.g. methane contributes more to the global warming than one kg of CO_2. Still, there is a lot more CO_2 in the atmosphere, and therefore it is the largest contributor to global warming [4].

The huge increase in concentration of atmospheric CO_2 is due to excessive combustion of fossil fuels. Today about 85% of the world's commercial energy needs are produced by the fossil fuels coal, oil and natural gas [5]. Of these fuels, coal is the highest emitter of CO_2 per produced GJ. In 2008, 27% of the total primary energy supply and 41% of the electricity generation in the world were produced by coal or peat [6]. With the world population rapidly growing the demand for energy will increase from its level in 2008 with 36% until 2035 [7]. This development is expected to make the demand for fossil fuels increase by 50%, which would have a significant impact on the climate.

An overall global mean temperature of more than 2°C above pre-industrial levels is estimated to cause irreversible damage to the environment [8]. The European Union aims at making sure that this level is not exceeded [9]. According to the International Energy Agency this is possible if the atmospheric CO_2 levels are kept below 450 ppm [7].

There are three ways to mitigate the effects of global warming from the energy supply sector:

- Use less energy. However, with a steady increase in the world population and a rapid development in developing countries, the demand for energy is expected to increase to a great extent. Therefore, this goal can only be reached by improving the efficiency of energy processes.
- Use energy from less GHG-emitting energy sources. Examples of technologies that do not emit any green house gases are renewable energy sources (wind, hydro, solar and biomass) and nuclear power. The renewable energy sources have a large potential and are steadily expanded, but still need lots of time before they can compete with fossil fuels on a high level. Nuclear energy provides GHG-clean energy, but faces other problems (waste issues, weapon proliferation, accident hazards) [10]. The next generations of nuclear power plants may

overcome most of the problems and thus become an excellent provider of energy. However, this technology needs at least several decades before it can be commercially available. Since both renewable and nuclear technologies need time before they can challenge fossil fuels for the dominance of the energy supply sector, fossil fuels will be a major part of the energy mix for a long time. Thus, bridging technologies are needed, which utilize fossil fuels with low or no emissions of greenhouse gases, until the clean options can take over.

- Utilize carbon capture and storage (CCS). This mitigation option suggests that CO_2 emissions from fossil power plants and process industries shall be captured before they reach the atmosphere and shall be securely stored for a significant period of time, hence protecting the environment. This could be one of the bridging technologies mentioned earlier.

Carbon capture and storage consists of three major parts: capture-, transportation- and storage of CO_2 [11].

The capture part of CCS requires both additional energy input to the power plant and new equipment to handle the separation [12]. This makes the capture process the most expensive part of the carbon capture and storage sequence. Currently, about two thirds of the total CCS costs have been suggested to originate from this part [13]. There are three main routes to capture the CO_2 from power processes: post-combustion, pre-combustion and oxy-fuel combustion. These concepts will be presented in detail.

Transportation of large quantities of CO_2 is preferably performed by pipelines, for travelling distances up to about 1,000 km. For small amounts of gas that needs to be transported overseas, ships may be economically feasible [11]. The gas must not contain moisture, otherwise it is corrosive to the pipeline. The gas must have a CO_2 purity of over 90-95.5% to make the transport satisfactory [14].

Suitable CO_2 storage sites could be depleted oil and gas reservoirs or deep saline aquifers [15]. A schematic diagram showing different storage options and transport of CO_2 is shown in Figure 2.1.

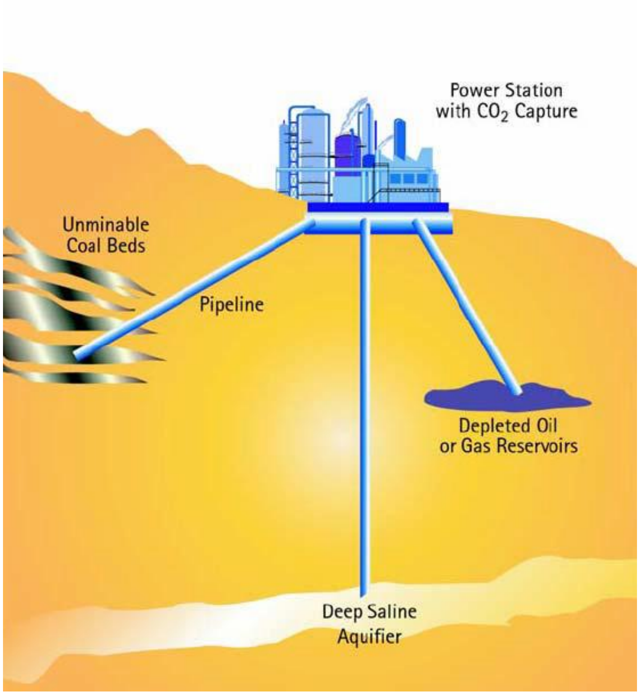

Figure 2.1. Picture of potential storage sites [16].

2.2 Capture routes

There are three main CO2 capture technologies: post-combustion, pre-combustion and oxy-fuel combustion. These processes involve different type of separation steps such as absorption, adsorption, membrane or cryogenic fractionation. In general, such state-of-the-art capture techniques require very high investment and lead to a substantial drop in power plant efficiency.

2.2.1 Main capture routes

The three capture routes are presented in the following pages.

2.2.1.1 Pre-combustion

The pre-combustion technology is applied in so called Integrated Gasification Combined Cycle (IGCC) power plants. In a pre-combustion system the primary fuel is made to react with oxygen or air and/or steam prior to combustion, which creates a synthesis gas that is mainly composed of carbon monoxide and hydrogen [11]. This synthesis gas is then processed in a shift reactor where additional steam is added, which results in more hydrogen and makes the CO convert to CO_2 [15]. CO_2 is then separated before combustion, usually by a physical or chemical absorption process. The resulting flue gas will be hydrogen rich, which makes it useful in furnaces, boilers, gas turbines, etc [11]. The general procedure is shown in Figure 2.2.

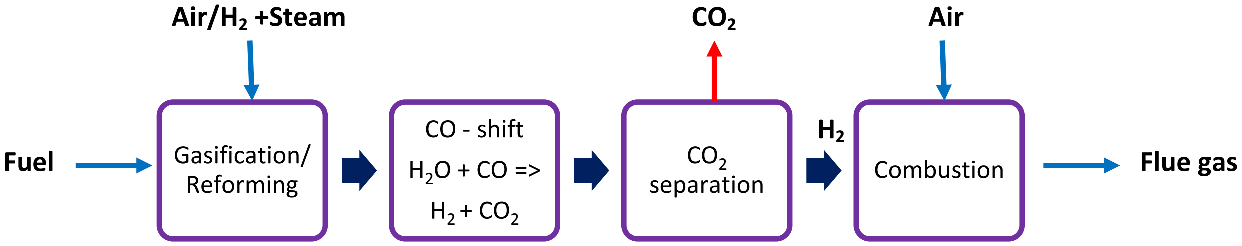

Figure 2.2. Schematic illustration of the principle of pre-combustion with inspiration from [62].

An advantage with this technology is that it generates CO_2 with high pressure, which consequently means that less energy is needed to compress the gas for transportation. It is also appropriate to natural gas and coal fired combined cycles and can produce both hydrogen and electricity [17].

There are some challenges that the pre-combustion technology must face in order to be competitive. First, the technology is mainly applicable for new power plants and not as retrofits for existing ones [18]. Also, the extended chemical plant that is needed in front of the turbine may cause extra shut-downs and lower power output [17]. Another challenge is to make turbines operate well with hydrogen rich gas [18].

2.2.1.2 Oxy-fuel combustion

In oxy-fuel combustion, oxygen is separated from nitrogen and the fuel is combusted in nearly pure oxygen instead of air [11], [15]. The resulting flue gas contains mainly CO_2 and H_2O. Combustion in pure oxygen gives very high flame temperatures. Therefore, the flue gas is recirculated to the burners in order to ascertain that the flame temperature is within acceptable limits of the boiler material [19]. The procedure is shown in Figure 2.3.

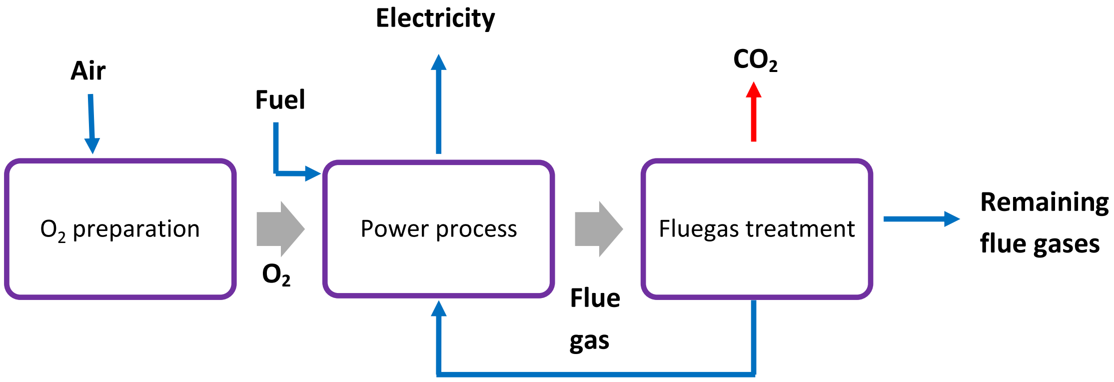

Figure 2.3. Schematic illustration of the principle of oxy-fuel combustion processes [62].

Oxy-fuel combustion has some appealing advantages and is expected to be a very good alternative for CO_2 capture in the future [20]. Combustion in oxygen results in a much higher CO_2 partial pressure in the flue gas compared to regular combustion in air, since the flue gases are not diluted with nitrogen from the air [21]. This is naturally an advantage for the CO_2 separation. The stream can be purified to a level of 99% of CO_2 [21].

However, before oxy-fuel combustion can be competitive with other capture technologies it has to overcome a few challenges. The oxygen rich stream is usually produced by cryogenic distillation in an air separation unit (ASU), which results in a large energy penalty for the plant [19]. After the combustion, the flue gas consists of about 75% CO_2. An extra flue gas treatment process is needed to obtain a stream that is as pure of CO2 as possible. For example, a condenser is needed since the flue gas in this part consists of a lot of water.

2.2.1.3 Post-combustion

In post-combustion processes the CO_2 is captured from flue gases produced by combustion of fossil fuels and biomass [11], or from gases produced by industrial processes. In a typical flue gas train in a power generation process there is a so called deNO_x unit that removes nitrogen oxides from the flue gas, followed by an electrostatic precipitator (ESP) that removes particulates and a flue gas desulphurisation unit (FGD). Normally, the post combustion technologies are designed to operate after the FGD [22]. Typically, the CO_2 concentration is 13-15% at this point for coal-fired power plants [17]. Post-combustion processes using chemical absorption are today the leading strategy to capture CO_2 [5]. The principle layout of the system is shown in Figure 2.4.

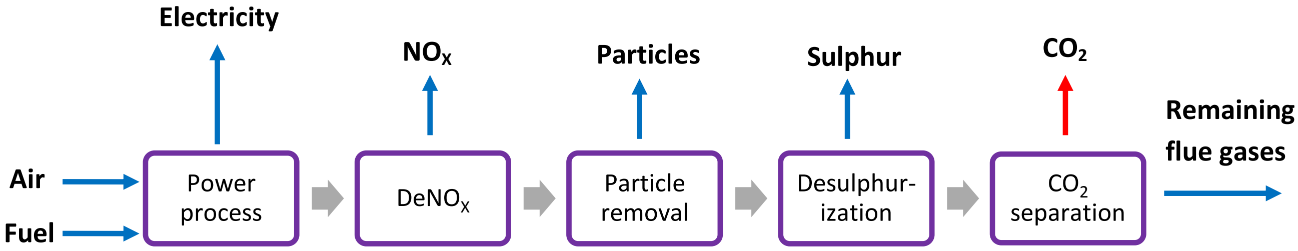

Figure 2.4. Schematic illustration of the principle of post combustion processes.

A major advantage with post-combustion is that it can be implemented in most existing plants, though with some technological adjustments [23]. The technology is also much more mature than pre- and oxy-fuel combustion and is expected to be the choice for many years [24].

The challenges with post combustion are to decrease the major energy penalty that the systems have on the power plant and to test it in large scale [24].

2.2.2 Main capture methods for post-combustion

The capture procedure can be performed in several different ways that each has its own advantages and drawbacks.

2.2.2.1 Chemical Absorption

In chemical absorption processes with liquids the CO_2 separation is achieved by putting the flue gas in contact with a liquid absorbent or a solid sorbent that selectively absorbs the CO_2 by chemical reactions[11], [25]. The sorbent loaded with the CO_2 is then transported to a regenerator where the CO_2 is released under pressure or heating. In most cases the absorbent is then recirculated to capture more CO_2, creating a cycle [11]. Most often amines are used as absorbent, particularly mono-ethanolamine (MEA). Alternative solvents like ammonia, alkali-compounds and aminosalt can also be used [26].

A major advantage with amine scrubbing is that it is suitable for the low CO_2 partial pressures that often occur in flue gases. Other post-combustion technologies are dependent on high CO_2 partial pressure levels [17].

The most significant drawback of chemical absorption is that the regeneration step requires a large amount of energy [27]. Moreover, reactions with NO_2 and SO_X lead to high levels of solvent degradation [5].

It has been proven that use of amine scrubbing can yield CO_2 purities above 99% and degrees of CO_2 separation between 80 and 95% [11].

2.2.2.2 Physical Absorption

The driving force for CO_2 separation in physical absorption processes is solubility [25]. Different species in the flue gas have different solubility in a liquid solvent, which makes it possible to extract the CO_2 from the flue gases if a proper solvent is used.

The main advantage of this process is that less energy is needed for regeneration of the solvent [25]. However, high CO_2 partial pressure is needed to achieve an acceptable CO_2 separation. Thus, physical absorption is mainly suitable for high pressure gas streams and CO_2-rich streams [28].

2.2.2.3 Adsorption with solids

When adsorption is used to separate CO_2 from the flue gas a material that CO_2 is adhesive to is used to selectively extract the CO_2 from the flue gas. Activated carbons and zeolites are examples of materials that can be used for this [29]. This can be done by the different methods: electric swing adsorption, thermal swing adsorption and pressure swing adsorption.

All these methods share the major drawback of high necessity to treat the flue gas before it reaches the adsorber [11].

2.2.2.4 Cryogenics

In cryogenic processes the flue gas is treated in a sequence consisting of cooling and expansion steps, resulting in a three-phase mixture [30]. The components of this mixture can then be separated in a distillation column.

An advantage with the system is that no elevated pressures are needed. Furthermore, the compressed and cooled gases make it possible to separate NO_2 and SO_2 with high efficiencies [31].

The major drawback is that the method is most suitable for gas streams with high CO_2 concentrations, and thereby less appropriate for post-combustion in power generation. Moreover, the procedure requires a considerable amount of energy [29].

2.2.2.5 Carbonate looping combustion

Carbonate looping combustion is a second generation method to remove CO_2 in pre- and post-combustion processes. It is still in an early stage of development. The process consists of a carbonation reactor and a calcination reactor. The first step in post-combustion processes is the carbonation reactor, where reactions of CO_2 in the flue gases and calcium oxide produce calcium carbonate in an exothermic reaction. This is then transported to the calcination reactor where heat is added and the CO_2 is released from an endothermic reaction. The calcium oxide is then recirculated to the flue gas where a new carbonation process is started [32].

The advantage of this process is that it may be less energy demanding and less expensive than amine scrubbing methods. The biggest drawback is that the reactivity of the calcium sorbents decrease rapidly with number of cycles [33].

2.2.2.6 Membrane-absorption hybrid systems

Research has been conducted in combining different carbon capture technologies in order to find an optimal system. Membrane contactors can be used in a hybrid system with chemical absorption to intensify the absorption processes. This is done by a porous membrane which improves gas/liquid interfacial contact [27]. The system also has the advantage of making it possible to control the gas and liquid flow rates independently [34]. A challenge with this technology is to find a membrane material that increases the gas-liquid interfacial area without a too high penalty on the mass transfer coefficient. Moreover, tests have only been performed on small and short time scale [14].

2.2.2.7 Gas separation membranes

The CO2 separation can also be performed by gas separation membranes. The driving force for a gas separation membrane is the partial pressure difference across the membrane. Owing to the limitation of the CO_2/N_2 selectivity of state-of-the-art membranes [35] and the operating conditions in a post-combustion process (1 bar, 13-15 mol% CO_2), multi-stage membrane systems must be applied[36], [22], [37]. This leads to relatively high energy consumption. Whereas, the distinguishing features are: potentially low environmental impact and as add-on equipments used in power plants in comparison with chemical absorption method. This technology has not been evaluated in large scale operation. The current research focuses on developing more CO_2 selective membrane materials and more energy efficient processes.

2.3 Membrane technology in post-combustion systems

The concept of using membranes to separate CO_2 from the rest of the gas is not yet fully competitive with the conventional scrubbing methods [27]. To be able to be competitive, the membrane systems must achieve as high quality results as the conventional methods and with lower costs.

When evaluating membrane systems for CCS the following parameters are of vital importance:

- Degree of CO_2 separation
- CO_2 purity
- Investment costs
- Energy consumption

Membranes are often classified in two categories: polymeric and inorganic [25]. Polymeric membranes are dominant in gas separation systems, since they have the highest selectivities.

2.3.1 Inorganic membranes

Inorganic membranes can be classified in ceramic and metallic membranes. These membranes have the advantage of being able to operate in higher temperatures than polymeric membranes. The gas separation is governed by the following mechanisms: molecular sieving, surface diffusion, Knudsen diffusion and capillary condensation [38].

In molecular sieving processes small particles pass through the pores of the membrane and are adsorbed, but large particles are not. This process has high separation factor but low permeability [38]. Zeolites are often used as molecular sieves [39].

Adsorbing gas that is adsorbed at the surface of the membrane pores is undergoing the surface diffusion mechanism. The gas component that should permeate through the membrane may diffuse faster than the other components under a pressure gradient [40].

The Knudsen mechanism is the process where gas molecules diffuses into the membrane pores and then advance only by collisions with the pore wall. This process shows a high permeance but a low selectivity.

Capillary condensation is adsorption from vapour into the pores of the membrane which results in that the pores become filled with condensed liquid of the vapour. This can occur in the pores of the membrane in the presence of condensable gas species. The filled pores in the membrane lead to high permeance and high selectivity [38].

2.3.2 Polymeric membranes

There are many different polymeric membranes suitable for CO_2 separation [41]. The gas separation process can be described with the solution-diffusion mechanism, consisting of sorption in membrane structure, diffusion through membrane and desorption on the permeate side of the membrane [38].

The properties of the membrane must allow the CO_2 to pass through the membrane in order to achieve a high degree of separation. Thus, the permeability of the membrane is of vital importance. It is defined as follows:

$$P_{CO_2} = S_{CO_2} \cdot D_{CO_2} \tag{2.1}$$

where S_{CO_2} is the solubility coefficient of CO_2 and D_{CO_2} is the diffusion coefficient of CO_2.

However, to achieve a high quality carbon capture it is also imperative that as far as it is possible, only CO_2 is allowed to penetrate the membrane so that the purity of the permeate stream is high. Low purities can lead to corrosion of the pipes during transportation of the gas. Since the flue gases mainly contain nitrogen and CO_2, the CO_2/N_2-selectivity is an important parameter. It can be expressed as:

$$\alpha = \frac{Permeance\ of\ CO_2}{Permeance\ of\ N_2} \tag{2.2}$$

Membranes with high permeability and selectivity are wanted. But materials with high selectivity usually have a low permeability and a high permeability usually means a low selectivity [42].

2.3.3 The CO_2 partial pressure difference

The basic theory of post-combustion membrane technology is to let the flue gas pass a membrane, which, using CO_2 partial pressure difference as driving force, separates the CO_2 from the other gases. The general procedure for a single-stage process is shown in Figure 2.5.

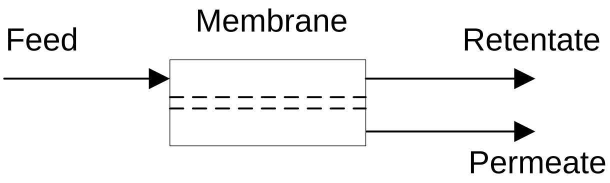

Figure 2.5. Principal sketch of a single-stage membrane system.

The partial pressure difference can be expressed as:

$$\Delta p_{CO_2} = p_{feed,CO_2} - p_{permeate,CO_2} = p_{feed} \cdot y_{feed,CO_2} - p_{permeate} \cdot y_{permeate,CO_2} \tag{2.3}$$

Thus, post-combustion membrane systems suffer from the fact that the CO_2 partial pressure is low in flue gases. It follows from the expression that a high pressure difference can be achieved by:

1. increasing the pressure of the feed gas
2. decreasing the pressure of the permeate gas
3. increasing the CO_2 concentration on the feed side
4. decreasing the concentration of CO_2 on the permeate side

The first option can be done by using a compressor. This has the advantage that then an expander can be coupled on the retentate stream to recover some of the work performed by the compressor [23], see Figure 2.6. Moreover, the capital cost for compressor equipment is less than for other alternatives and less membrane area is needed than for option 2 [22].

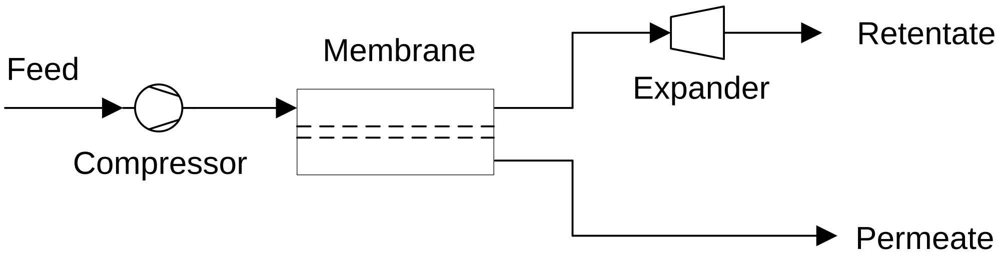

Figure 2.6. Single-stage membrane system with a compressor and an expander.

Option two can be performed by a vacuum pump on the permeate side, as is shown in Figure 2.7. This is not possible to combine with an expander on the retentate side, but it has the advantage that the energy needed for the vacuum pump is much smaller than for the compressor, since the flow rate on the permeate side is much smaller than on the feed side [27].

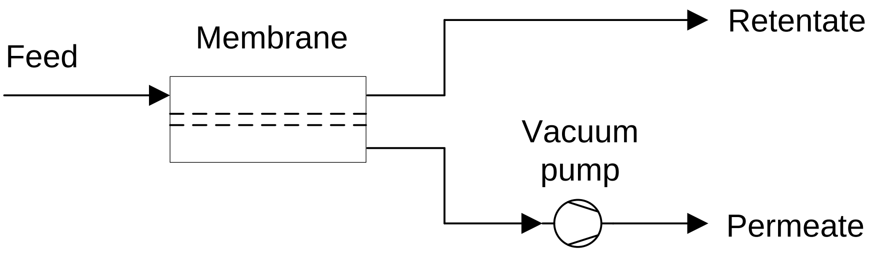

Figure 2.7. Single-stage membrane system with a vacuum pump installed on the permeate side.

The third option can be achieved by recirculating a CO_2 rich stream to the feed gas.

Sweep gas can be used to realise option four. This means that a small fraction of one of the streams is decreased in pressure and introduced to the permeate side of the membrane [22]. The increased driving force gained by introducing a CO_2 lean stream (in accordance with Equation (2.3)), makes sure that the CO_2 purity is not negatively affected. The result of sweep gas utilization is that the required membrane area is dramatically reduced [22].

2.3.4 Requirements for membrane systems

To be able to transport and store the CO_2 a purity of at least 95% is required as product from the CCS plants [14]. The goal is to reach 80 or 90% recovery rate as well as a high enough purity [27]. To be truly competitive with the industrially favoured scrubbing methods, this must be done at low costs. The major costs of scrubbing methods are associated with the high energy consumption of the process, which decreases the efficiency of the plant. The energy needed for amine absorption processes range from 4 to 6 $GJ_{thermal}$/tonne CO_2 recovered [27].

In coal based power processes the flue gas typically contains 13-15 vol% CO_2 at the point where post-combustion systems are implemented [17]. A number of studies have shown that a single-stage membrane system cannot fulfil both the recovery rate and the purity requirements simultaneously when the CO_2 concentration is that low [36],[29]. However, for processes that have a content of CO_2 in the flue gases of 20-30% the requirements can be met [27]. This can be the case for steel and iron production facilities.

To be able to reach the requirements on purity and recovery rate when the gas contains less CO_2, like in coal fired power plants, either membranes with very high selectivity (over 200) [43], or a multi stage system of membranes must be used [36]. However, membranes with selectivity above 200 have very low permeance, which would make the system need unfeasibly large membrane area [23]. Multi stage system consists of two or more membranes connected in series. Different properties of the membranes make it possible to achieve the requirements of CO_2 purity and recovery rate.

There are two basic ways to configure a multi stage system: the enricher and the stripper concept. The enricher is configured so the permeate of the first membrane is sent as feed gas to another membrane, as presented in Figure 2.8.

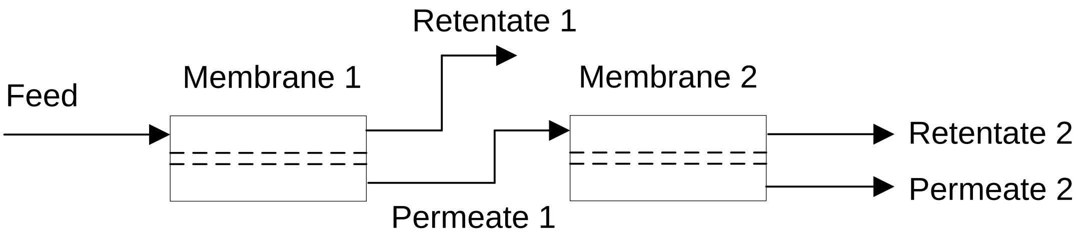

Figure 2.8. Two-stage membrane system configured according to the enricher concept.

In the stripper concept the retentate stream of the first membrane is sent as feed gas to another membrane [23], see Figure 2.9. There are then numerous ways to configure vacuum pumps and compressors to achieve as high performance as possible of the system. However, these components require additional energy input.

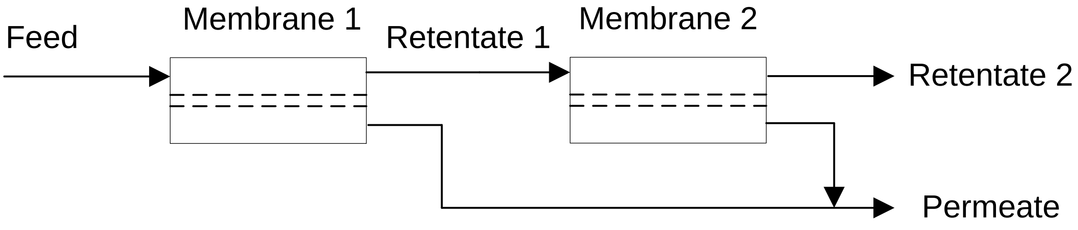

Figure 2.9. Two-stage membrane system configured according to the stripper concept.

It is important to investigate avoidance cost behaviour of membrane systems and to study the components to get a comprehensive analysis of the system.

2.4 Components used in membrane capture processes

The additional equipment needed in CCS plants leads to additional investment and maintenance costs and, as mentioned above, that extra energy is required to operate the plant. The variable cost of certain components, such as compressors and vacuum pumps, during its lifetime is generally much larger than the investment and maintenance costs [44], [45]. It is therefore important to base the selection of the new components on the amount of energy they need to perform their tasks (efficiencies) rather than only on the cost of investment.

2.4.1 Compressors

The required CO_2 partial pressure difference between the feed and the permeate side of the membrane can be achieved by increasing the pressure on the feed side using a compressor. There is a wide range of different kinds of compressors and they are classified in groups and sub-groups according to their working principles. The classification system of some of the most important compressor types are shown in Figure 2.10.

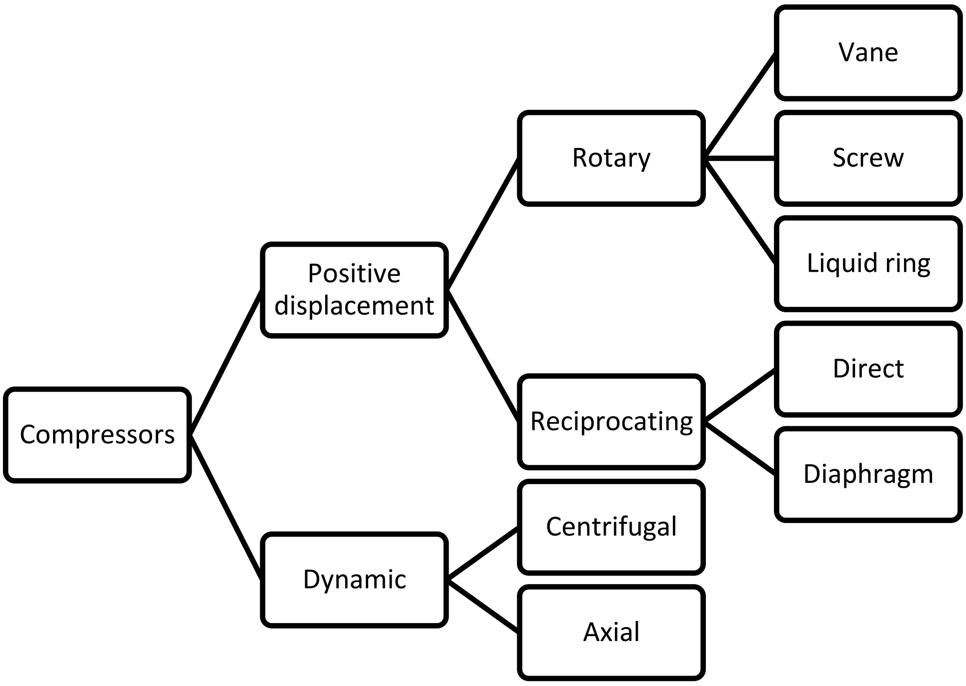

Figure 2.10. Overview of compressor types.

In accordance with Figure 2.10, compressors are often classified as either positive displacement compressors or dynamic compressors. A positive displacement compressor takes a given quantity of the gas into a confined volume and then decreases the volume, causing the pressure to rise [46]. Dynamic compressors bestow a velocity upon the gas, thereby giving it velocity energy that is afterwards converted to pressure energy [47].

Positive displacement compressors are categorized as rotary or reciprocating. Examples of the rotary type are rotary vane-, rotary screw- and liquid ring compressors. The reciprocating type consists of direct and diaphragm compressors.

Dynamic compressors are either of centrifugal or axial types, depending on which direction the flow of gas has through the compressor. Centrifugal machines represent about 80% of all dynamic compressors [47].

Compressors used in membrane systems need to be able to handle large flow rates of gas and high efficiencies are certainly desirable. Axial compressors can handle up to 1 million Nm^3/s and centrifugal ones up to 340 000 Nm^3/s, which is much higher than positive displacement compressors are capable of [48]. However, axial compressors are vulnerable to corrosion, erosion and deposits; hence they are mostly useful in streams with clean gases. Despite this, the axial compressors are used in air separation systems [47].

To be able to handle large flow rates it is possible to use a system with many small compressors working together. In coal power plants the flow rate of the flue gases is usually very high, thus it may be necessary with a multisystem of compressors.

The isentropic efficiency depends on the flow rate through the compressor. Positive displacement compressors have their peak efficiencies at low flow rates. Mechanical friction, flow discontinuities, seal- and valve leakages increases at large flow rates, which lowers the efficiencies. Dynamic compressors, on the other hand, operate most efficiently with higher flow rates. The axial compressors reach the highest efficiency of all compressor types, with values up to and sometimes over 90% [49].

2.4.2 Vacuum pumps

Instead of compressing the feed gas, the necessary partial pressure difference can be obtained by decreasing the pressure of the permeate gas by using a vacuum pump. Since the pump is located at the permeate side of the membrane it doesn’t need to handle as high flows as the compressor, but a high capacity is still necessary. Like for the compressors, a multi system of vacuum pumps may be more profitable than using one single vacuum pump. Different kinds of vacuum pumps can be classified as shown in Figure 2.11.

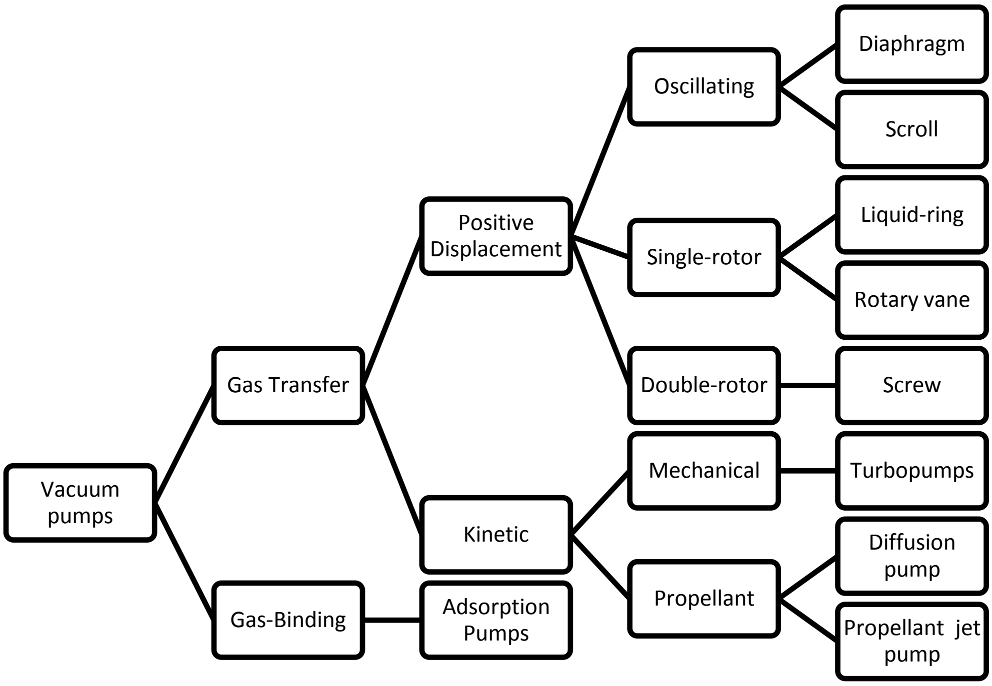

Figure 2.11. Sketch of a basic classification of types of vacuum pumps.

The first classification is between gas transfer and gas binding vacuum pumps. Gas-binding pumps have a limited gas adsorption ability capability and must therefore be regenerated at certain intervals. Gas transfer pumps can operate without limitation [50].

The gas transfer category can be divided in the positive displacement and kinetic groups. Kinetic pumps accelerate the gas in order to create vacuum at the inlet port. This can be done by a mechanical drive system (e.g. turbo pumps) or by using a propellant (e.g. propellant jet pumps and diffusion pumps).

Positive displacement pumps isolates and compresses a constant volume of the gas. Then the gas is vented out at one port while a vacuum is created at the inlet port. Positive displacement pumps can be operated by single-rotor, double-rotor or oscillating movements. Diaphragm and scroll vacuum pumps are examples of the oscillating kind. The single-rotor group includes liquid-ring pumps and rotary vane pumps. Screw pumps are double-rotor pumps.

Positive displacement vacuum pumps cannot handle as high flow rates as kinetic pumps but have higher isentropic efficiencies [48].

After discussing the membrane system with different vacuum pump manufacturers, the author of the thesis has received different recommendations regarding the types of vacuum pump that can be suitable for the process. Proposed types were liquid ring pumps, diaphragm pumps and scroll vacuum pumps. However, none of these kinds can handle as large flow rates as occurs in membrane processes. Therefore, it may be necessary to use a parallel arrangement of vacuum pumps in order for the process to work properly.

2.4.3 Heat exchangers

The temperature of the gas is inadvertently increased during the compression process in vacuum pumps and compressors. For optimal membrane operation a temperature between 40 and 60°C is desired [14]. This can be achieved by introduction of recuperative heat exchangers.

Heat exchangers can be classified in a number of different ways. They can be classified according to their transfer process, which is either of indirect contact type or direct type. In indirect contact heat exchangers the fluids that exchange heat are separated and the heat transfers through a wall from one fluid to the other. In direct heat exchangers the fluids are mixed and the heat transfers directly between the fluids [51].

Heat exchangers can also be classified according to their construction. This can be done according to Figure 2.12.

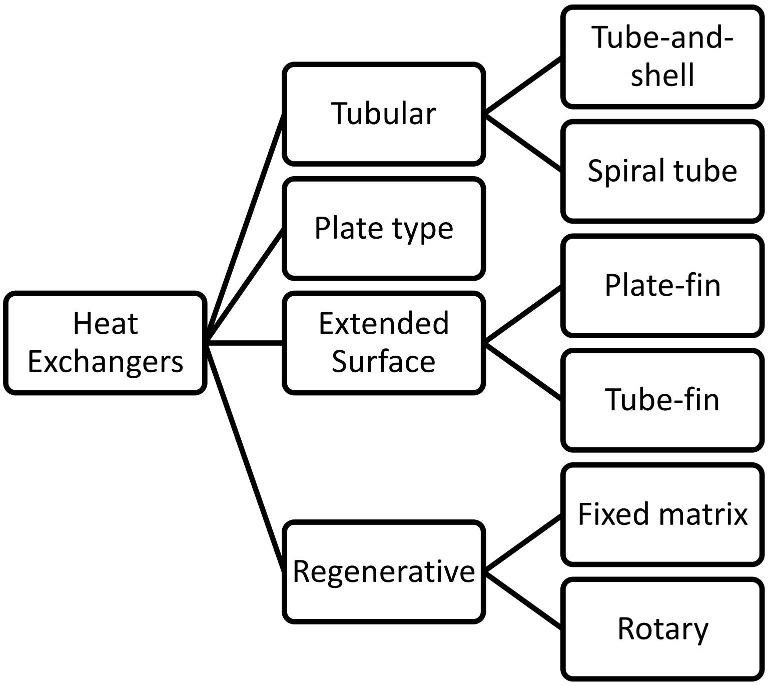

Figure 2.12. Basic classification of heat exchangers based on the construction.

Tubular design is flexible since the dimensions and arrangement of the tubes easily can be organized in many different ways. Also, the design makes it possible to handle high pressure differences between the fluids. The most commonly used heat exchangers in chemical processes are of the tube-and shell type [52]. As the name implies, one fluid is transported through tubes and the other outside the tubes but inside the shell of the heat exchanger, as shown in Figure 2.13. They can be designed so that the different fluids go through the unit in parallel-, counter- or cross-current flow. Using spiral tubes is a way to increase the heat transfer but the shape makes cleaning very difficult [51].

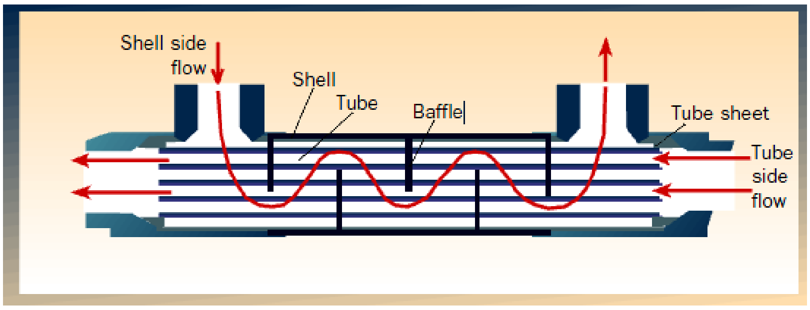

Figure 2.13. Tube-and-shell heat exchanger with counter current flow [53].

Another common type is the plate heat exchanger which is composed of thin plates slightly separated from each other with passages for the fluids as shown in Figure 2.14. These heat exchangers have the advantages of being easy to maintain and that the minimum temperature difference between the hot and the cold stream can be lower than for other types, but they cannot handle as high flow rates as is needed in this process [54].

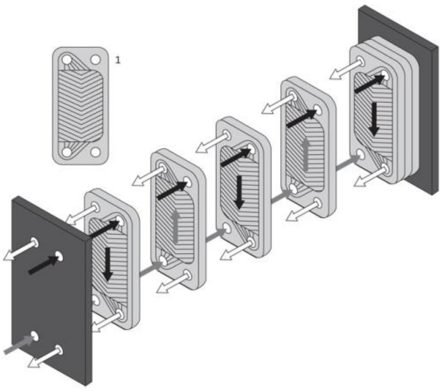

Figure 2.14. Sketch of plate heat exchanger [55].

A method to improve the efficiencies of heat exchangers is to increase the heat exchange area by extending the surface with the introduction of fins. Components with this design are called extended surface heat exchangers. The most common types are the plate-fin and tube-fin designs.

In regenerative heat exchangers the heat exchange between the fluids is occurring in two steps. In fixed matrix regenerators the fluids flow through the same passages in the heat exchangers at different times. First the hot stream heats up the heat transfer surface (often called matrix). Then the cold stream is led through the heat exchanger and the heat is transferred from the matrix to the fluid. Thus the heat transfer between the fluids is not occurring constantly. A drawback of this configuration is that some of the fluid will be trapped in the passage and transferred to the other fluid and at high pressure differences there will also be leakages from the high pressure fluid to the low pressure fluid. Another method is the rotary regenerator type, in which the matrix is moved periodically between the fixed streams of fluids [51].

In an ideal counter-flow heat exchanger the hot stream would be cooled to the same temperature as the ingoing cold stream. However, in real heat exchangers the temperature of the outgoing hot stream will always be higher than that, see Figure 2.15 [53]. The difference between these two temperatures is called the terminal temperature difference and it should be as low as possible. In parallel flow heat exchangers the terminal temperature difference is the difference between the outgoing temperatures of the cold and hot streams.

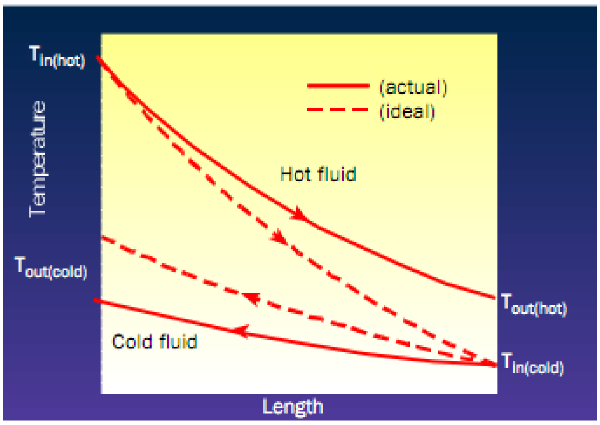

Figure 2.15. Graph of ideal and actual stream temperatures in counter current heat exchanger [53].

2.4.4 Utilization of components in membrane systems

The vacuum pumps and compressors in membrane CO_2 capture systems are most often performed in stages. A stage-arranged compressor leads to lower energy consumption than a single-stage process [36]. Each stage is composed of a compressor or vacuum pump unit, a heat exchanger and a water separator, as shown in Figure 2.16. As mentioned above, the temperature of the gas is inadvertently increased during the vacuum pump and compression operation. The heat exchanger (sometimes called intercooler or aftercooler depending on its location in the system) cools the gas in order to avoid extreme temperatures and to maintain a suitable temperature for the membrane operation. In this heat exchanger, some of water contained in the gas may condense. This liquid water is then removed in a water knock-off unit.

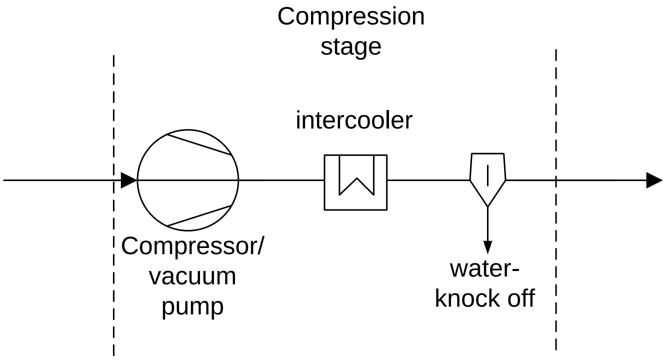

Figure 2.16. Illustration of a compression stage in vacuum pumps and compressors.

Expansion processes are also advantageous to perform in stages, since it is possible to reheat the gas between the stages in order to recover as much energy as possible. Each step contains a reheater and an expander, as shown in Figure 2.17.

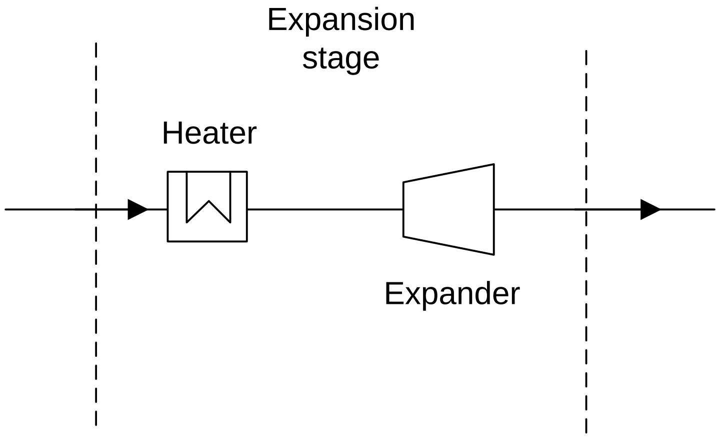

Figure 2.17. Illustration of an expansion stage in an expander.

The heat that is recovered in the intercoolers and aftercoolers in the compressors and vacuum pumps are expected to be sufficient to heat the gas in the expander process.

2.5 CO_2-capture and CO_2-avoidance

As previously mentioned, CO_2 capture increases the energy requirement of the power plant, which reduces the efficiency of the plant since more fuel is needed to produce the same amount of energy [23]. Consequently, a power plant with CCS technology produces more CO_2 per kWh than a similar plant without CCS technology.

Because of this, the amount of captured CO_2 is not the same as the amount of avoided CO_2 in the atmosphere. The amount of avoided CO_2 emissions is lower than the amount captured. Therefore, the difference of CO_2 capture cost and CO_2 avoidance cost should be emphasized and the latter should be prioritized [21]. Figure 2.18 shows a schematic of the concept.

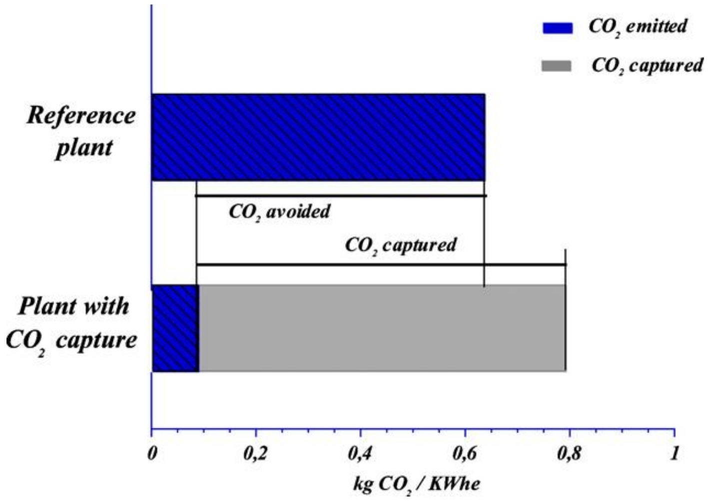

Figure 2.18. Chart of the difference in amount of CO_2 produced in a reference plant and a plant with CO_2 capture, and the difference between CO_2 avoided and CO_2 capture [14].

As a result, reducing energy input is more important in CO_2 capture processes than in regular traditional processes [56].

3 Reference power plant and simulation method

This chapter introduces the reference power plant and the computer software that has been used in the thesis.

3.1 Reference power plant

A reference power plant of 600 MW, RKW-NRW (Reference Power Plant North Rhein-Westphalia [57]), was used in the simulations. The flow rate and the elemental analysis of the flue gas were simulated using the bituminous coal "Klein Kopje".

The capture system should be implemented downstream from the $DeNO_X$-unit, the dust removal unit and the flue gas desulphurization, since this section has been recognized as most suitable for polymeric membrane separation [40].This configuration is shown in Figure 3.1. The power plant has the properties shown in Table 3.1.

Table 3.1. Data of RKW-NRW [57].

Power plant RKW-NRW	
Output gross	600 MW
Output net	555 MW
Net efficiency	45.9%
Annual operation time	8000 h
Fuel input	1.33 million ton CO_2/year
Steam parameters	285bar/600°C/620°C
Investment costs	534.4 million €
O & M costs	6.4 million €/year
Fuel cost	78 €/ton
Cost of electricity	4.355 cent/kWh
Flow rate of flue gas after removal of pollutants	1.6 million m^3/h
Temperature of flue gas after removal of pollutants	50°C
Pressure of flue gas after removal of pollutants	1.05 bar

The composition of a quasi real flue gas is listed in Table 3.2.

Table 3.2. Properties of the gas before the CO_2 capture system [23].

Feed gas properties	
Pressure [bar]	1.05
Temperature [°C]	50
Flow rate [m^3/s]	440
CO_2 fraction [mol%]	13.5
N_2 fraction [mol%]	70.1
O_2 fraction [mol%]	3.7
H_2O fraction [mol%]	11.9
Ar fraction [mol%]	0.8

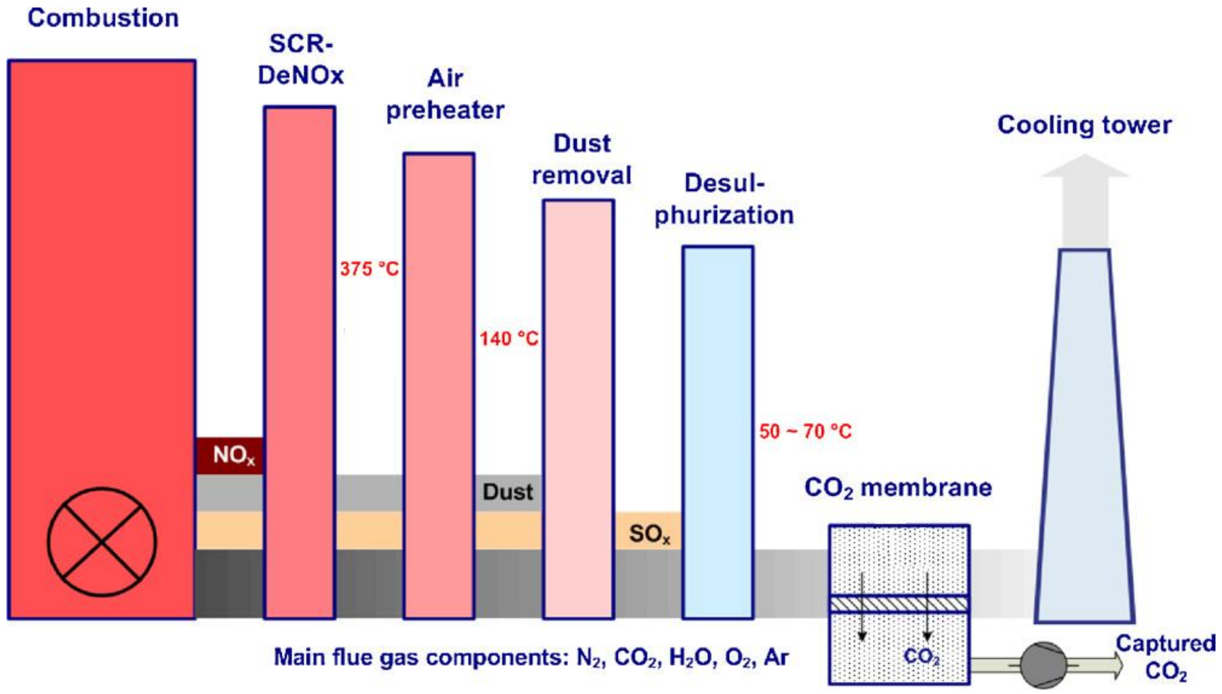

Figure 3.1. Post-combustion flue gas train and the position of CO_2 membrane separation [36].

3.2 Simulation tools

RKW-NRW was used as a platform and the computer programs PRO/II and Aspen Plus were used as tools for the simulations performed in this thesis.

When power processes are modelled it is common practice to use either of the thermodynamic models Soave-Redlich-Kwong (SKR) equation of state or Peng-Robinson (PR). The simulations in this thesis were made with PR in PRO/II and with both RKS and PR in Aspen Plus.

3.2.1 PRO/II 8.3

PRO/II is a steady-state process simulator developed by Invensys SimSci-Esscor. The program is well suited to simulate membrane systems, since user-friendly membrane gas separation units are included in the software.

In PRO/II there is an optimizer component that makes it possible to find the lowest or highest value of an objective function by varying the values of process sheet variables. This can be done with certain specifications that define values for flow sheet parameters that must be obtained while finding the optimal value of the objective function. The optimizer thus makes it possible to find the lowest energy consumption that is needed to achieve specified requirements on the CO_2 purity, by using membrane area as process sheet variables.

The operation of the vacuum pumps, compressors and expanders were modelled as adiabatic, in other words irreversible and without heat losses.

A flow sheet showing the input and output parameters in PRO/II is presented in Figure 3.2.

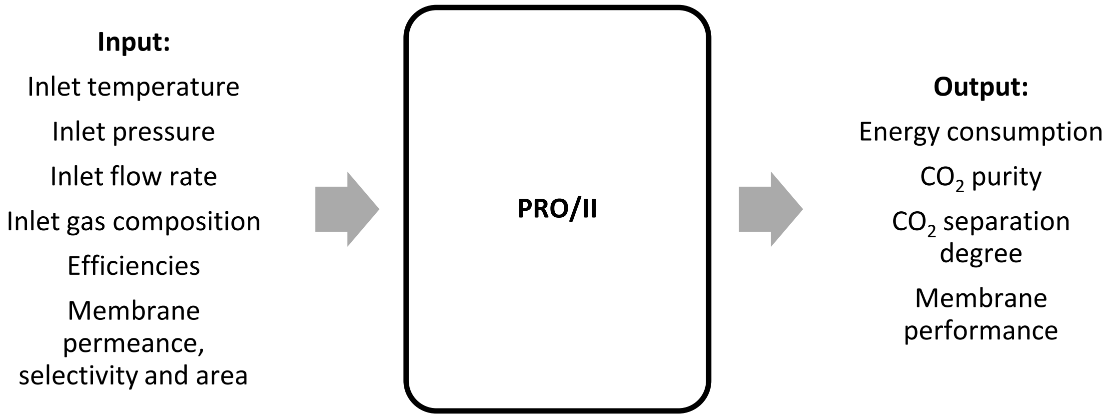

Figure 3.2. Flow sheet of the input and output parameters in PRO/II.

3.2.2 Aspen Plus 7.2

Aspen Plus is a process simulation software that is widely used in both industry and education. It has most of the qualities that PRO/II has, but it lacks membrane components. The membranes have therefore been modelled in PRO/II first in order to find the compositions and flow rates of the permeate and retentate. The membrane systems have then been modelled in Aspen Plus with separator components that act as membrane units. The outlets of these separator components have been taken from the PRO/II simulations. This procedure has made it possible to simulate membrane systems in Aspen Plus even though there are no membrane units in the program.

Compression and expansion cannot be modelled as adiabatic processes in Aspen Plus. Instead, the expansion was modelled as an isentropic process, which is an adiabatic reversible process. The vacuum pumps and compressors were modelled as polytropic processes, since this is a more accurate way of modelling compression operation. The expanders, however, cannot be modelled as polytropic processes in Aspen Plus.

The input parameters used in Aspen Plus and the resulting output are shown in Figure 3.3.

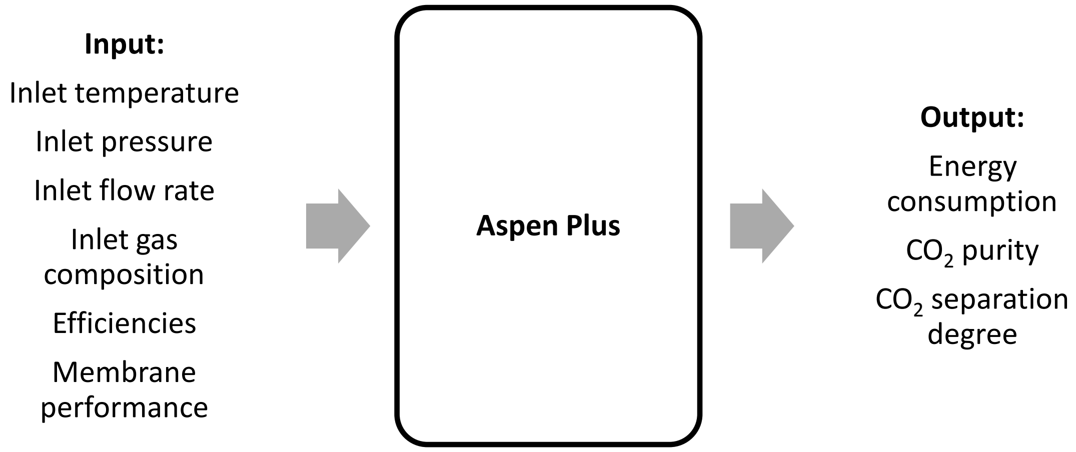

Figure 3.3. Flow sheet of the input and output parameters in Aspen Plus.

4 Simulations of multi-stage membrane systems

In a CCS chain, the purity of the captured CO_2 and the impurities are limited by the downstream CO_2 pipeline transport and the storage specifications. In the investigations in this thesis, 95 mol% has been taken as a target for CO_2 purity. The degree of CO_2 separation has been treated as a variable. In addition to the CO_2 purity, the separation degree is an important factor that influences the energy demand of the capture process.

It is suggested by Hildebrand & Herzog [58] that it may be advantageous to only capture parts of the emissions instead of full capture. With only partial capture, the efficiency loss would be lower, the plant output higher and the capital and operational costs lower. With a cap-and-trade emissions reduction program it is likely that natural gas plants will be built instead of coal power plants. This would most likely have the consequences of higher prices on natural gas and thus higher electricity prices. If 40-65% of the CO_2 from coal power plants can be captured, the emissions would be in the same parity as the emissions from natural gas power plants. This way, the economic and energy security benefits of coal can be maintained, while the CO_2 emissions decrease and over reliance on natural gas is avoided.

Two different 2-stage membrane systems were investigated in PRO/II with quasi real flue gas composition. The chosen systems have been proved to have the optimal configurations to reach a separation degree of 50%, 70% (Cascade A) and 90% (Cascade B) respectively in the reference power plant when an ideal gas mixture of CO_2 and N_2 is used [40]. Cascade A and Cascade B are shown in Figure 4.1 and Figure 4.2 respectively. Both systems have the enricher configuration, since this arrangement has been proven to be able to reach higher CO_2 purities than the stripper concept for the same degree of CO_2 separation [23].

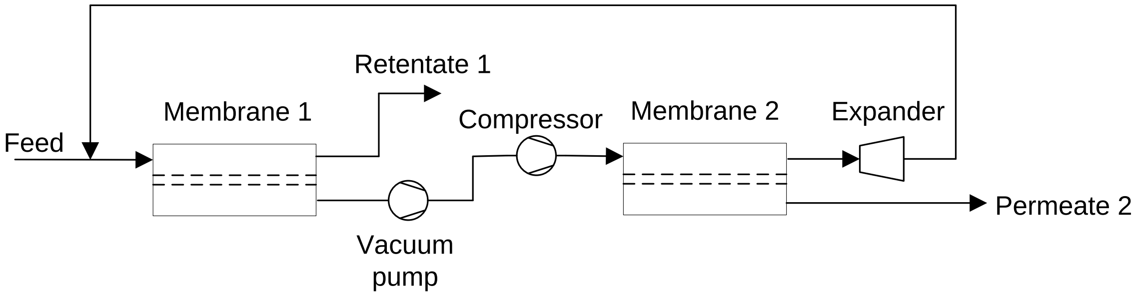

Figure 4.1. Cascade A: Enricher configuration of two-stage membrane system with vacuum pump on first membrane permeate, compressor on second membrane feed, expander on second membrane retentate and re-circulation of second membrane retentate.

The pressure difference over the first membrane is generated by a vacuum pump and the second membrane has a compressor-expander design. The retentate of the second membrane has a higher concentration of CO_2 than the feed stream and is therefore re-circulated to a point prior to the first membrane in order to increase the driving force of CO_2 separation. The vacuum pump, compressor and expander were all simulated as two-stage units.

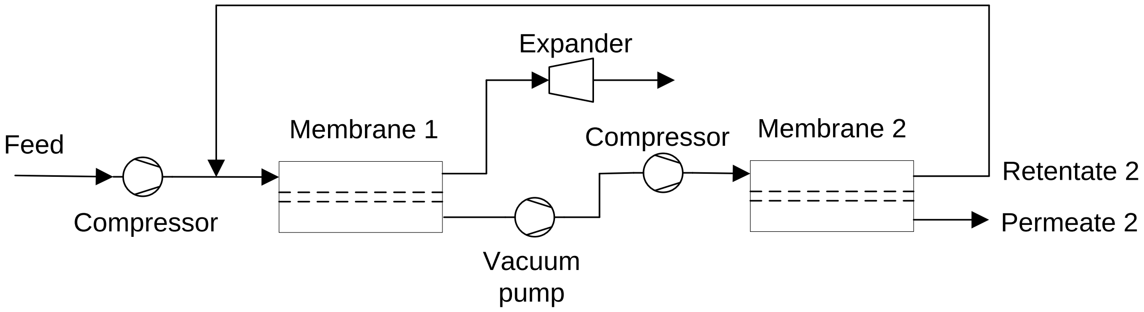

Figure 4.2. Cascade B: Configuration of two-stage membrane system with compressor on feed gas, vacuum pump on first membrane permeate, compressor on second membrane feed, expander on first membrane retentate and re-circulation of second membrane retentate.

Cascade B is configured with a vacuum pump on the first membrane permeate and a compressor on the second membrane feed. Instead of having an expander on the second membrane retentate, this system has an expander on the first membrane retentate. It also has a compressor before the feed stream is mixed with the re-circulated retentate of the second membrane. The vacuum pump, expander and each compressor are simulated as two-stage units.

The membranes used in the simulations are polymeric membranes of the type Polyactive, which is a membrane developed by Helmholz-Zentrum Geesthacht [59]. The characteristics of this membrane are shown in Table 4.1.

Table 4.1. Characteristics of the membrane [60].

Membrane characteristics	
CO_2 Permeance [$Nm^3/m^2 \cdot h \cdot bar$]	3
N_2 Permeance [$Nm^3/m^2 \cdot h \cdot bar$]	0.06
O_2 Permeance [$Nm^3/m^2 \cdot h \cdot bar$]	0.12
H_2O Permeance [$Nm^3/m^2 \cdot h \cdot bar$]	6000
Ar Permeance [$Nm^3/m^2 \cdot h \cdot bar$]	0.06
CO_2/N_2 Selectivity	50
O_2/N_2 Selectivity	2
H_2O/N_2 Selectivity	10^5
Ar/N_2 Selectivity	2

It is assumed that there is no pressure drop for the intercoolers and membranes. The vacuum pumps, compressors and expanders have an adiabatic efficiency of 85% in the PRO/II simulations. In Aspen Plus, the vacuum pumps and compressors have a polytropic efficiency of 85% and the expanders have an isentropic efficiency of 85%. Another important assumption is that the recovered heat in the stages of the vacuum pumps and compressors are sufficient to supply the heat needed in the expander stages.

The specific energy consumption was calculated with the following formula:

$$Specific\ energy\ consumption = \frac{Total\ energy\ consumption}{Amount\ of\ captured\ CO_2} \tag{4.1}$$

4.1 Removal of water

The final CO_2 stream must be of high quality to be suitable for pipeline transport [60]. In addition to a high CO_2 molar fraction (>95 mol%), the final stream must meet the following requirements:

1. There can be no free water, so that corrosion, hydrate formation and two phase flow is prevented. The water content must be lower than 500 ppm.
2. The concentration of contaminants (SO_2, H_2S and O_2) must be limited for safety and acceptance reasons.
3. The concentration of non-condensable gases (N_2, NO_X, CH_4, Ar and H_2) must be limited to below 4 mol% in total.

In post-combustion processes it is therefore important to remove the water from the flue gas in addition to separating CO_2. There are three ways to remove water from the system [60]:

- Removal of water before the CO_2 separation. A very small partial pressure difference of H_2O can be achieved by connecting a condenser with a water dehydrating SPEEK-membrane [61]. A steam partial pressure of about 40 mbar can be achieved without extra energy consumption. Therefore, the energy consumption of the pre-drying process can be neglected when dehydration membranes are used.
- Removal of water during the compression of the flue gas, in combination with intercooling.
- Removal of small amounts of water using desiccant after the CO_2 separation.

These three options are illustrated in Figure 4.3 for Cascade A.

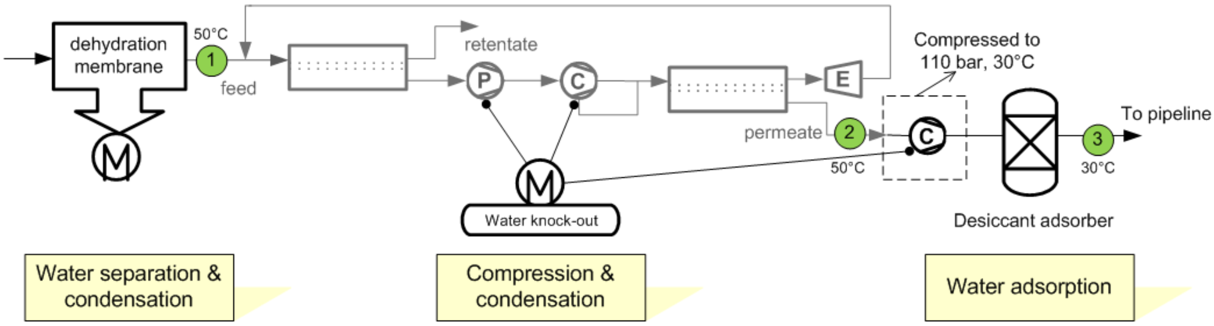

Figure 4.3. Schematic illustration of water removal options for Cascade A [60].

All of the three water removing options were used simultaneously in the models throughout this thesis. After each intercooler that caused water condensation in the flue gas, a flash unit was placed that removed the liquid water. Four cases were investigated for the dehydration unit located prior to the CO_2 separation:

- No removal of the water in the flue gas
- Removal of 30% of the total water in the flue gas
- Removal of 60% of the total water in the flue gas
- Complete removal (ideal gas)

4.2 50% and 70% degree of CO_2 separation

The initial investigations were based on Cascade A, shown in Figure 4.1.

4.2.1 50% and 70% separation degree with ideal flue gas

Cascade A has been proved to be able to reach a 50% separation degree and 95 mol% CO_2 purity with a membrane area of 1.13 km^2 for the first membrane and 0.04 km^2 for the second when an ideal gas mixture is used [40]. If a separation degree of 70% is wanted, a membrane area of 2.39 km^2 is needed for the first membrane and 0.06 km^2 for the second. The data of the system when an ideal gas mixture is used is shown in Table 4.2. The specific energy for compression is the energy needed to compress the stream to a suitable pressure for pipeline transport (110 bar). The efficiency loss in Table 4.2 is the reduction in net efficiency of the reference power plant from its initial value of 45.9%. The energy gain of the expanders is included in the compressors energy consumption.

The vacuum pump has a pressure of 100 mbar and the compressor increases the pressure to 4 bar before the gas enters the second membrane. The expander decreases the pressure of the second retentate to 1 bar. Permeate 2 has a pressure of 1 bar.

Table 4.2. Data of Cascade A when an ideal gas mixture is used.

CO_2 separation degree	Membrane area [km^2]		CO_2 purity [mol%]	Specific energy for vacuum pumps [kWh_e/t_{CO2}]	Specific energy for compressors [kWh_e/t_{CO2}]	Specific energy for compression [kWh_e/t_{CO2}]	Efficiency loss imposed on reference power plant [%-points]
	1st	2nd					
50%	1.13	0.04	95	87	37	105	4.1
70%	2.39	0.06	95	110	41	105	6.5

4.2.2 50% separation degree with real flue gas

Cascade A was first simulated with the same membrane areas that are needed to reach 50% separation degree and 95 mol% CO_2 purity when an ideal gas mixture is used. The four cases for the water removal unit located before the capture system were investigated. The results of the simulations are presented in Table 4.3. First, only the CO_2 capture process was simulated. The energy consumption of the CO_2 compression process is calculated in section 4.4.

The results show that the more water the gas contains, the more energy is needed to complete the process. The component that accounts for most of the increase is the vacuum pump. It is evident that it is advantageous to remove as much of the water as possible before the capture sequence.

Given the same membrane area, the separation degree of CO_2 is significantly higher when real flue gas is used compared to when an ideal N_2-CO_2-gas is used. The water has a positive sweeping effect, since it decreases the CO_2 concentration on the permeate side of the membrane, which increases the driving force for CO_2 separation. It should be remembered that the permeance of H_2O is very high, see Table 4.1.

Table 4.3. Comparison of the energy consumption and separation degree of different dehydration cases for Cascade A with membrane areas that result in a separation degree of 50% for the ideal gas mixture case.

Water removal prior to CO_2 separation	**CO_2 separation degree [%]**	**Membrane area [km^2]**		**Specific energy for vacuum pumps [kWh_e/t_{CO_2}]**	**Specific energy for compressors [kWh_e/t_{CO_2}]**
		1st	2nd		
0	63	1.13	0.04	141	41
30%	62	1.13	0.04	133	41
60%	61	1.13	0.04	113	42
Ideal gas	50	1.13	0.04	87	37

The gas compositions in the positions 1, 2 and 3 in Figure 4.3 are presented in Table 4.4. It can be seen that by using the above mentioned measures, the water can be removed from the flue gas. The two main components CO_2 and H_2O can be regulated to the requirement of the pipeline transport.

Table 4.4. The CO_2 purity in positions 1, 2 and 3 according to Figure 4.3 for the 50 % separation degree case.

Point in process according to Figure 4.3	**Water removal prior to CO_2 separation**	**Total flow rate of entire stream [kmol/h]**	**CO_2 [mol%]**	**N_2 [mol%]**	**O_2 [mol%]**	**Ar [mol%]**	**H_2O [mol%]**
1	0	70 499	13.50	70.10	3.70	0.80	11.90
	30%	68 147	14.00	72.70	3.83	0.82	8.64
	60%	65 624	14.54	75.49	3.98	0.86	5.13
2	0	6 654	92.18	2.68	0.53	0.03	4.58
	30%	6 467	91.93	2.82	0.55	0.03	4.66
	60%	6 330	91.79	2.92	0.57	0.03	4.68
3	0	6 353	96.56	2.81	0.55	0.03	500 ppm
	30%	6 168	96.38	2.96	0.58	0.03	500 ppm
	60%	6 036	96.25	3.06	0.60	0.03	500 ppm

4.2.3 70% separation degree with real flue gas

With membrane areas of 2.39 km^2 for the first membrane and 0.06 km^2 for the second, the CO_2 purity becomes 95 mol% and the separation degree 70% if an ideal gas mixture of N_2 and CO_2 is modelled. When this system is simulated with a real composition of the flue gas, the separation degree is increased to about 79%, which confirms the good effect the water has on this parameter. The results are shown in Table 4.5.

As in the case with 50% separation degree, the energy requirement of the vacuum pump clearly increases with a higher content of water in the flue gas.

Table 4.5. Comparison of the energy consumption and separation degree of different dehydration cases for Cascade A with membrane areas that result in a separation degree of 70% for the ideal gas mixture case.

Water removal prior to CO_2 separation	CO_2 separation degree [%]	Membrane area [km^2]		Specific energy for vacuum pumps [kWh_e/t_{CO2}]	Specific energy for compressors [kWh_e/t_{CO2}]
		1st	2nd		
0	79	2.39	0.06	167	47
30%	79	2.39	0.06	150	47
60%	78	2.39	0.06	133	48
Ideal gas	70	2.39	0.06	110	41

The compositions of the gas in the three points are shown in Table 4.6. The CO_2 purity after the entire system is above 95 mol% for each dewatering case. The gas is thereby suitable for CO_2 transport in pipelines.

Table 4.6. The CO_2 purity in positions 1, 2 and 3 according to Figure 4.3 for the 70 % separation degree case.

Point in process according to Figure 4.3	Water removal prior to CO_2 separation	Total flow rate of entire stream [kmol/h]	CO_2 [mol%]	N_2 [mol%]	O_2 [mol%]	Ar [mol%]	H_2O [mol%]
1	0	70 499	13.50	70.10	3.70	0.80	11.90
	30%	68 147	14.00	72.70	3.83	0.82	8.64
	60%	65 624	14.54	75.49	3.98	0.86	5.13
2	0	8 382	90.07	3.55	0.70	0.04	5.63
	30%	8 366	90.06	3.56	0.71	0.04	5.63
	60%	8 293	89.99	3.61	0.72	0.04	5.64
3	0	7 914	95.40	3.76	0.75	0.04	500 ppm
	30%	7 900	95.39	3.77	0.75	0.04	500 ppm
	60%	7 830	95.32	3.82	0.76	0.04	500 ppm

4.3 90% degree of CO_2 separation

When using an ideal gas mixture, the Cascade B system shown in Figure 4.2 reaches a separation degree of 90% and a CO_2 purity of 95 mol% if the first membrane has an area of 0.45 km^2 and the second an area of 0.08 km^2 [40]. The higher separation degree is due to the higher pressure of the flue gas into membrane 1 which enhances the driving force for separation.

Like in Cascade A, the vacuum pump operates at a pressure of 100 mbar, the compressor between the membranes increases the pressure to 4 bar and the first retentate is expanded to 1 bar. The first compressor induces a pressure of 4 bar on the feed stream. The adiabatic efficiency of the vacuum pump, compressor and expander were set to 85%.

When simulating with real flue gas, the separation degree increases and the CO_2 purity decreases compared to the ideal gas case. The results are presented in Table 4.7 and Table 4.8.

The energy demand is not as dependent on the amount of water in the flue gas in this system as in Cascade A. Higher water content only results in a slight increase in compressor energy. The reason for this is that the compressor that is located before the first membrane functions as a water removal unit that makes the flue gas conditions similar no matter how much water is removed in the SPEEK-membranes. However, the difference between ideal flue gas and real flue gas simulations is still significant.

Table 4.7. Comparison of the energy consumption and separation degree of different dehydration cases for Cascade B with membrane areas that result in a separation degree of 90% for the ideal gas mixture case.

Water removal prior to CO_2 separation	CO_2 separation degree [%]	Membrane area [km^2]		Specific energy for vacuum pumps [kWh_e/t_{CO2}]	Specific energy for compressors [kWh_e/t_{CO2}]
		1st	2nd		
0	93	0.45	0.08	100	156
30%	93	0.45	0.08	100	154
60%	93	0.45	0.08	100	148
Ideal gas	90	0.45	0.08	86	139

Table 4.8 shows that the amount of water that is removed prior to the CO_2 capture process is of insignificant importance for the composition of the gas, since all dewatering options provide approximately the same results.

An issue with Cascade B is that the final CO_2 stream does not reach 95mol% CO_2 purity, which is desired, but a high CO_2 separation degree is reached instead.

Table 4.8. CO_2 purity in positions 1, 2 and 3 according to Figure 4.3 for the 90% separation degree case.

Point in process according to Figure 4.3	Water removal prior to CO_2 separation	Total flow rate of entire stream [kmol/h]	CO_2 [mol%]	N_2 [mol%]	O_2 [mol%]	Ar [mol%]	H_2O [mol%]
1	0	70 499	13.50	70.1	3.7	0.8	11.9
	30%	68 147	14.00	72.70	3.84	0.83	8.64
	60%	65 624	14.54	75.49	3.98	0.86	5.13
2	0	9 834	90.17	4.26	0.83	0.05	4.69
	30%	9 834	90.17	4.26	0.83	0.05	4.69
	60%	9 834	90.22	4.25	0.83	0.05	4.65
3	0	9 378	94.55	4.47	0.87	0.05	500 ppm
	30%	9 378	94.55	4.47	0.87	0.05	500 ppm
	60%	9 378	94.55	4.47	0.87	0.05	500 ppm

The simulations of Cascade A and B show that a real gas mixture provides different results than ideal gas simulations. Thus, modeling as close to the real conditions as possible is important in order to make a valid assessment of membrane systems.

4.4 Compression system

The CO_2 needs to be compressed after the separation in order to be suitable for pipeline transportation. The end condition is assumed to be at a pressure of 110 bar and a temperature of 30°C.

For a real flue gas system, each compression stage is composed of a compressor, an intercooler and a water separator, as was discussed in chapter 2.4.4. After the CO_2 compression system, a desiccant adsorber is implemented to ensure that the water content is maximum 500 ppm.

The arrangement of compressor stages was investigated in this thesis. On the basis of Cascade A with 70% degree of separation, several arrangements were explored. The results are shown in Table 4.9. The energy requirement of 3-stage compression were taken from previous studies [60].

Table 4.9. Specific energy requirement of CO_2 compression process for different gas mixtures and number of compression stages[60].

Gas mixture	Number of stages	Specific energy requirement [kWh_e/t_{CO2}]
Ideal	3	105
	8	92.9
Real	3	110
	8	93.7

Table 4.9 shows that it is clearly energetic advantageous to perform the CO_2 compression in eight stages instead of three. Therefore, eight-staged compression was chosen for the further simulations in the thesis.

The compression system was simulated for Cascade A for the cases with 60% dewatering prior to CO_2 capture. The results are shown in Table 4.10.

Table 4.10. Comparison of the energy consumption of the CO_2 compression for the cases with removal of 60% of the water prior to CO_2 capture.

Cascade	CO_2 separation degree (ideal gas) [%]	Specific energy for CO_2 compression [kWh_e/t_{CO2}]
A	61	92.50
A	78	93.74
B	93	94.50

4.5 Comparison of different concepts

On the basis of the aforementioned results, a detailed comparison was performed in order to investigate how the energy consumption of different components, i.e. vacuum pump, compressor and final compression for transportation distribute in the total energy demand. Figure 4.4, Figure 4.5

and Figure 4.6 show the results of the four water removal cases for at 50%, 70% and 90% degree of CO_2 separation respectively.

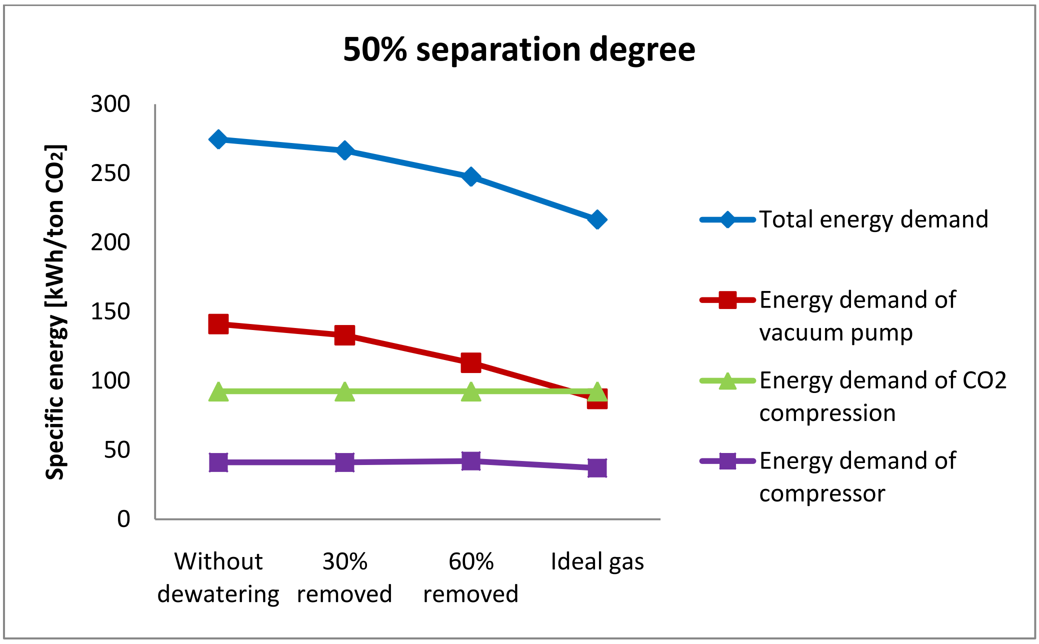

Figure 4.4. Energy demand profile for the capture and CO_2 compression processes for the 50% separation degree case.

The two cases of Cascade A (Figure 4.4 and Figure 4.5) have similar distribution of the energy demand. The vacuum pump is the major contributor to the total energy demand and is also the component that benefits most from a decrease in water content in the flue gas.

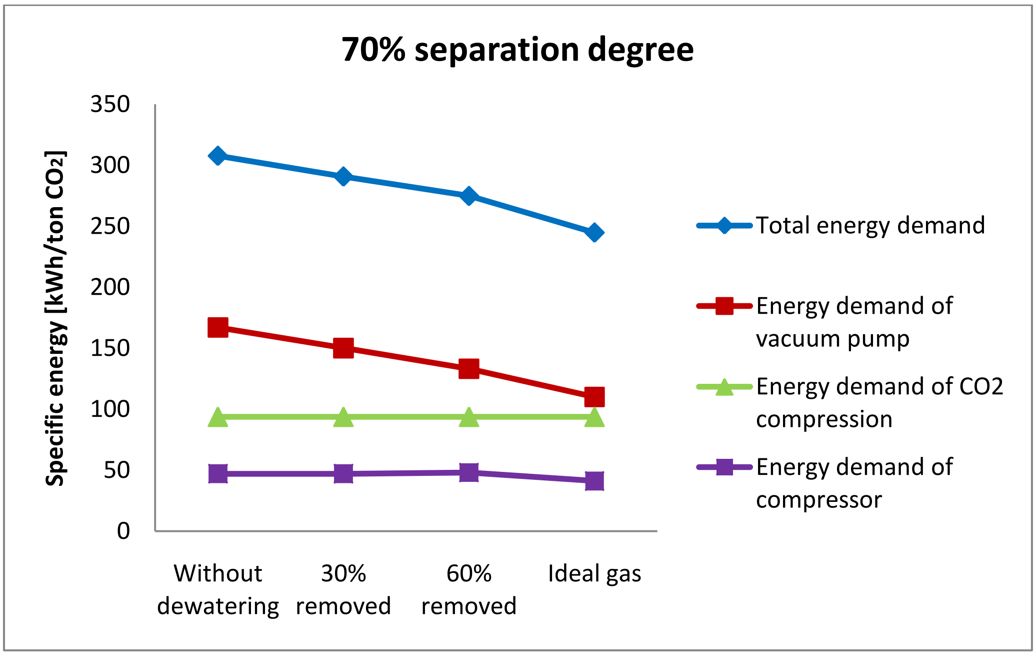

Figure 4.5. Energy demand profile for the capture and CO_2 compression processes for the 70% separation degree case.

Figure 4.6 show how small the difference in energy consumption is between the different water removal options for Cascade B.

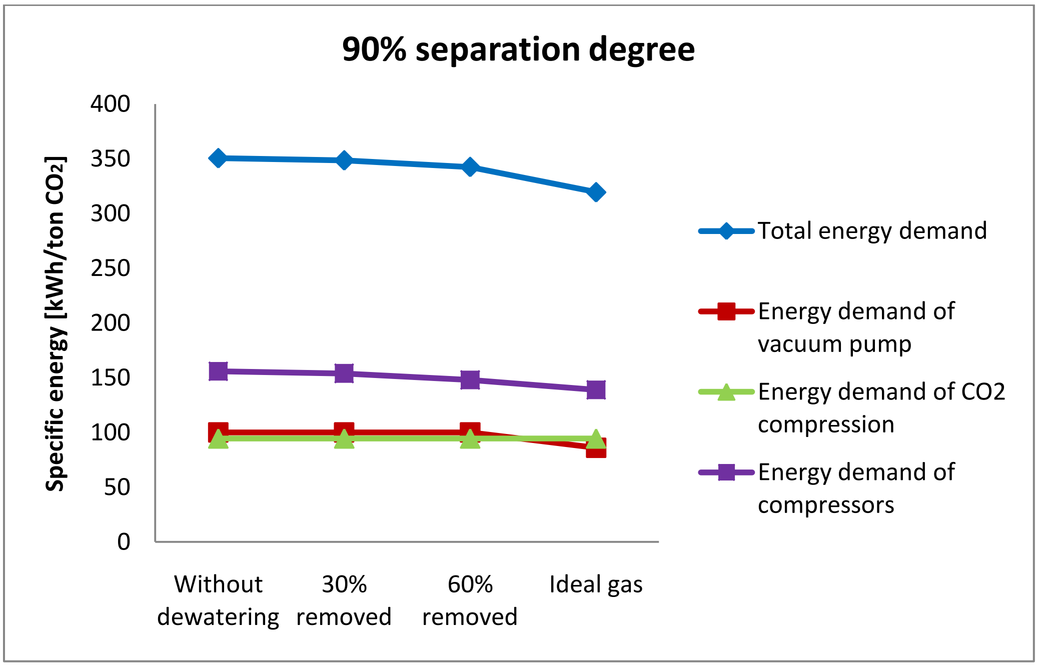

Figure 4.6. Energy demand profile for the capture and CO_2 compression processes for the 90% separation degree case.

The efficiency penalty that each of the different cases inflict on the power plant is shown in Table 4.11.

Table 4.11. Efficiency penalty imposed on the power plant by each case for different separation degrees.

CO_2 separation degree	0	30%	60%	Ideal gas
50%	6.0	5.7	5.2	4.1
70%	8.4	8.0	7.4	6.4
90%	11.3	11.2	11.0	10.7

The efficiency penalties of the cases with 60% water removal prior to CO_2 capture were compared to the efficiency penalties imposed by the market leading MEA-absorption technology. The results are shown graphically in Figure 4.7.

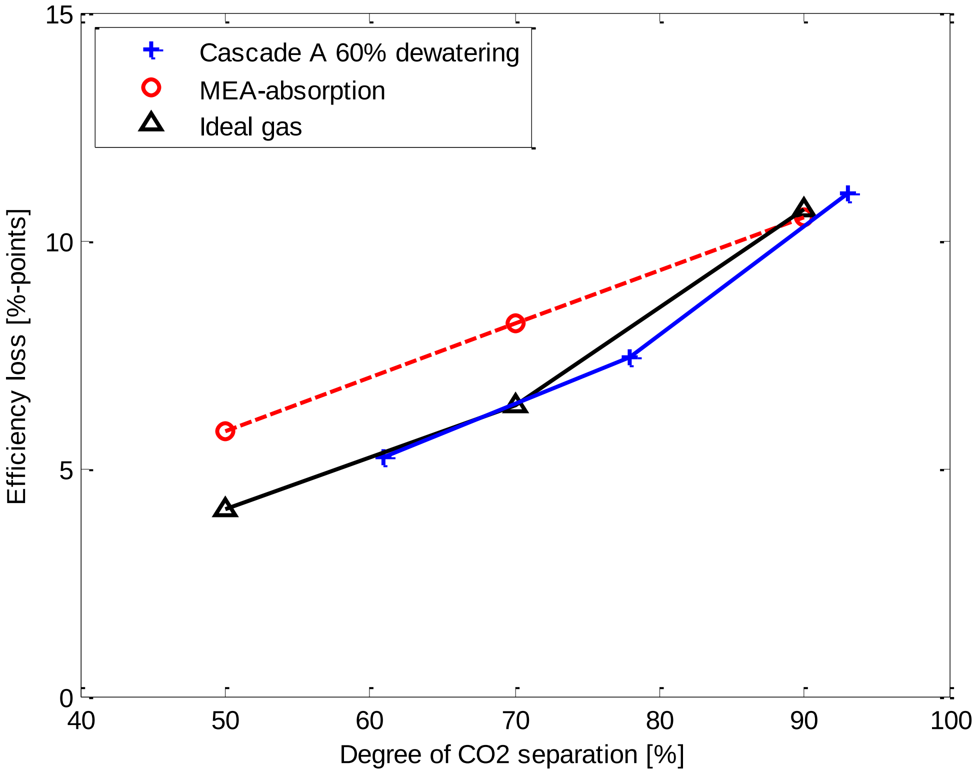

Figure 4.7. Comparison of membrane CO_2 separation based on ideal and quasi real flue gas and MEA-absorption.

It can be concluded that the membrane systems have an energetic advantage compared to MEA absorption for separation degrees of 61% and 78% if 60% of the water is removed prior to the CO_2 capture. For a separation degree of 90% the membrane separation and MEA-absorption stand almost in the same level.

4.6 Summary

When applying the real flue gas for the optimized membrane cascades based on ideal flue gas simulations, the following results were obtained:

- The water in the flue gas has a positive sweep gas effect that increases the degree of CO_2 separation.
- Under the defined boundary conditions, the energy consumption increases significantly with higher water content for Cascade A and modestly for Cascade B.
- The investigated membrane systems have an energetic advantage compared to MEA-absorption for CO_2 separation degrees up to 79% if 60% of the water is removed prior to CO_2 separation, provided that the defined boundary conditions are respected.

5 Heat exchanger design

The simulations in this thesis have so far been based on the assumption that the recovered heat in the stages of the vacuum pumps and compressors is sufficient to heat the gas in the expansion process. The intercoolers and aftercoolers play an essential role in fulfilling this requirement. However, so far in this thesis as well as in previous studies, these heat exchangers have not been investigated in detail.

The heat exchangers also have the important task of making sure that the inlet temperature to the second membrane is about 50°C, which is the optimal temperature for membrane separation in multi-stage systems with polymeric membranes.

As discussed in chapter 4, the combination of intercooler and water separator for each compression stage is an effective measure to remove water in a real flue gas membrane separation system. It was concluded in chapter 4 that more water removal results in less energy consumption. Thus, it is of great interest to investigate the heat exchanger process further.

This chapter aims to give a description of how the heat exchangers are designed to be able to fulfil the requirements of the membrane systems.

5.1 Basic parameters

Heat exchange between two fluids is governed by the following parameters:

- The hot stream's inlet- and outlet temperatures $T_{h.in}, T_{h.out}$
- The cold stream's inlet- and outlet temperatures $T_{c.in}, T_{c.out}$
- The mass flow rates of both streams $\dot{m}_h, \dot{m}_c$
- The heat capacities of both streams c_{p_h}, c_c
- The overall heat transfer coefficient U
- The heat transfer area A
- The logarithmic mean temperature difference ΔT_m

5.1.1 T-Q diagrams

The performance of a heat exchanger can be shown in a T-Q (temperature-heat transfer) diagram. Such a diagram makes it easy to see if the second law of thermodynamics is obeyed or not. Figure 5.1 shows how a T-Q diagram can look, with the red arrow representing the stream that is cooled down (the hot stream) and the blue arrow representing the stream that is heated (the cold stream). The opposite directions of the arrows show that this is a heat exchanger with counter current flow.

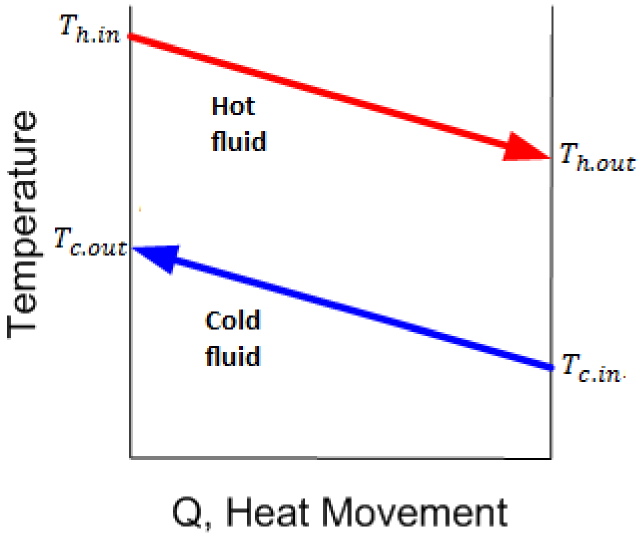

Figure 5.1. Sketch of a basic T-Q diagram.

According to the second law of thermodynamics, heat can only move from a higher to a lower temperature fluid. Figure 5.2 illustrates a T-Q diagram with a violation to this law. In other words, Figure 5.2 shows an impossible heat exchanger design.

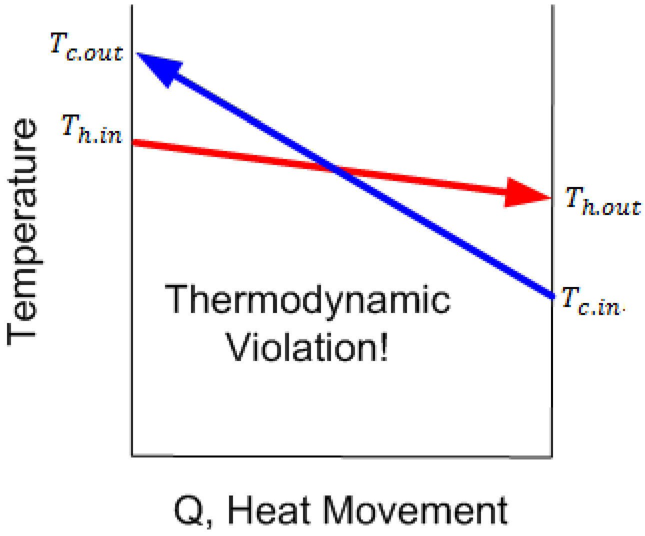

Figure 5.2. T-Q diagram with highlighting a thermodynamic violation

Sometimes one of the fluids undergoes a phase change during the heat exchange. An example of this is shown in Figure 5.3, where the curve symbolises a liquid water stream that is heated to 100°C, where it is completely vaporized and then heated to 150°C. It is obvious that most of the heat is transferred when the water is changing phase, because the latent heat is required for the phase transition.

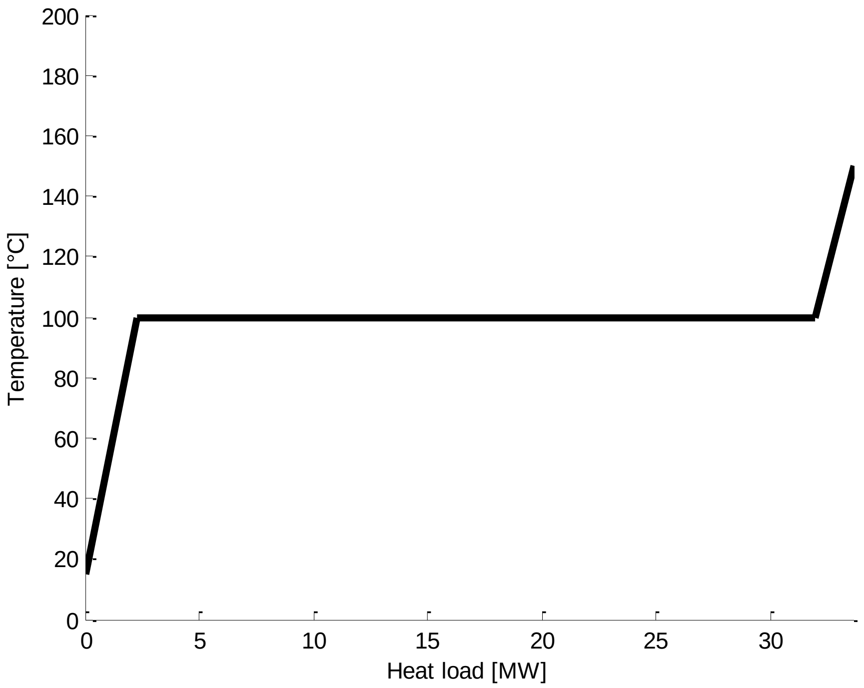

Figure 5.3. T-Q diagram representing a water stream that is undergoing complete phase change.

The heat exchangers that have been investigated in this thesis use a flue gas with a quasi realistic composition on the hot side. When cooling such a gas, the water contained in the flue gas may start to condense. In this case the phase change will not occur during constant temperature. This is explained more in section 5.2.

5.1.2 Heat exchanger equations

The amount of transferred heat in a counter current heat exchanger can be calculated with any of the three following formulas:

$$\dot{Q} = \dot{m}_h c_{p_h} (T_{h.in} - T_{h.out}) \tag{5.1}$$

$$\dot{Q} = \dot{m}_c c_{p_c} (T_{c.out} - T_{c.in}) \tag{5.2}$$

$$\dot{Q} = UA\Delta T_m \tag{5.3}$$

The logarithmic mean temperature difference can be calculated from:

$$\Delta T_m = \frac{(T_{h.in} - T_{c.out}) - (T_{h.out} - T_{c.in})}{\ln\left(\frac{T_{h.in} - T_{c.out}}{T_{h.out} - T_{c.in}}\right)} = \frac{\Delta T_1 - \Delta T_2}{\ln\left(\frac{\Delta T_1}{\Delta T_2}\right)} \tag{5.4}$$

The main objective for the investigated heat exchangers is to intercool the flue gas, in other words to achieve a low value of the hot stream's outlet temperature $T_{h.out}$. From equation (5.1) it can be seen that $T_{h.out}$ can be decreased if:

- The heat transfer is increased
- The hot stream inlet temperature is decreased
- The hot stream flow rate is decreased

Equation (5.2) show that the heat transfer rate can be increased by:

- Increasing the cold stream flow rate
- Increasing the cold stream outlet temperature
- Decreasing the cold stream inlet temperature

In order to make CCS systems attractive and a worthwhile investment, the systems must be kept at a cost as low as possible. Thus, the best kind of heat exchanger would be one that provides a sufficiently low hot outlet temperature and is as inexpensive as possible. The major cost factor for heat exchangers is the size of them. Therefore, it is important to minimize the heat transfer area without decreasing the performance of the heat exchanger. From equation (5.3) it can be seen that the area will be low if:

- The logarithmic mean temperature difference is high
- The heat transfer coefficient is high
- The heat transfer rate is low

However, the heat transfer rate must be high enough to achieve a sufficiently low value on $T_{h.out}$. Thus, it is clear that there is a trade-off relationship between the area and the hot stream outlet temperature.

5.2 Heat exchangers in real flue gas systems

The issue of water condensation during a compression process distinguishes a real flue gas simulation from an ideal flue gas mixture. More influence factors must be considered for a realistic heat exchanger design.

Normally when there is a phase change in a heat exchanger, the temperature of the medium is constant during the phase change. When there is flue gas condensation, the phase change of the water will occur in a temperature range instead [62]. Figure 5.4 shows the temperature profiles of flue gases from combustion of heating oil and natural gas.

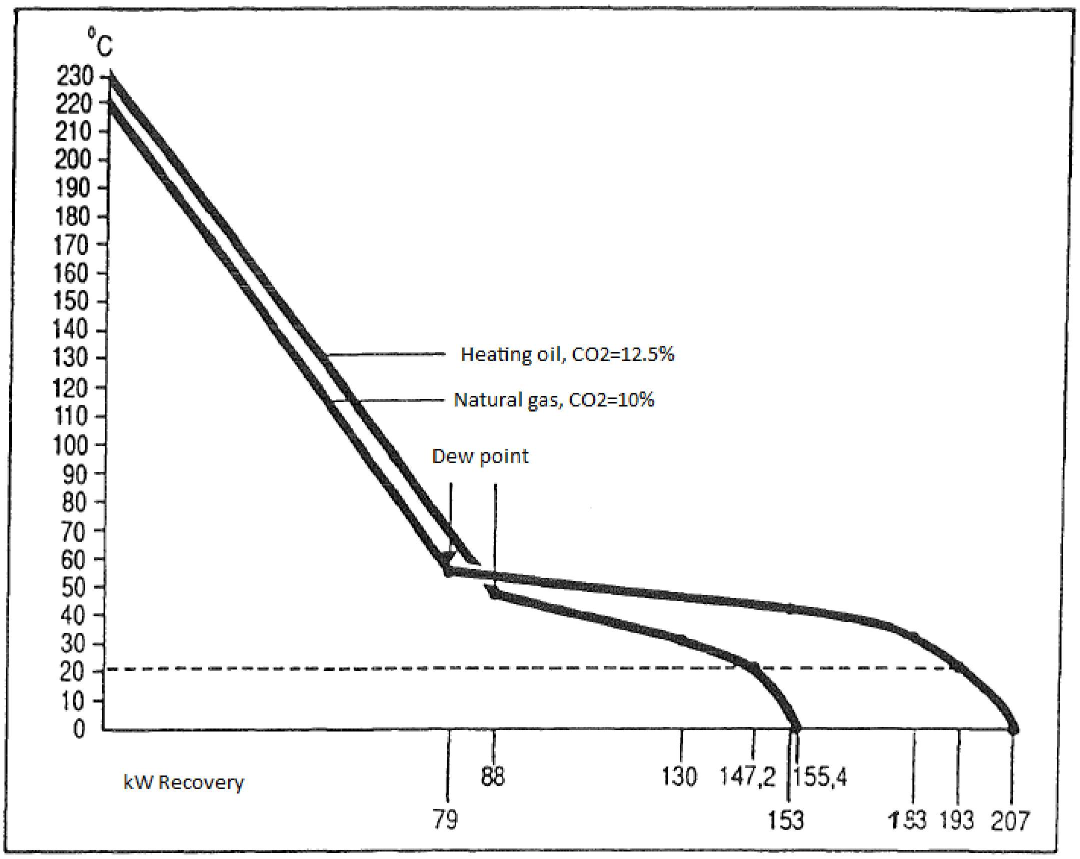

Figure 5.4. Illustration of how the temperature changes during flue gas condensation for heating oil and natural gas [62].

5.3 An initial attempt

Cascade A with 70% degree of CO_2 separation was chosen for an initial investigation. 60% of the water in the flue gas is removed using dehydration membranes prior to the capture process.

If it would be possible, a uniform design of each heat exchanger is desired, because it is manufacturing friendly. On the basis of this rule, the same pressure ratio was applied for the vacuum pump, compressor and expander, instead of using the square root method for calculating the inter-stage pressure [36]. A tube-and-shell recuperator made for flue gas with condensation was chosen for the simulations (taken from [62]), since this design is flexible and can operate in many different conditions. The cooling media that is used to cool the flue gas and then reheat it during expansion is river water at 15°C and 1 bar. The heat exchangers may be positioned at elevated locations. Therefore the water is pumped to a pressure of 3 bar, so that there is a driving force that makes the water flow to its destination. The heat exchangers were assumed to cause a pressure drop on the flue gas stream of 30 mbar. Counter current flow is simulated, since this is the most effective and common flow pattern in heat exchangers. The assumptions are summarized in Table 5.1.

Table 5.1. Assumptions made for the capture process.

Assumptions	Unit	Value
Cooling water pressure	bar	3
Cooling water temperature	°C	15
Polytropic efficiencies of compressors and vacuum pumps	-	0.85
Isentropic efficiency of expanders	-	0.85
Hot stream pressure drop in each heat exchanger	mbar	30

An initial investigation was focused on the aftercooler prior to the 2nd membrane, in order to understand how the different parameters influence the heat exchanging performance. This aftercooler plays an important role, because the stream should be cooled to approximately 50°C, since the polymer membrane has an optimum separation behavior at this temperature. The hot feed stream of this aftercooler is assumed to have a pressure of 2 bar and a temperature of 158°C. The data were taken from the previous system design.

A parametric study was carried out for the following parameters:

- The temperature difference between the ingoing flue gases and the outgoing water stream
- The cooling water pressure
- The cooling water flow rate

The parameter set for a base case is shown in Table 5.2. Under these boundary conditions, the T-Q diagram of this aftercooler was developed, as is shown in Figure 5.5.

Table 5.2. Parameter set for a base case.

Basic case values		
$T_{h.in} - T_{c.out}$	K	5
Cooling water pressure	bar	3
Cooling water flow rate	kmol/h	2 335

There is an obvious thermodynamic violation in this heat exchanger. The problem is that the cooling water is heated above its boiling point and is therefore undergoing a phase change.

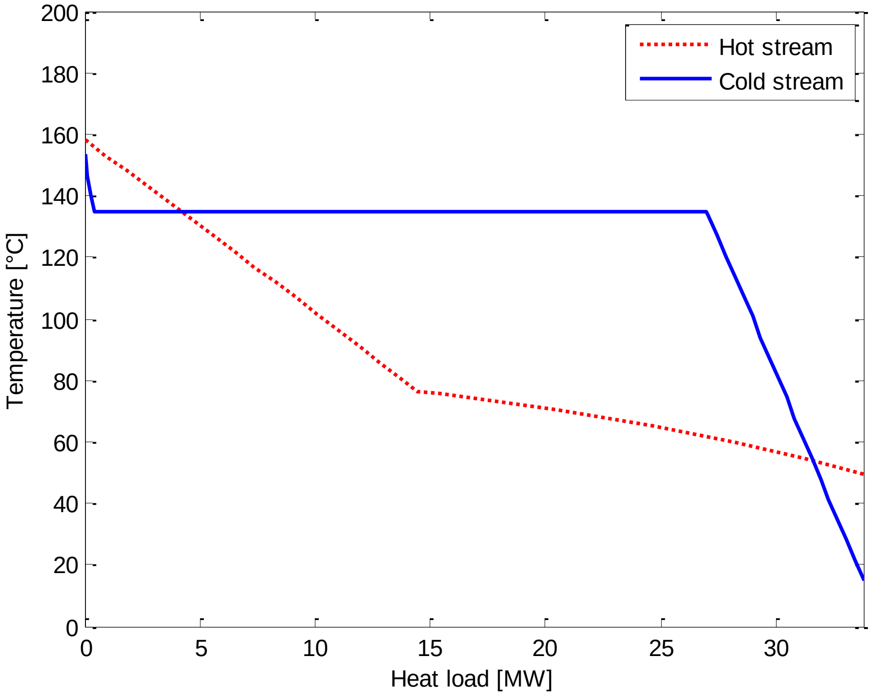

Figure 5.5. T-Q diagram of the base case with the parameter set shown in Table 5.2.

If the temperature difference between $T_{h.in}$ and $T_{c.out}$ is increased to 20 K, the T-Q-diagram will not change much. However, if the temperature difference is increased to above 23.4, as shown in Figure 5.6, the cooling water will never reach its boiling temperature, but the cooling medium cannot take away enough heat to ensure that the $T_{h.out}$ is lowered to 50°C.

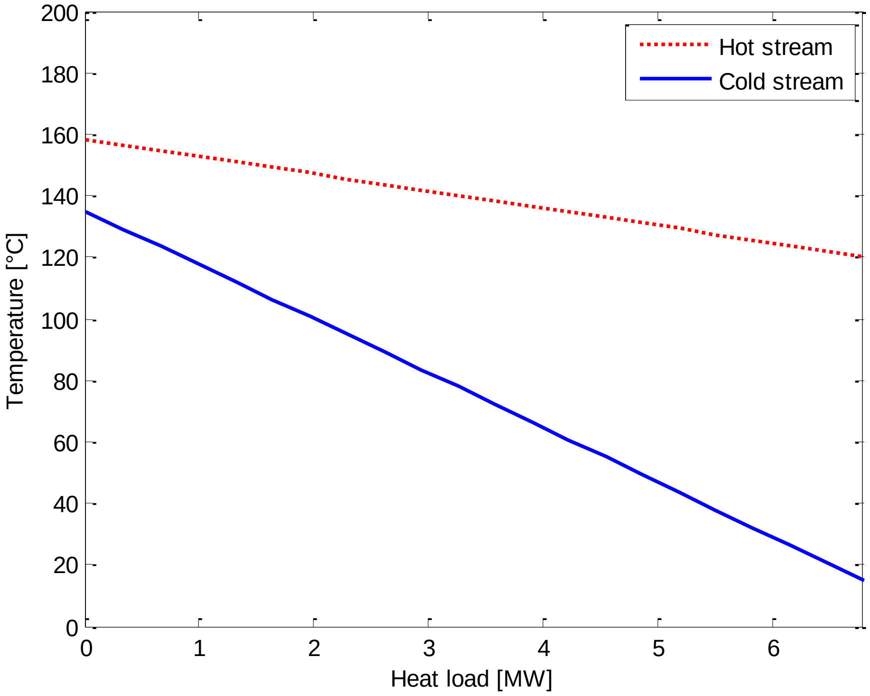

Figure 5.6. T-Q diagram of the base case but with a temperature difference of 23.4 K between $T_{h.in}$ and $T_{c.out}$.

By increasing the pressure of the cooling water to 6 bar, the cooling water will have a boiling point that is higher than $T_{h.in}$, which would prevent the water from boiling and there would be no thermodynamic violation. However, $T_{h.out}$ would be too high, since the heat transfer would not be high enough. This is shown in Figure 5.7.

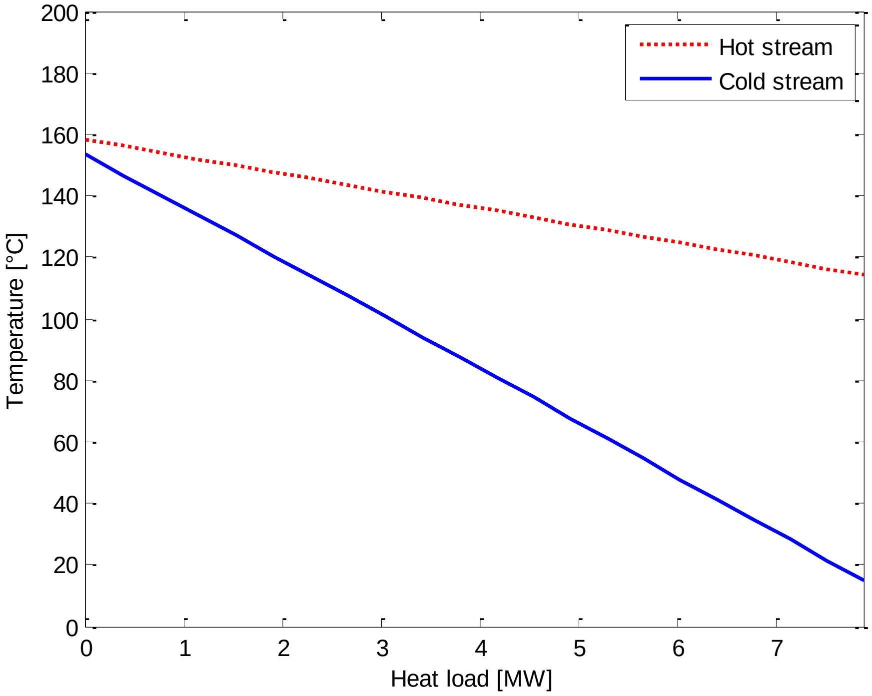

Figure 5.7. T-Q diagram of the base case but with cooling water at 6 bar.

If the pressure of the cooling water is decreased to 0.1 bar the boiling point would be so low that the water could evaporate completely under the hot curve without causing any violations (Figure 5.8), but such a low pressure is not practical in reality.

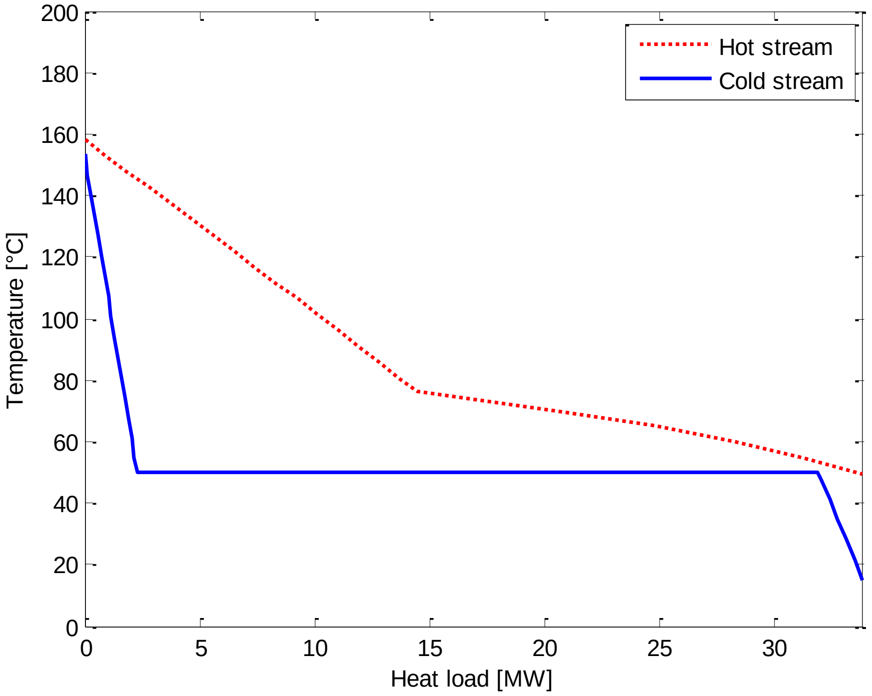

Figure 5.8. T-Q diagram of the base case but with cooling water at 0.1 bar.

If the cooling water flow rate is decreased it will result in a lower heat transfer rate and thus a higher $T_{h.out}$. With a cooling water flow rate of 300 kmol/h, there would be no thermodynamic violations, but $T_{h.out}$ would be approximately 135°C, as is shown in Figure 5.9

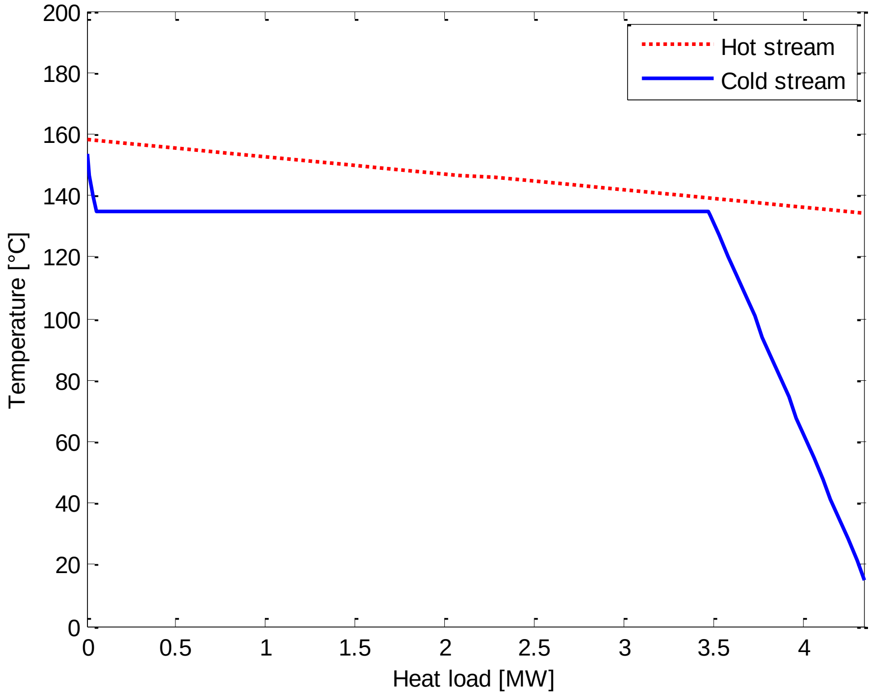

Figure 5.9. T-Q diagram of the base case but with a cooling water flow rate of 300 kmol/h.

On the basis of the above simulations, Table 5.3 was made that shows how different parameters influence the T-Q-diagram.

Table 5.3. Influences of different parameters on the cold and hot fluid temperature profiles.

	Temperature difference	**Flow rate of cooling water**	**Pressure of cooling water**
Cold fluid temperature profile	High➔ No water evaporation ➔cold fluid temperature profile below the hot profile	The shape of the profile is unaffected	High➔ No water evaporation Low➔ Water evaporation below hot stream
Hot fluid temperature profile	The shape of the profile is unaffected	High➔ Higher heat transfer ➔ Lower $T_{h.out}$ Low➔ Lower heat transfer ➔ Higher $T_{h.out}$	The shape of the profile is unaffected

These results lead to a preliminary design of the last heat exchanger prior to the second membrane. This design is called “Case A1” and has a cooling water pressure of 3 bar, a flow rate of 12 400 kmol/h and a temperature difference of 39 K between the hot inlet stream and the cold outlet stream. This results in a hot outlet stream temperature of about 60°C, which is above the preferred temperature of 50°C. As an initial result the deviation from the target is accepted.

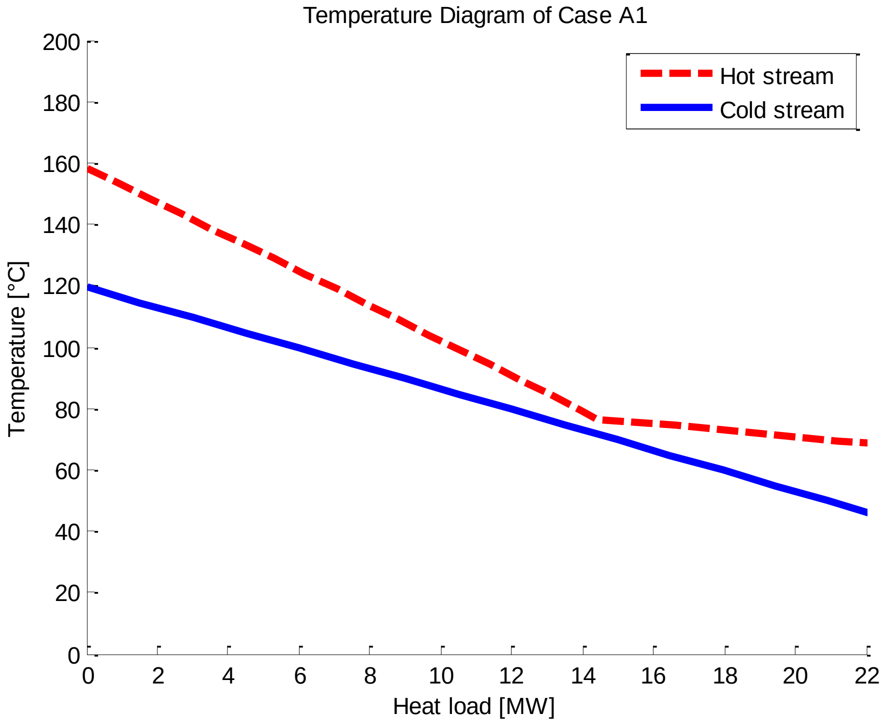

Figure 5.10. Temperature diagram of an aftercooler in case A1.

5.4 Heat exchanger design in membrane capture system

The membrane capture system was investigated first with Case A1 as a basis.

5.4.1 2 stage-vacuum pump

2-stage arrangements of the vacuum pump, compressor and expander were investigated initially. The cold outlet stream from each heat exchanger is mixed together into one stream and then divided into two equal streams, of which one goes to each heat exchanger in the expansion process. After the water has been used to heat the gas in the expander sequence, it is mixed again into one final water stream. The Aspen Plus model of the entire capture system is shown in Figure 5.11.

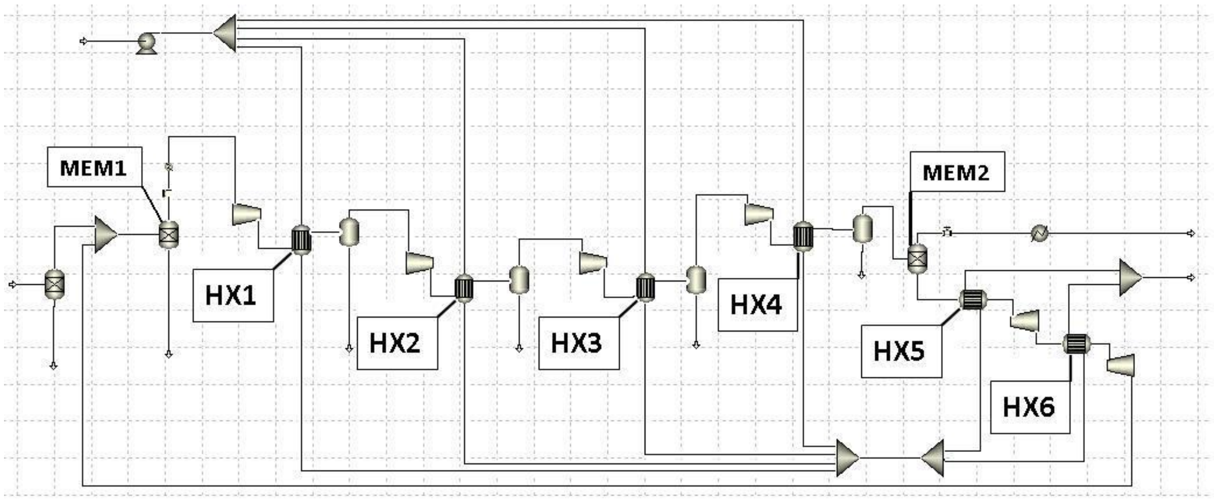

Figure 5.11. Flow diagram of the membrane capture system with 2-stage vacuum pump design in Aspen Plus.

The so called optimal pressure ratio was used in the vacuum pumps, compressors and expanders in order to minimize the energy consumption of the system. The optimal pressure ratios were calculated to the values shown in Table 5.4.

Table 5.4. Pressure ratios of vacuum pump, compressor and expander when each of them has two stages.

Pressure ratios	
Vacuum pump	3.36
Compressor	2.02
Expander	0.51

The aim of this point is to find a heat exchanger design that could be used for each intercooler, so that the temperature going to the second membrane can reach approximately 50°C and the recovered heat is enough to heat the gas in the expansion sequence.

The following attempt is to implement the parameters, obtained from Case A1, to the membrane capture system for each heat exchanger. Unfortunately, this design doesn't work for the all heat exchangers. Two causes can be explained:

- Owing to the different pressure ratios used for the vacuum pump and compressor, the heat exchanger cannot be identical for each intercooling state.
- The hot inlet stream temperature of HX4, analyzed in Case 1, was obtained from the previous system design. This value is changed if a 30 mbar pressure drop for each intercooling stage is considered, since the pressure ratio must be increased in this case. The deviation of the inlet hot stream temperature leads to that the desired 50°C is not reachable.

The heat exchangers in the vacuum pump, HX1 and HX2, have a much larger ingoing flue gas temperature than the heat exchangers in the compression part of the system, HX3 and HX4. For example, $T_{h.in}$ is about 183°C in the first heat exchanger. If the temperature difference $T_{h.in} - T_{c.out}$ is 39 K, $T_{c.out}$ would be 144°C, which is above the boiling temperature of water at 3 bar. This is not desirable. Moreover, the first heat exchanger, HX1, is different from the others, since there is no water condensation in the flue gas in that unit.

The different conditions for the heat exchangers make it difficult to achieve the desired temperature to the second membrane at the same time as the heat exchangers have the same water flow rates and hot inlet-cold outlet temperature differences.

A further attempt is to rearrange the number of stages of the vacuum pump. The aim is try to regulate the pressure ratio of each vacuum pump stage to give each intercooler or aftercooler of the vacuum pump and compressor identical boundary conditions.

5.4.2 4 stage-vacuum pump

With a 4-stage vacuum pump, the capture system has the configuration shown in Figure 5.12.

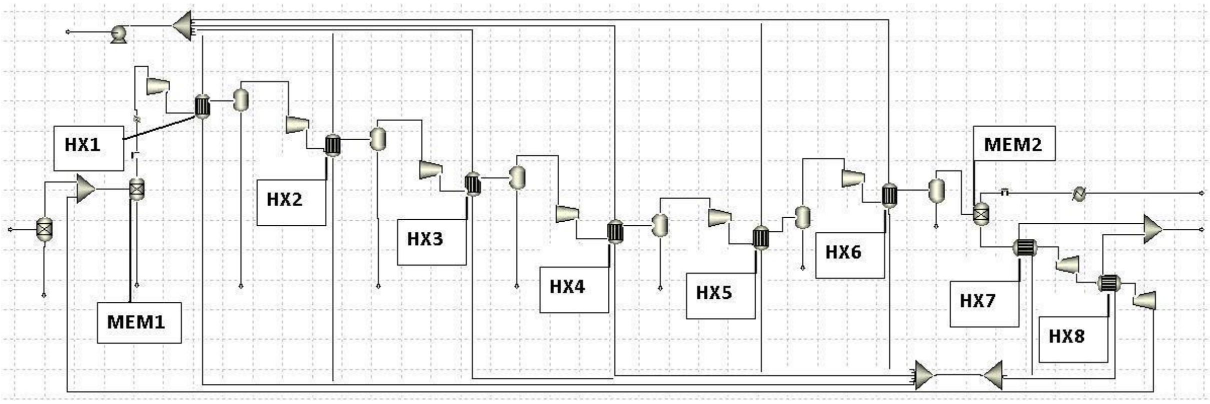

Figure 5.12. Flow diagram of the membrane capture system with 4-stage vacuum pump design in Aspen Plus.

The pressure ratio for each vacuum pump stage, compressor stage and expander stage are shown in Table 5.5.

Table 5.5. Pressure ratios of vacuum pump, compressor and expander when the vacuum pump has two stages and the other units have two stages.

Pressure ratios	
Vacuum pump	1.94
Compressor	2.02
Expander	0.51

Now there is flue gas condensation and similar values on the ingoing flue gas temperature in each heat exchanger. However, even now it is difficult to reach a low outlet temperature from the last heat exchanger before the second membrane of the same reasons as in the previous attempt. A lot of different combinations of parameters were tested and finally the following values were chosen for each heat exchanger:

- Hot inlet-cold outlet temperature difference of 12.5 K
- Cooling water flow rate of 8 400 kmol/h
- Cooling water pressure of 3 bar

The temperature of the flue gas when it reaches membrane 2 is almost 60°C, which is a bit higher than preferred, but not completely out of range. The amount of heat that is recovered from the intercoolers is enough to heat the flue gas in the expansion sequence to 95°C in both the reheating expansion heat exchangers. The T-Q-diagram of every heat exchanger in the vacuum pump sequence, compressor sequence and expander sequence are shown in Figure 5.13, Figure 5.14 and Figure 5.15 respectively.

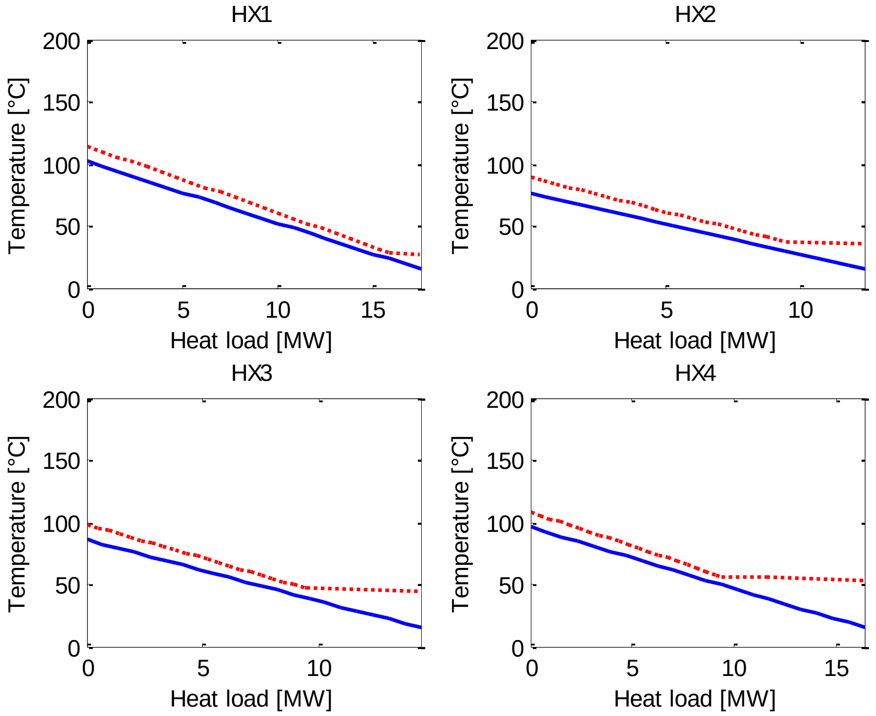

Figure 5.13. T-Q-diagrams for the heat exchangers in each vacuum pump stage.

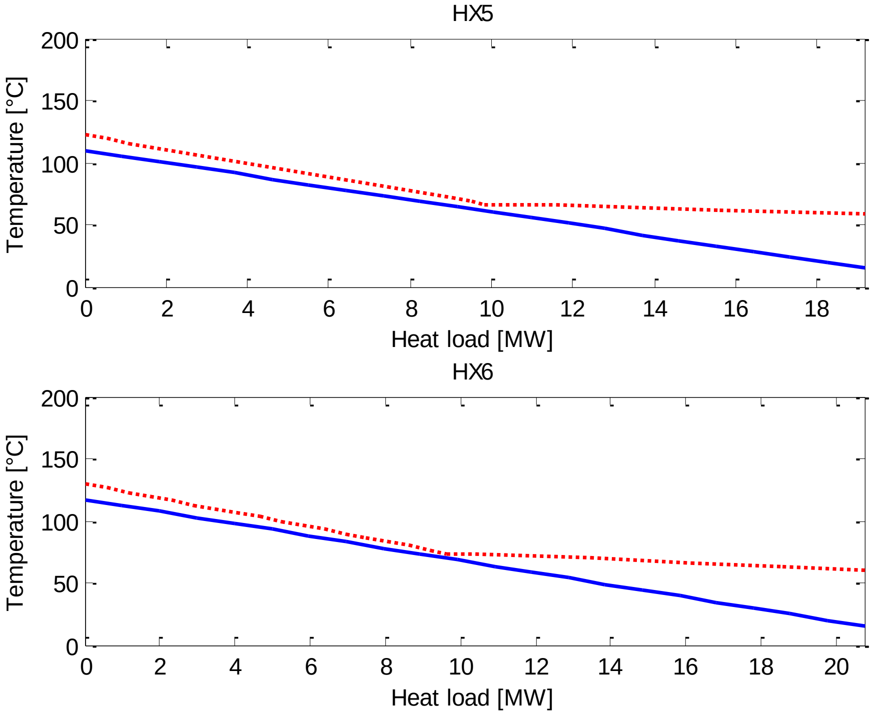

Figure 5.14. T-Q-diagrams for the heat exchangers in each compressor stage.

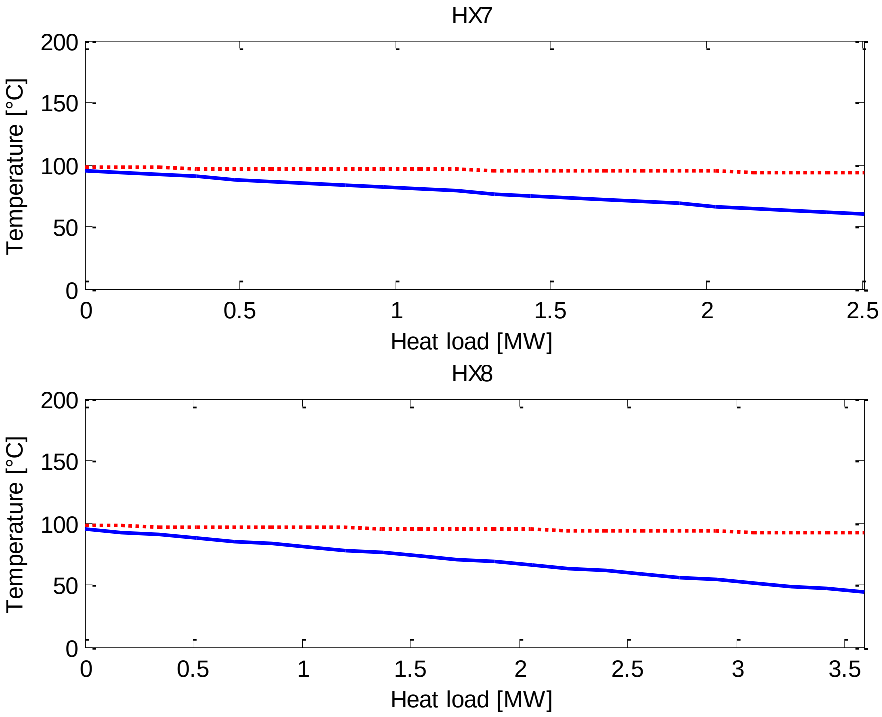

Figure 5.15. T-Q-diagrams for the heat exchangers in each expander stage.

The energy requirement of the entire capture system was then calculated. The results are summarized in Table 5.6.

Table 5.6. Required energy of the capture system.

ENERGY	
Power requirement [kW]	
Vacuum pump 1	12021
Vacuum pump 2	11143
Vacuum pump 3	11313
Vacuum pump 4	11397
Compressor 1	12121
Compressor 2	11894
Expander 1	-3 546
Expander 2	-3 549
Pump	78
Total power	62 872
Final CO2 flow [kmol/h]	7 444
Specific energy in capture process [kWh/t CO_2]	191.9

The specific energy requirement in this process is higher than the one that was simulated in chapter 4. There it was calculated to be 181 kWh/ton CO_2. The increase is a result from more vacuum pump stages, since more heat exchangers are needed and each heat exchanger impose a pressure drop that increases the energy demand in the vacuum pumps.

5.4.3 Calculation of heat transfer area

The major cost factor for a heat exchanger is the heat exchanger area. According to Equation (5.3), the size of the area depends on the heat transfer rate, the overall transfer coefficient and the logarithmic mean temperature. The equation can be rewritten as:

$$A = \frac{\dot{Q}}{U \Delta T_m} \tag{5.5}$$

The heat transfer rate and logarithmic mean temperature difference can be calculated according to equations (5.1), (5.2) and (5.4). The overall heat transfer coefficient is a bit more difficult to determine. It is a measure of how much energy flux is transferred per square meter and Kelvin. It is thus easy to understand that it is dependent on which fluids the heat exchange takes place between and the state of each fluid. In addition, the fouling effect each fluid has on the heat exchanger must be taking into account, since this decrease the performance of the heat exchanger.

The overall heat transfer coefficient can be calculated as [52]:

$$\frac{1}{U} = \frac{1}{h_g} + \frac{1}{h_{d.g}} + \frac{d}{\lambda} + \frac{1}{h_{d.w}} + \frac{1}{h_w} \tag{5.6}$$

$h_{d.g}$ and $h_{d.w}$ are the fouling factor on the flue gas side and on the water side respectively. h_g and h_w are the heat transfer coefficients for each fluid, d is the thickness of the heat transfer wall and λ is the thermal conductivity of the material.

The values for these different parameters can be found in tables. The heat exchange that takes place in the capture and compression processes are of three different types:

- heat exchange with flue gas condensation in heat exchanger in vacuum pump
- heat exchange with flue gas condensation in heat exchanger in compressor
- heat exchange without flue gas condensation in heat exchanger in compressors and expanders

Thus, three different values of U must be used in the calculation of the heat transfer area. In the simulations in this thesis, the parameters are chosen according to Table 5.7.

The chosen heat exchanger material is stainless steel, since this is most suitable when the flue gas condenses [62]. According to Bettge et al. [63], all of the stainless steels 1.4006, 1.4313, 1.4542, 1.4562 and 3.7165 (with European standard number designations) are anti-corrosive and of a high enough quality to handle compression processes in CCS systems.

The heat transfer coefficient of condensing flue gas is very high, which makes the area smaller, in accordance with Equation (5.5). The difference in heat transfer coefficient on the flue gas side between vacuum pump and compressor heat exchangers is due to the different construction of vacuum pumps and compressors. The table also shows the heat transfer coefficients in an air cooler.

Flue gas is not considerably fouling according to Kuhn et al, hence the fouling factor for flue gas is neglected.

Table 5.7. Parameters needed to calculate the overall heat transfer coefficient.

Parameter	Abbreviation	Unit	Value	Reference
Thermal conductivity	λ	W/(mK)	16	[62], [52]
Wall thickness	d	mm	0.1	[64]
Fouling factor for water	$h_{d.w}$	W/(m^{2}K)	6 000	[52]
Fouling factor for flue gas	$h_{d.g}$	W/(m^{2}K)	-	[62]
Heat transfer coefficient for water	h_w	W/(m^{2}K)	1 000	[62]
Heat transfer coefficient for flue gas with condensation in vacuum pump	h_g	W/(m^{2}K)	5 000	[62]
Heat transfer coefficient for flue gas with condensation in compressor	h_g	W/(m^{2}K)	15 000	[62]
Heat transfer coefficient for flue gas without condensation in compressor	h_g	W/(m^{2}K)	8 000	[62]
Heat transfer coefficient for air	h_a	W/(m^{2}K)	250	
Heat transfer coefficient for flue gas without condensation in air cooler	h_g	W/(m^{2}K)	10 000	[62]

When applying the values in Table 5.7 to Equation (5.6), the overall heat transfer coefficients shown in Table 5.8 are obtained.

Table 5.8. The three different overall heat transfer coefficients.

Overall heat transfer coefficients U [W/(m^{2}K)]	
U for vacuum pump with flue gas condensation	728
U for compressor with flue gas condensation	807
U for expanders without flue gas condensation	770

With these U-values set and the heat transfer rates and logarithmic mean temperature differences calculated for each heat exchanger by Aspen Plus, the area of each heat exchanger was calculated by Equation (5.5). The results are shown in Table 5.9.

Table 5.9. Required heat transfer area in the capture process.

Heat Transfer Area [m^2]	
HX1	2609
HX2	1586
HX3	1699
HX4	1817
HX5	1871
HX6	2025
HX7	268
HX8	301
Total area	12 175

The heat duty is much smaller in the heat exchangers in the expansion sequence. That is why the area requirement is significantly smaller in these units. The reason for the larger area requirement in HX1 is that more heat is transferred in this heat exchanger than in the others. This is because HX1 has the highest flue gas inlet temperature, which leads to that the water is heated to a higher temperature, which in turn increases the heat duty of the heat exchanger. In HX6 the flue gas inlet temperature is almost as high as in HX1, but the logarithmic mean temperature difference and the U-value are larger than those of HX1, so that the area will be smaller than that of HX1.

5.5 Heat exchanger design in compression process

The compression process was simulated in a similar way as the capture process, with cooling water at 15°C and a mixer that collects all the water after the heat exchangers. The compression is performed in eight stages with 30 mbar pressure drop in each heat exchanger and the polytropic efficiency of each compressor is 85%. The Aspen Plus flow sheet is shown in Figure 5.16.

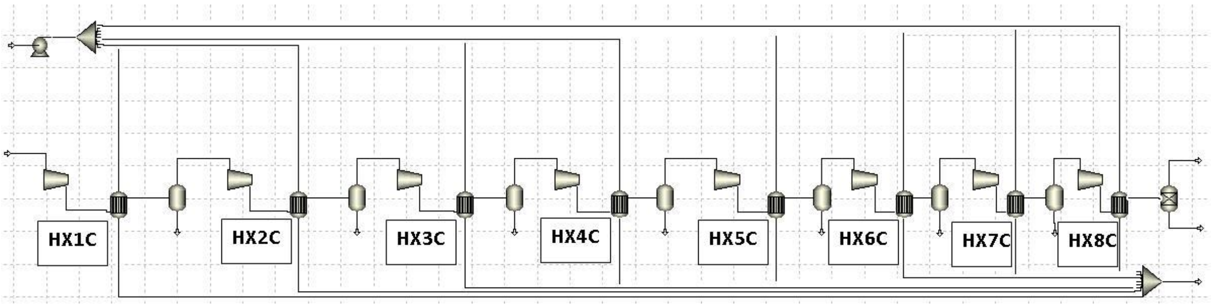

Figure 5.16. Aspen Plus model of the CO_2 compression system.

The most important requirement on this system is that the final CO_2 stream shall meet the requirements of CO_2 transport. This means that the pressure shall be 110 bar, the temperature 30°C and the water content less than 500 ppm.

The procedure for finding a heat exchanger design (hot inlet-cold outlet temperature difference, cooling water flow rate and pressure) was the same as in the capture system.

The problem when simulating this system is that the pressure of the hot stream in the last heat exchanger is significantly higher than in the other heat exchangers. Because of this, the last heat exchanger needs a very high cooling water flow rate so that the hot stream can reach the suitable temperature 30°C. In fact, the flow rate that is needed in HX8C is much higher than the other heat exchangers can handle.

For a system with a temperature difference between the hot inlet stream and the cold outlet stream of 10 K, the highest possible flow rate that every heat exchanger can handle is 4125 kmol/h. With this flow rate in each heat exchanger, the temperature leaving the last heat exchanger will be about 59°C. To reach 30°C, a flow rate of 10 800 kmol/h in the last heat exchanger would be needed.

A system with 5 K temperature difference can reach a temperature as low as 55.7°C, but then a much higher heat exchange area is needed. This follows from Equation (5.3); the logarithmic mean temperature difference will be lower, which leads to a higher area requirement if the overall heat transfer coefficient is the same in both cases. Because of this, the 10 K temperature difference case was chosen for further studies. A comparison between these two cases is presented in Table 5.10.

Table 5.10. This table shows the differences if 5 or 10 K is used as hot inlet-cold outlet temperature difference in the compression process.

Compression system		
ΔT [K]	5	10
Total water flow rate [kmol/h]	34 000	33 000
Water flow rate in each HX [kmol/h]	4 250	4 125
Out temp [°C]	56	59

5.5.1 Reaching 30°C

The problem with reaching the desired temperature of 30°C can be met with two different approaches:

- install an additional heat exchanger after the last compression stage
- have a different water flow rate in the last heat exchanger, which is a possible solution in the CO_2 compression process

The extra heat exchanger can be of either gas-liquid type or gas-gas type. The gas-gas type would cool the CO_2-stream with air as cooling medium. If water is used as cooling source, the total amount of water in the system would be higher than if the flow rate of water in HX8C was increased, which means that the pump work would also be higher. But the difference is only about 10 KW, which does not make a significant impact on the total specific energy requirement of the system. The energy demand for each option is shown in Table 5.11.

If an air-cooled heat exchanger was used the area would be higher than in the other cases, because of the lower overall heating coefficient. Table 5.11 shows the area requirement for the different options. The values for the overall heat transfer coefficient U were calculated according to the principle explained in chapter 5.4.3. The flow rate of air would have to be quite high if an air cooled heat exchanger was to be used.

From these results the option with an extra gas-liquid heat exchanger seems to be the best option. One way to make the area smaller is to increase the temperature difference between the hot inlet and cold outlet. This would increase the demand for water flow rate and thus increase the pump work, but since the pump work is a less significant factor than area it might be a good idea to do this anyway.

Therefore, an extra heat exchanger with 15 K temperature difference was tested (it would not be possible to reach 30°C with a higher value). This design has the lowest area and highest pump work, but the pump work only has a minor influence on the total specific energy requirement of the system. Consequently, this design is chosen for the extra heat exchanger in the CO_2 compression system.

Table 5.11. Comparison of different ways to achieve an outlet temperature of 30°C.

	Increased cooling water flow rate in HX8C	**Extra gas-liquid HX**	**Extra gas-gas HX**	**Extra gas-liquid HX 15 K**
U phase change [W/(m^{2}K)]	806.72	806.72		806.72
U no phase change [W/(m^{2}K)]	770.47	770.47		770.47
U in air-air HX [W/(m^{2}K)]			244.88	
Area [m^2]				
HX8C	1853.34	368.33	368.33	368.33
Extra HX		1191.79	3719.45	970.58
Total area in HX8C and extra unit	1853.34	1560.12	4087.78	1338.91
Total area	6699.67	6406.46	8934.12	6185.25
Energy requirement [kW]				
Pump	55.25	65.62	45.49	68.93
Total energy	33160.63	33227.73	33207.60	33231.04
Final CO2 flow [kmol/h]	7443.78	7443.78	7443.78	7443.78
Specific energy in compression process [kWh/t CO_2]	101.25	101.45	101.39	101.46

The final layout of the compression system is shown in Figure 5.17.

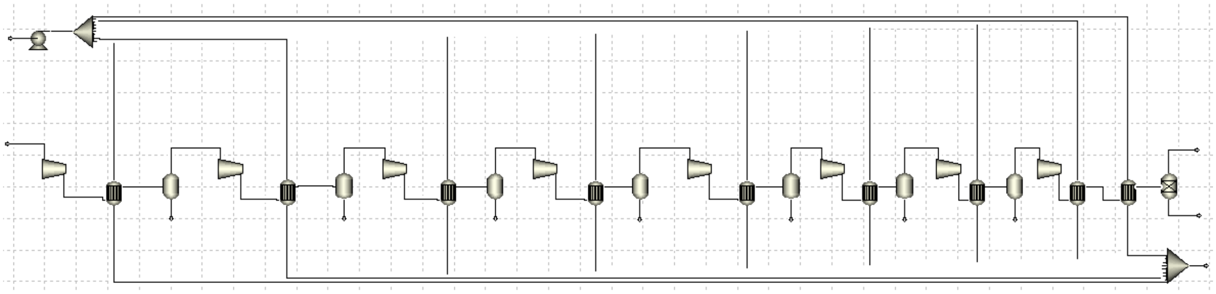

Figure 5.17. Aspen Plus model of the CO_2 compression system with an extra gas-liquid heat exchanger.

Figure 5.18 and Figure 5.19 shows the T-Q diagrams of the heat exchangers in every compression step. Water in the flue gas condenses only in the four first heat exchangers.

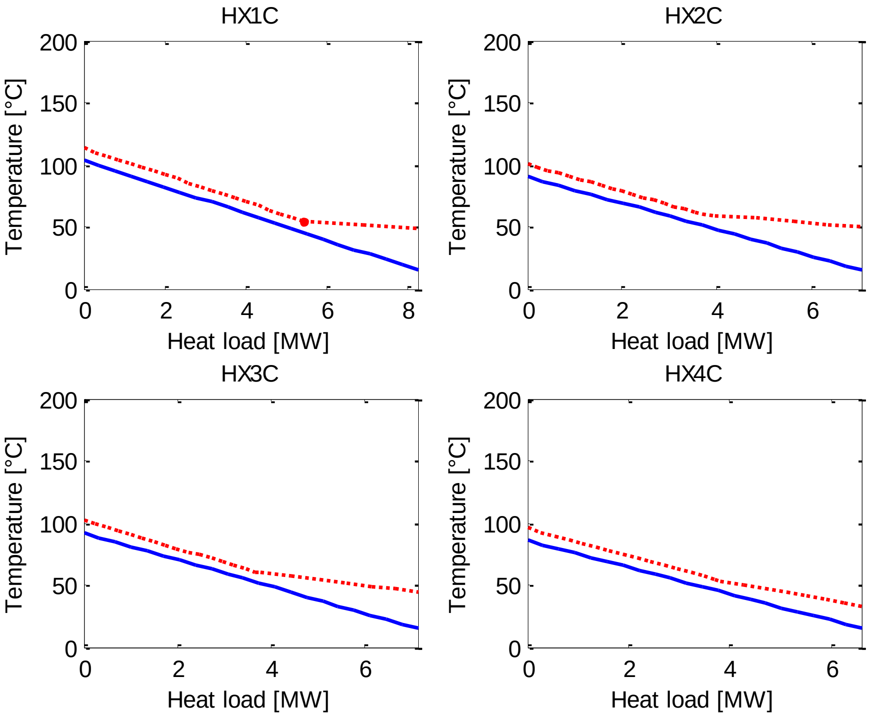

Figure 5.18.The T-Q diagrams of the four first heat exchangers in the compression process.

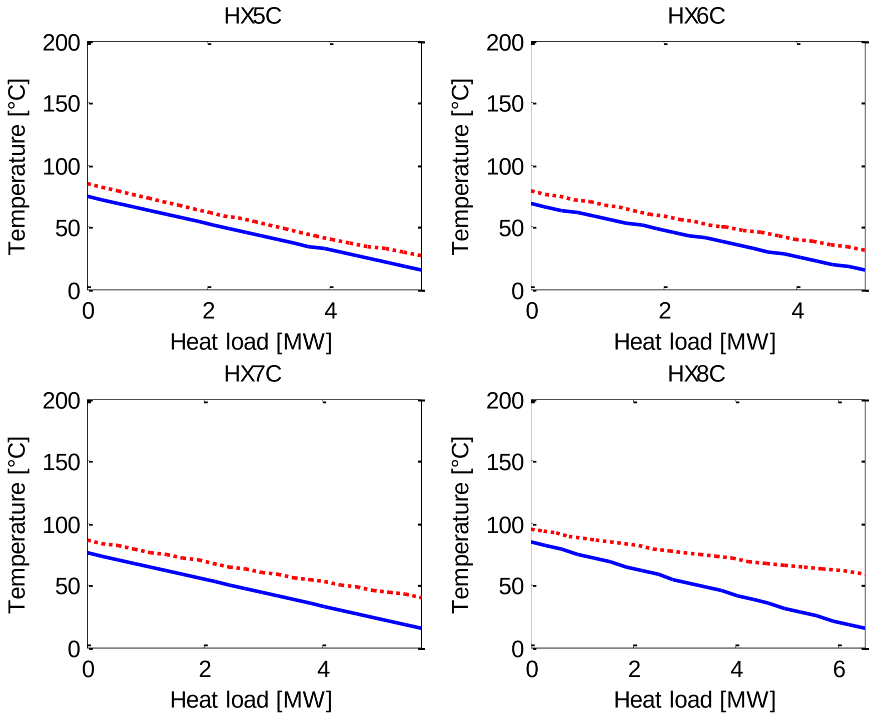

Figure 5.19. The T-Q diagrams of heat exchangers 5-8 in the compression process.

The extra heat exchanger is shown in Figure 5.20.

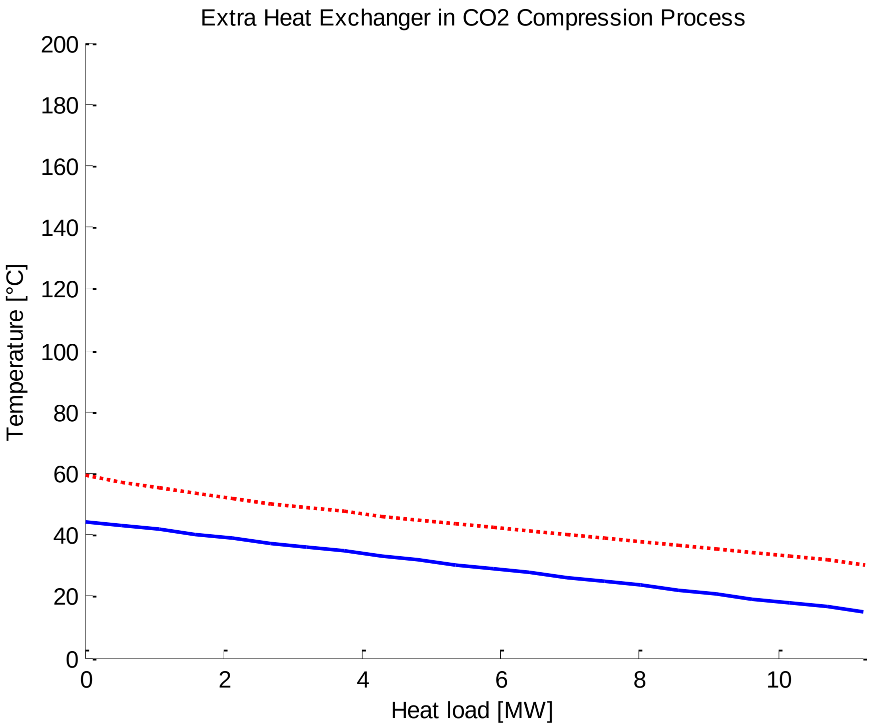

Figure 5.20. T-Q diagram of the extra heat exchanger in the compression process.

The energy requirement of the entire CO_2 compression system was calculated and the results are presented in Table 5.12.

Table 5.12. Required energy of the compression system.

Energy requirement of compression system	
Power requirement [kW]	
Compressor 1	**4970**
Compressor 2	**4678**
Compressor 3	**4555**
Compressor 4	**4337**
Compressor 5	**4037**
Compressor 6	**3760**
Compressor 7	**3506**
Compressor 8	**3098**
Pump	**69**
Total energy	**33 009**
Final CO_2 flow [kmol/h]	**7 444**
Specific energy in compression process [kWh/t CO_2]	**100.6**

The specific energy requirement of the compression process is about 101 kWh/ton CO_2, which is a bit higher than was calculated in section 4.4 where it was determined to 93 kWh/ton CO_2. The reason for the increase is the pressure drop of the stage-arranged intercoolers.

5.5.2 Heat transfer area in compression process

The calculation of the required heat transfer area for the compression system was done in the same way as for the capture system. Flue gas condensation occurred only in the four first heat exchangers in the compression process, which means that two different U-values were used. The results of the area calculations are shown in Table 5.13.

Table 5.13. Required heat transfer area in the compression process.

Area [m^2]	
HX1C	**889**
HX2C	**704**
HX3C	**749**
HX4C	**787**
HX5C	**730**
HX6C	**515**
HX7C	**446**
HX8C	**367**
Extra HX	**967**
Total area	**6 154**

5.6 Combined capture and compression process

The characteristics of the system where the capture and compression processes are combined are shown in Table 5.14.

Table 5.14. Data of the combined capture and compression system.

Entire system for capture and compression of CO_2	
Heat transfer area [m^2]	18 329
Energy consumption [kW]	95 881
Efficiency penalty on power plant [%-points]	7.9
Efficiency of power plant [%]	38.0
Specific energy requirement [kWh/ton CO_2]	292.3
CO_2 separation degree [%]	78.2
CO_2 purity [%]	95.3

The efficiency penalty (7.9%-points) is lower than that of a system with MEA-absorption with the same CO_2 separation degree [40]. In other words, membrane systems can be competitive with MEA-absorption for a separation degree of this magnitude. But a further economic evaluation has to be made.

5.7 Summary

The design of the intercoolers and aftercoolers in the CO_2 capture and compression processes is a complex procedure, in which a number of parameters have an influence. The following results were found in the heat exchanger investigation for the chosen boundary conditions:

- Vacuum pump operation may be advantageous to perform in four stages instead of two, since this makes the conditions of each intercooler and aftercooler similar.
- The heat recovered in the compressors and vacuum pumps is sufficient to heat the recycled flue gas in the expansion process to 95°C.
- In order to reach a temperature of 30°C after the CO_2 compression process, an extra aftercooler is needed.

6 Cost calculations

An economic analysis is necessary for any process development. In addition to high energy efficiency, a beneficial investment cost also plays an important role for a feasible capture technology.

6.1 Heat exchanger cost

The calculation of the heat exchanger cost follows the procedure presented by Kuhn et al [62]. The chosen heat exchanger is as previously mentioned a tube-and-shell heat exchanger made for flue gas condensation processes. The cost per square meter of such a heat exchanger is predicted to be 750 DM/m^2 by the year 2020 [62]. Using a currency conversion rate of 0.51129 €/DM [65], the cost of the heat exchanger could be calculated. The installation cost was calculated as 20% of the area cost, in accordance with [62]. The results of these cost calculations are presented in Table 6.1.

Table 6.1. Cost of the heat exchangers that was used in the capture and compression processes.

Heat exchanger costs [€]	Capture process	Compression process
Area cost	4 918 738	2 371 843
Installation cost	983 748	474 369
Total cost	5 902 485	2 846 212
Total cost of entire system	8 748 697	

In previous work about multi-stage membrane systems, the cost of the heat exchangers have been approximated to 3.5 million € [23]. Obviously, the cost is much higher in this thesis. The influence of this cost on the capture cost is investigated in the following sections.

6.2 Cost of water removing SPEEK-membrane

The water removing membrane that is used in the first step of the capture process was assumed to have a cost of 30 €/m^2. These membranes have been proved to be able to remove 1 kg/(m^{2}h) of water vapour from flue gas [61]. Thus, the area and cost of the SPEEK-membrane was calculated with the equation:

$$Area_{SPEEK} = \frac{Flow\ rate\ [kg/h]}{Removal\ rate\ [kg/(m^2h]} \tag{6.1}$$

$$Cost_{SPEEK} = Area_{SPEEK}\ [m^2] \cdot Area\ cost\ [€/m^2] \tag{6.2}$$

60% of the water vapour in the flue gas was removed in the investigated capture system. This corresponds to a flow rate of 90 682 kg/h. Hence, an area of 90 682 m^2 was needed, which results in a cost of 2 720 465 €.

6.3 Capture cost

The calculations of the capture costs for the combined capture and compression process were performed with a similar simulation method as has been used in previous studies for the same reference plant [23], [43].

When the capture cost of a CCS-system is calculated the following cost factors should be taken into account: capital cost, energy cost, and operation & maintenance cost. The equations used for the cost calculations are shown in Table 6.2.

Assumptions regarding cost and process parameters are shown in Table 6.3. The depreciation time of membrane module, compressor, vacuum pump, expander and heat exchangers is 35 years. The lifetime of the membrane is 3 years and the interest rate is 7.5% [66].

The operation & maintenance (O&M) cost of the membrane and membrane frame is assumed to be 1% of their capital cost, and for the heat exchangers, compressor, vacuum pump and expander it is assumed to be 3.6% of their capital cost [43].

The compressor cost consists of two parts: one for the capture process and one for the compression process. The vacuum pump is assumed to cost four times as much as the compressor used in the capture process.

Another factor that can be taken into account is the European Union Emission Trading System (EU ETS) cost of CO_2 emission permits. When a CCS system is introduced, it means that less carbon dioxide is emitted to the atmosphere, which in turn means that less finances has to be spent on buying CO_2 permits. The current cost of these permits is 12.22 €/ton CO_2 [67]. In 2020 the cost is expected to have increased to about 30 €/ton CO2 [68]. The capture cost has been calculated both with this cost included and excluded.

The conventional way of capturing CO_2, with mono-ethanolamine, has a capture cost (the cost of CO_2 permits excluded) in the range of 30-38 €/ton CO_2 [69].

Table 6.2. Calculations used to determine CO_2 capture cost.

Investments		
$I_m = A \cdot K_m$	(6.3)	Membrane cost
$I_{mf} = (\frac{A}{2000})^{0.7} \cdot K_{mf}$	(6.4)	Permanent membrane frame cost
$I_c = K_{c1} \cdot F_h + K_{c2} \cdot F_h$	(6.5)	Compressor cost
$I_{vp} = K_{vp} \cdot F_h$	(6.6)	Vacuum pump cost
$I_{ex} = P_{ex} \cdot K_{ex} \cdot F_h$	(6.7)	Expander cost
$I_{he} = C_{he}$	(6.8)	Heat exchangers and cooling facilities
Energy consumption of compression equipment		
$P_{tot} = \sum P_c + \sum P_{vp} + \sum P_{ex} + \sum P_{pump}$	(6.9)	Total energy consumption
Annual costs		
$C_{cap} = \left(\sum I_c + \sum I_{vp} + \sum I_{ex} + \sum I_{he}\right) \cdot a + I_m \cdot a_m$	(6.10)	Capital cost
$C_{O\&M} = 0.036 \cdot \left(\sum I_c + \sum I_{vp} + \sum I_{ex} + \sum I_{he}\right) + 0.01 \cdot (I_m \cdot I_{mf})$	(6.11)	O&M
$C_{en} = t_{op} \cdot P_{tot} \cdot K_{el}$	(6.12)	Energy cost per year
$C_{tot} = C_{cap} \cdot C_{en} \cdot C_{O\&M}$	(6.13)	Total cost
Specific CO_2 separation cost		
$\dot{C}_{CO_2} = \frac{C_{tot}}{M_{CO_2,separated\ annually}}$	(6.14)	

Table 6.3. Assumptions for cost and process parameters [23], [43].

Parameter	Value	Unit	Parameter	Value	Unit
K_m	50	€/m^2	K_{mf}	0.25	Million €
K_{c1}	3	Million €	K_{ex}	0.3	€/watt
K_{c2}	30	Million €	K_{vp}	$4K_{c1}$	Million €
C_{he}	3.5	Million €	F_h	1.8	-
a	0.081	-	a_m	0.385	-
t_{op}	8000	h	K_{el}	4.335	Cent/kWh

When these equations were calculated the results shown in Table 6.4 were obtained. The costs of the reference power plant were calculated with basic data of the plant [57].

Table 6.4.Capture costs for the investigated system.

Cost	Unit	CCS
Net power	MW	459
Efficiency	%	38.0
Costs		Additional costs with CCS
Capital cost	Million €/yr	59.00
Membrane	Million €	125.22
Membrane frame cost	Million €	39.89
Compressor	Million €	21.6
Vacuum pump	Million €	59.4
Expander	Million €	3.83
Heat exchanger	Million €	8.43
O&M cost	Million €/yr	5.01
Energy cost	Million €/yr	33.40
		Value
Emitted CO_2	Ton CO_2	730 646
Captured CO_2	Ton CO_2	2 620 210
Emission cost	Million €/yr	21.87
Savings	Million €/yr	78.43
		Additional costs
Total cost	Million €/yr	97.42
Specific CO_2 capture cost	[€/ton CO_2]	37.18

The calculated value of the specific CO_2 capture cost is in the same order of magnitude as what have been calculated for membrane systems elsewhere [59]. In a study by Zhao et al. [59] the specific capture cost was calculated to 31 €/ton CO_2 with no CO_2 costs included. The higher value in this thesis is due to higher energy costs and equipment cost to remove the water content in the flue gas, a shorter lifetime of the CO_2 separation membranes and an increased fuel cost. The cost of the heat exchangers are more than doubled compared to what have been used in other work ([23], [43], [59]), but since the major cost factors is the membrane cost, the heat exchangers have a minor influence on the total costs.

The extra capture cost of the membrane system is in the same range as CO_2 separation with MEA-absorption [69]. It should however be noted that the costs for MEA-absorption were calculated for a system that had a higher separation degree than this membrane system has (78%).

6.4 Avoidance cost

The efficiency penalty that is imposed to the power plant when CCS is introduced makes it necessary to add more fuel to the plant in order to produce the same amount of energy as before the CCS introduction. As mentioned in the introduction, section 0, the cost of interest is therefore the CO_2 avoidance cost.

The avoidance cost for plants with MEA-absorption is in the range 33-75 €/ton CO_2 [70].

6.4.1 Avoidance cost equations

The energy needed to operate a reference non-CCS power plant that produces a certain energy output E_{out} and has an efficiency η_{ref} can be calculated as follows:

$$E_{in_{ref}} = \frac{E_{out}}{\eta_{ref}} \tag{6.15}$$

The energy needed to operate a plant with the same energy output but with CCS installed is calculated in the same way.

$$E_{in\_CCS} = \frac{E_{out}}{\eta_{CCS}} \tag{6.16}$$

The amount of CO_2 produced by a reference power plant depends on the energy input and the carbon content of the fuel (in grams of carbon per MJ).

$$Produced\ CO_{2_{ref}} = E_{in_{ref}} \cdot Carbon\ content \cdot \frac{M_{CO_2}}{M_C} \tag{6.17}$$

The last term is a conversion factor that converts the carbon content to CO_2 emissions. The amount of produced CO_2 in a CCS power plant is determined correspondingly.

$$Produced\ CO_{2_{CCS}} = E_{in.CCS} \cdot Carbon\ content \cdot \frac{M_{CO_2}}{M_C} \tag{6.18}$$

It is important that as much of the CO_2 in the flue gas as possible is extracted, so that the degree of separation is as high as possible. This parameter must also be determined considering the extra production of CO_2. The Capture separation rate is the degree of separation without considering that extra energy is needed to operate the plant. It can be expressed in the form:

$$Capture\ Separation\ Rate = \frac{Captured\ CO_2}{Produced\ CO_{2_{CCS}}} \tag{6.19}$$

The amount of CO_2 that is captured in a CCS plant can thus be calculated as follows:

$$Captured\ CO_2 = Produced\ CO_{2_{CCS}} \cdot Capture\ Separation\ Rate \tag{6.20}$$

The amount of avoided CO_2 can then be calculated.

$$Avoided\ CO_2 = Produced\ CO_{2_{ref}} - (Produced\ CO_{2_{CCS}} - Captured\ CO_2) \tag{6.21}$$

The avoidance rate (the degree of separation considering the extra energy requirements) can now be calculated as follows.

$$Avoidance\ rate = \frac{Avoided\ CO_2}{Produced\ CO_{2_{ref}}} \tag{6.22}$$

This expression can be treated to a more practical form in the following way.

$$Avoidance\ rate = \frac{Avoided\ CO_2}{Produced\ CO_{2_{ref}}} = \frac{Produced\ CO_{2_{ref}} - (Produced\ CO_{2_{CCS}} - Captured\ CO_2)}{Produced\ CO_{2_{ref}}}$$

$$= 1 + \frac{Captured\ CO_2 - Produced\ CO_{2_{CCS}}}{Produced\ CO_{2_{ref}}} =$$

$$= 1 + \frac{Produced\ CO_{2_{CCS}} \cdot Capture\ Separation\ Rate - Produced\ CO_{2_{CCS}}}{Produced\ CO_{2_{ref}}} =$$

$$= 1 + \frac{E_{in.CCS} \cdot Carbon\ content \cdot \frac{M_{CO_2}}{M_C} \cdot Capture\ Separation\ Rate - E_{in.CCS} \cdot Carbon\ content \cdot \frac{M_{CO_2}}{M_C}}{E_{in_{ref}} \cdot Carbon\ content \cdot \frac{M_{CO_2}}{M_C}}$$

$$= 1 + \frac{\frac{1}{\eta_{CCS}} \cdot Capture\ Separation\ Rate - \frac{1}{\eta_{CCS}}}{\frac{1}{\eta_{ref}}} = 1 + \frac{\frac{1}{\eta_{CCS}}(Capture\ Separation\ Rate - 1)}{\frac{1}{\eta_{ref}}}$$

$$\Rightarrow Avoidance\ rate = \frac{\eta_{ref}}{\eta_{CCS}}(Capture\ Separation\ Rate - 1) + 1 \tag{6.23}$$

Equation (6.23) is useful when the impact on the efficiency and the capture separation rate is known. The specific avoidance cost can, in accordance with Andersson et al.[71], be calculated with the following equation:

$$Avoidance\ cost\ \left[\frac{Cost}{tonne\ CO_2}\right] = \frac{\left(\frac{Cost}{MWh}\right)_{ref} - \left(\frac{Cost}{MWh}\right)_{CCS}}{\left(\frac{tonne\ CO_2}{MWh}\right)_{CCS} - \left(\frac{tonne\ CO_2}{MWh}\right)_{ref}} \tag{6.24}$$

The goal of this thesis is to take the avoidance cost aspect into account in order to make a valid assessment.

6.4.2 Avoidance cost calculations

From previous simulations the capture separation rate was found to be 0.7821 and the efficiency of the CCS plant was calculated to 38.0%. With these values and the efficiency of the reference power plant (45.9%), the avoidance rate was determined using Equation (6.23). The result was 0.736.

In order to determine the avoidance cost, a CCS plant that produces as much energy as the reference plant shall be considered. The efficiency loss caused by the introduction of CCS increases the capital costs of membrane, membrane frame, expanders and heat exchangers. Thus, the O&M costs increase as well. The fuel demand for a CCS power plant is also higher than for the reference plant. The capital costs and the fuel costs increase by the ratio between the reference power plant net output and the CCS plant net output (555/459).

The costs associated with the avoidance calculations are shown in Table 6.5. Fuel is assumed to cost 72.8 €/ton coal [66].

Table 6.5. A comparison between the annual costs of the reference plant and the avoidance costs of the CCS plant.

Cost	Unit	CCS-plant
Net power	MW	555
Efficiency	%	38.0
Fuel input	Ton coal	1 611 782
Costs		Additional costs
Capital cost	Million €/yr	69.94
Membrane	Million €/yr	151.37
Membrane frame cost	Million €/yr	48.22
Compressor	Million €/yr	21.60
Vacuum pump	Million €/yr	59.40
Expander	Million €/yr	4.63
Heat exchanger	Million €/yr	10.20
O&M cost	Million €/yr	5.45
Additional energy cost	Million €/yr	33.40
Fuel cost	Million €/yr	20.73
		Value
Emitted CO_2	Ton CO_2	883 039
Captured CO_2	Ton CO_2	3 167 600
Avoided CO_2	Ton CO_2	2 467 821
Emission cost	Million €/yr	26.43
Savings	Million €/yr	73.87
		Additional costs
Total cost	Million €/yr	129.52
Specific CO_2 avoidance cost	[€/ton CO_2 avoided]	52.48

The specific CO_2 avoidance cost is about 52.5 €/ton CO_2. The average CO_2 avoidance cost for coal fired CCS plants in the OECD countries is about 36 €/ton CO_2 [72]. For post combustion systems the average cost is about 40 €/ton CO_2 [72]. A comparison between the specific capture cost and the specific avoidance cost for the membrane system is shown in Table 6.6.

Table 6.6. Comparison between capture and avoidance costs.

	Capture cost	Avoidance cost
Specific cost [€/ton CO_2]	37.18	52.48

It is clear that the avoidance cost is significantly higher than the capture cost. Therefore, cost calculations shall be made according to the avoidance cost concept so that unrealistically low values are not presented.

6.5 Cost of electricity

A detailed comparison between different cases was performed. The cost of electricity was calculated for the reference power plant and for the plant with CCS based on both capture and avoidance costs. The results are shown in Table 6.7. The costs of the reference power plant were taken from the MEM-BRAIN progress report 2011 [66].

The reference power plant costs were, in the avoidance calculations, multiplied with the factor $(P_{net_{ref}}/P_{net_{CCS}})$ in order to keep the CCS power plant constant with 555 MW net power output. The increase in wages, insurance and operating materials was calculated with a factor that was calculated as the ratio between the O&M costs of the reference power plant and the O&M costs of the power plant with CCS.

Table 6.7. Comparison of the electricity costs between the different cases.

	Units	Ref. PP	Capture	Avoidance
Net power	MW	**555**	**459**	**555**
Net efficiency	%	**45.9**	**38.0**	**38.0**
Fixed costs	*€/MWh*	***19.15***	***37.63***	***41.08***
Capital cost	*€/MWh*	***14.09***	*14.09+16.06 =* ***30.15***	*17.03+15.75 =* ***32.79***
Plant maintenance	*€/MWh*	***2.85***	*2.85+0 =* ***2.85***	*3.45+0 =* ***3.45***
Membrane plant maintenance	*€/MWh*	**-**	***1.36***	***1.23***
Wages	*€/MWh*	***1.41***	*1.41+0.67 =* ***2.08***	*1.70+0.61 =* ***2.31***
Insurance, overheads	*€/MWh*	***0.80***	*0.80+0.38 =* ***1.18***	*0.97+0.34 =* ***1.31***
Variable costs	*€/MWh*	***24.40***	***25.38***	***30.37***
Coal	*€/MWh*	***22.36***	*22.36+0 =* ***22.36***	*22.36*555/459 =* ***27.03***
Operating materials etc	*€/MWh*	***2.04***	*2.04+0.98 =* ***3.02***	*2.47+0.88 =* ***3.34***
COE	€/MWh	**43.55**	**63.01**	**71.45**
“COC” (cost of certificates)	€/MWh	**22.59**	**5.95**	**5.95**
COE + “COC”	€/MWh	**66.14**	**68.96**	**77.41**

It can be seen that under the above mentioned boundary conditions, the membrane CCS power plant is still not economically attractive.

6.6 Parametric investigation

An investigation was made to see how high the price on CO_2 emission permits must be in order to make the CCS-plant more economically feasible than the reference power plant. The result is shown in Figure 6.1, which shows the electricity costs for the reference power plant and for the CCS plant based on capture and avoidance cost simulations.

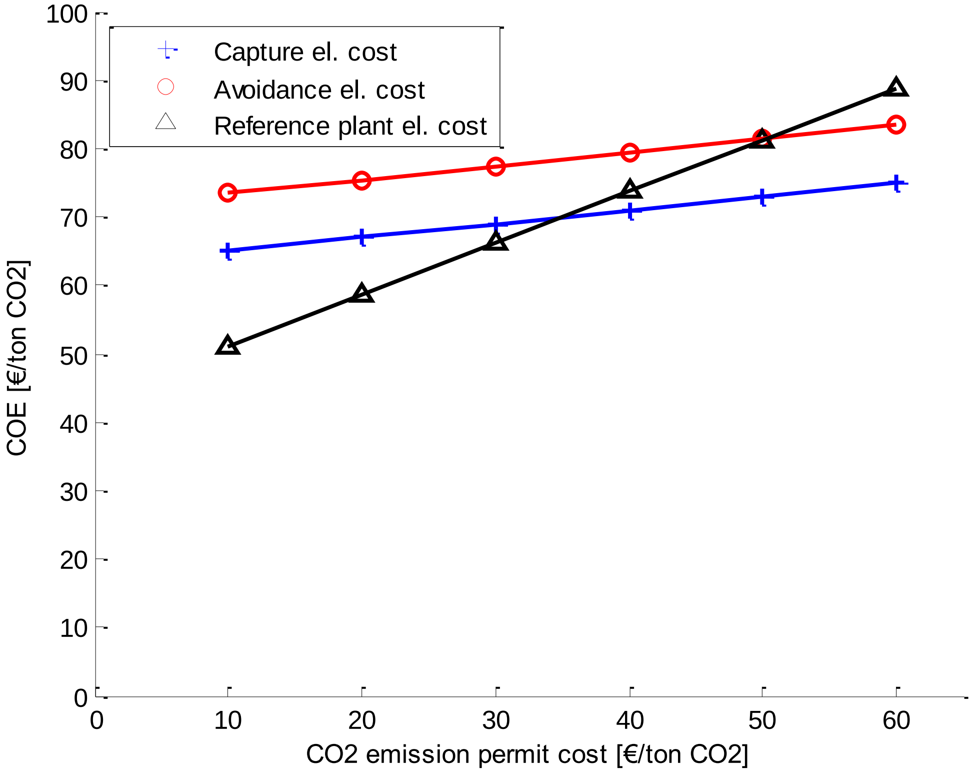

Figure 6.1. Impact of CO_2 emission permit cost on electricity costs.

The graph shows that the price on CO_2 emission permits must be higher than about 50 €/ton CO_2 in order for the CCS plant to be more economically feasible than the reference power plant according to avoidance calculations. If the capture cost is considered, the CO_2 would only need to be about 35 €/ton CO_2.

The effects of a higher membrane life time were also investigated, since this can give an idea about which direction the development of membrane materials shall take. The previous calculations in this thesis have been based on a membrane life time of three years. A possible future scenario is a lifetime of 5 years. The effects of such an increase are shown in Table 6.8.

Table 6.8. Effects of increased membrane lifetime on cost of electricity.

Membrane lifetime [years]	COE Ref. plant [€/MWh]	COE capture [€/MWh]	COE avoidance [€/MWh]
3	**66.14**	**68.96**	**77.41**
5	**66.14**	**64.28**	**72.72**

According to the table, a longer membrane life time makes membrane CO_2 capture more attractive. An increase to 5 years has a considerable impact. However, it is not enough to decrease the electricity cost of the avoidance case enough to make it competitive with that of the reference power plant.

A test was also carried out in order to investigate the economical consequences of an improved CO_2 permeance of the membranes, which is increased from 3 to 6 or 10 $Nm^3/m^2 \cdot h \cdot bar$. An increase in CO_2 permeance results in that less membrane area is needed to achieve the same CO_2 separation degree. The cost of electricity is shown in Figure 6.2.

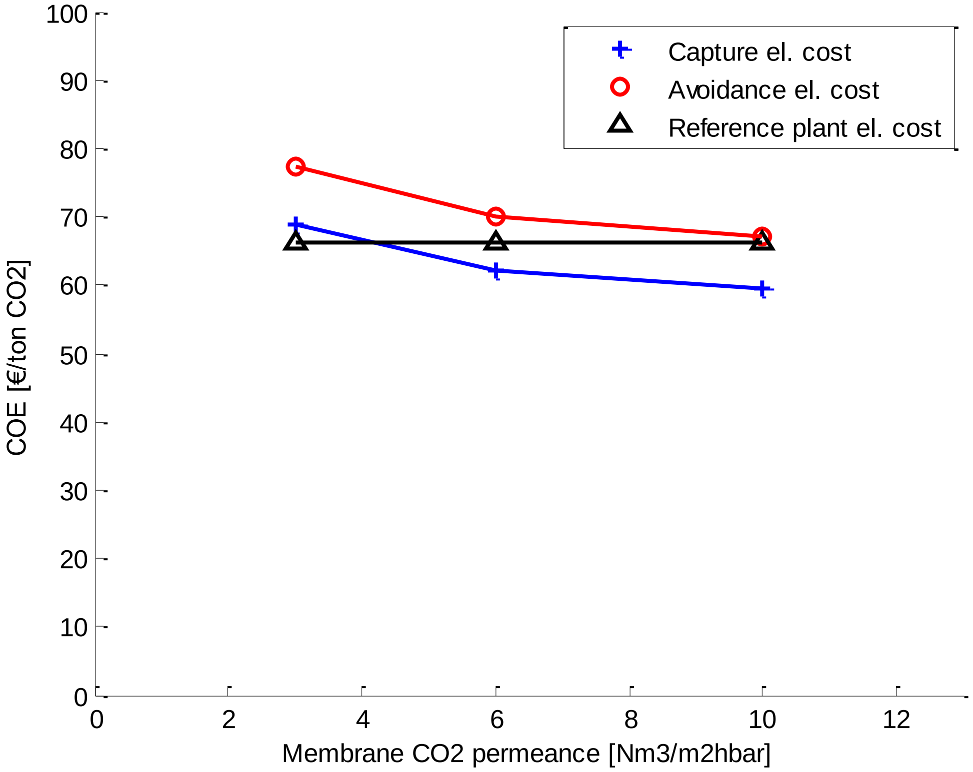

Figure 6.2. Effect on cost of electricity by increasing co_2 permeance.

The results show that if membranes with higher CO_2 permeance can be developed it will result in significantly lower electricity costs. More research of membrane materials could therefore be important in order to make membrane CO_2 capture more beneficial.

The price of the membrane material has in this thesis been assumed to be 50 €/m^2. If this cost could be reduced to 30 €/m^2, the costs cost of electricity would be decreased according to Table 6.9.

Table 6.9. Effect on cost of electricity by a cheaper membrane price.

Membrane cost [€/m^2]	COE Ref. plant [€/MWh]	COE capture [€/MWh]	COE avoidance [€/MWh]
50	**66.14**	**68.96**	**77.41**
30	**66.14**	**63.77**	**71.87**

Since the membranes in the system represent the largest share of the total costs, a reduced membrane price has a significant impact on the cost of electricity. Well performing membranes with less expensive materials could therefore be an important way to decrease the total cost of the system.

Finally, the combined effects of a higher membrane lifetime (5 years), higher membrane CO_2 permeance (10 $Nm^3/m^2 \cdot h \cdot bar$) and lower membrane cost (30 €/m^2) were investigated. The results are shown in Table 6.10.

Table 6.10. Effects of higher membrane CO_2 permeance, longer membrane lifetime and lower membrane price on COE.

	COE Ref. plant [€/MWh]	COE capture [€/MWh]	COE avoidance [€/MWh]
Base case	**66.14**	**68.96**	**77.41**
Improved membrane lifetime, permeance and cost	**66.14**	**56.13**	**64.57**

It can be concluded that membrane CO_2 capture can be profitable if the properties of the membrane material are improved.

The specific CO_2 avoidance cost, calculated by Equation (6.24), is affected by membrane development according to Figure 6.3.

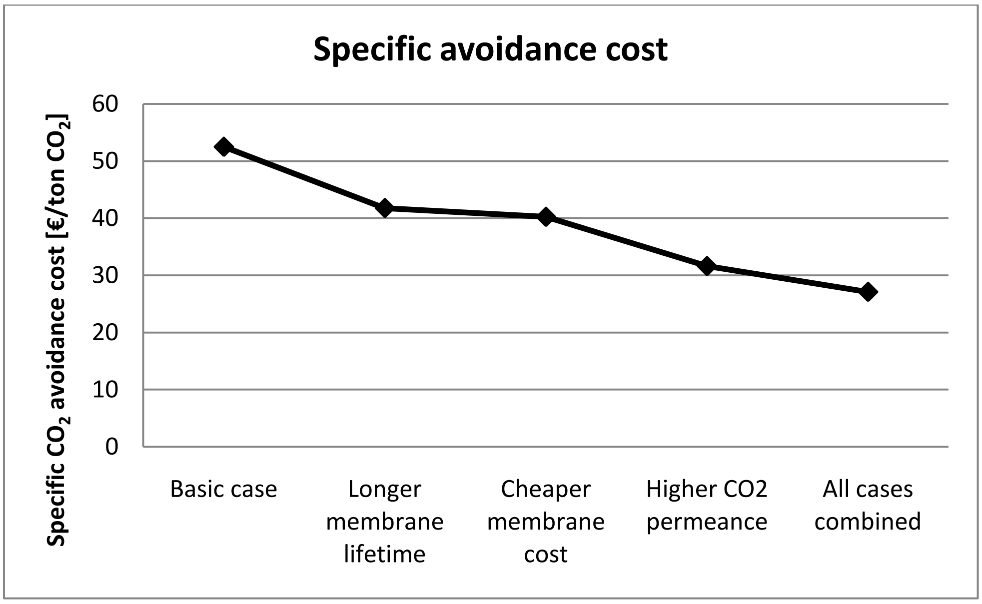

Figure 6.3. Effects on specific CO_2 avoidance cost by membrane improvements.

6.7 Summary

The following conclusions can be drawn from the economical investigation:

- The specific CO_2 capture cost of the chosen membrane system is about 37 €/ton CO_2, which is in the same range as for MEA-absorption systems.
- The heat exchanger cost has only a minor influence on the total costs of membrane systems.
- The CO_2 avoidance cost is about 52 €/ton CO_2, which is higher than the average avoidance cost of post combustion systems.
- According to the calculated costs of electricity for the reference power plant and for the plant with membrane CO_2 capture, membrane systems are not economically advantageous at current level of development.
- By increased effort and research in giving membrane materials longer lifetime, higher CO_2 permeance and lower manufacturing costs, membrane cascade systems can be made less more economically attractive.

7 Discussion and conclusions

This thesis focuses on the investigation of the performance of multi-stage membrane systems for CO_2 capture in post combustion systems. With a realistic composition for the flue gas, the energy consumption and the capture and avoidance costs were studied. Extra attention was paid to the design of the heat exchangers in the system, in order to be able to make an assessment of their influence on the system performance and design.

The results show that the membrane cascade systems consume more energy for real flue gas simulations than for ideal gas systems. In addition, the water content of real flue gas makes it necessary with additional components in the CCS system, in form of water removal units.

The energy demand is decreased accordingly if more water is removed before the CO_2 capture system. Energetically efficient flue gas dehydration at this point is thus of great importance in order to avoid large efficiency penalties for the power plant.

The heat that is recovered by the intercoolers in the vacuum pump and compressor units is sufficient to heat the flue gas in the expansion sequence.

A positive effect of the water content in the flue gas is that the degree of CO_2 separation is increased owing to the sweep gas effect of water.

The design of the heat exchangers in membrane systems is a complex procedure, since the water in the flue gas condenses out during the compression process. In this thesis each heat exchanger was designed to operate with the same cooling water flow rates and hot inlet-cold outlet temperature difference to make the system more practical. The problem with this strategy is that each heat exchanger work under different conditions on the hot stream side concerning temperature, flow rate and water content. It was found that it was less difficult to reach a low temperature of the flue gas going to the second membrane if the vacuum pump operation is performed in four stages instead of two. This increases the energy consumption of the system, because of the pressure drop in the staged heat exchangers, which increases the vacuum pump work.

The cost of heat exchangers was investigated to be more than doubled the amount of the values used in previous studies. However, these costs are small compared to the membrane costs, which makes the increase insignificant.

The extra capture cost for the investigated system was calculated to 37.2 €/ton CO_2. Compared to previous studies (31 €/ton CO_2), the value in this thesis is a bit higher, which is an expected result since the water content in the flue gas increases the energy consumption and there are different boundary conditions.

The avoidance cost is 52.5 €/ton CO_2, which is a bit higher than the average CO_2 avoidance cost for post combustion systems, but the difference is not large.

The cost of electricity of the system shows that the CCS plant is not economically feasible since the electricity is more expensive when CCS is installed, even though less funds needs to be put into paying emission permits. If the EU Emissions Trading System raises the price significantly, it could get feasible. Membrane systems can also be made more attractive if membrane materials with longer lifetimes, higher CO_2 permeance and cheaper manufacturing price can be developed.

Multi-stage membrane systems can reach high enough purities at a cost that is in similarity with competing technologies.

8 Recommendations

The following recommendations are made for future studies:

- Simulations of CCS-systems shall be carried out with as real composition of the flue gas as possible, in order to achieve valid results.
- As much water as possible shall be removed before the flue gas reaches the membrane, in order to minimize the energy consumption of the system.
- The intercoolers in the membrane systems shall be modelled and designed in detail. The total cost is not affected much by this, but it provides guidance for a feasible system design.
- The vacuum pump operation shall be performed in four stages instead of two. This is disadvantageous for the energy consumption, but necessary if the intercoolers shall have the same design.
- Membrane material with higher CO_2 permeance, longer lifetimes and cheaper manufacturing price shall be investigated and developed.
- A future investigation should be performed for the cases of 50% and 90% degree of CO_2 separation. The heat exchanger design should be done separately for each case.
- Integration of the exhausted heat from the CO_2 capture and compression processes to the water-steam cycle of the power plant should be investigated to improve the power plant efficiency.

More research and development will have to show the true potential of membrane technology in CCS systems. The results of this thesis show that it at least is one of the promising candidates for effective and inexpensive capture of carbon dioxide. The future will have to tell how large part it has to play in the struggle against climate change.

9 References

1. **IPCC.** *Climate Change 2007: Synthesis Report.* Geneva, Switzerland : s.n., 2007.

2. **CO2.org.** *CO2Now.org.* [Online] 8 Mars 2011. [Cited: 17 Mars 2011.] co2now.org.

3. **Carlson, Ola.** *Energy overview and wind power.* Göteborg, Sweden : Division of Electric Power Engineering, Department of Energy and Environment, Chalmers University of Technology, 30 August 2010. Presentation in the course Sustainable Power Production and Presentation.

4. **Rodhe, Henning.** A Comparison of the Contribution of Various Gases to the Greenhouse Effect. *Science.* 8, 1990, Vol. 248, pp. 1217-1219.

5. **Davison, John and Thambimuthu, Kelly.** *Technologies for Capture of Carbon Dioxide.*

6. **International Energy Agency.** Key World Energy Statistics. *International Energy Agency.* [Online] October 2010. [Cited: 1 April 2011.] http://www.iea.org/textbase/nppdf/free/2010/key_stats_2010.pdf.

7. **International Energy Agency IEA.** *World Energy Outlook 2010.* 2010.

8. **German Advisory Council on Global Change.** *New Impetus for Climate Policy: Making the Most of Germany's Dual Presidency.* Berlin : s.n., 2007. ISBN 978-3-936191-16-6.

9. **European Council.** Climate Change: Medium and longer term emission reduction strategies, including targets Council conclusions. *Consilium - Council of the European Union.* [Online] 11 Mars 2005. [Cited: 23 Mars 2011.] register.consilium.europa.eu/pdf/en/05/st07/st07242.en05.pdf. Document Number 7242/05.

10. **Nässén, Jonas.** *Kärnkraft.* Göteborg, Sweden : Division of Physical Resource Theory, Department of Energy and Environment, Chalmers University of Technology, October 2008. Presentation in the course Miljö- och energiteknik.

11. **IPCC.** *IPCC Special Report on Carbon Capture and Storage.* s.l. : Cambrigde University Press, 2005.

12. **International Energy Agency.** *CO2 capture ready plants.* 2007.

13. **Conturie, Michel.** *Reduction of Carbon Dioxide Emissions by Capture and Re-Injection.* Vrnjacka Banja, Serbia : Renewable Energy Sources and Environment, 17-24 October 2006.

14. **Favre, E.** Membrane processes and postcombustion carbon dioxide capture: Challenges and prospects. *Chem. Eng. J.* 2011.

15. **Gibbins, Jon and Chalmers, Hannah.** Carbon capture and storage. *Energy Policy.* 2008, Vol. 36, pp. 4317–4322.

16. **IEA.** *Energy Technology Essentials - CO2 Capture & Storage.* s.l. : OECD/IEA, December 2006.

17. **Blomen, Eliane, Hendriks, Chris and Neele, Filip.** Capture technologies: Improvements and Promising Developments. *Energy Procedia.* 2009, Vol. 1, pp. 1505–1512.

18. **Bellona.** Pre combustion. *Bellona CCS web.* [Online] [Cited: 23 August 2011.] http://www.bellona.org/ccs/Artikler/pre_combustion.

19. **Toftegaard, Maja B., et al.** Oxy-fuel combustion of solid fuels. *Progress in Energy and Combustion Science.* 2010, Vol. 36, pp. 581-625.

20. **Bellona.** Oxyfuel. *Bellona CCS web.* [Online] [Cited: 23 August 2011.] http://www.bellona.org/ccs/Artikler/oxyfuel.

21. **Kanniche, Mohamed, et al.** Pre-combustion, post-combustion and oxy-combustion in thermal power plant for CO2 capture. *Applied Thermal Engineering.* 2010, Vol. 30, pp. 53–62.

22. **Merkel, Tim C., et al.** Power plant post-combustion carbon dioxide capture: An opportunity for membranes. *Journal of Membrane Science.* 2010, Vol. 359, pp. 126–139.

23. **Zhao, Li, et al.** Multi-stage gas separation membrane processes used in post-combustion capture: Energetic and economic analyses. *Journal of Membrane Science.* 2010, Vol. 359, pp. 160–172.

24. **Bellona.** Post combustion. *Bellona CCS web.* [Online] [Cited: 23 August 2011.] http://www.bellona.org/ccs/Artikler/post_combustion.

25. **Riensche, Ernst, et al.** *Capture Option for Coal Power Plants.* Jülich : Wiley.

26. **Andesson, Klas.** *New Combustion Technologies with CO2 Separation.* Göteborg, Sweden : Division of Energy Technology, Department of Energy and Environment, Chalmers University of Technology, 6 October 2010. Presentation in the course Combustion Engineering.

27. **Bounaceur, Roda, et al.** Membrane processes for post-combustion carbon dioxide capture: A parametric study. *Energy.* 2006, Vol. 31, pp. 2556–2570.

28. **Keskes, Emmanuel, et al.** A Physical Absorption Process for the Capture of CO2 from CO2-enriched Natural Gas Streams. *UK Carbon Capture and Storage Community.* [Online] [Cited: 9 Mars 2011.] www.geos.ed.ac.uk/ccs/Publications/Keskes.pdf.

29. **Thiruvenkatachari, Ramesh, et al.** Post combustion CO2 capture by carbon fibre monolithic adsorbents. *Progress in Energy and Combustion Science.* 2009, Vol. 35, pp. 438–455.

30. **Hart, Allan and Gnanendran, Nimalan.** Cryogenic CO2 Capture in Natural Gas. *Energy Procedia.* 2009, Vol. 1, pp. 697–706.

31. *Cryogenic CO2 Capture to Control Climate Change Emissions.* **Baxter, L. L., P., Baxter A. and S., Burt S.** Clearwater, Florida, USA : s.n., 2009. in Coal: World Energy Security - The Clearwater Clean Coal Conference - The 34th International Technical Conference on Clean Coal & Fuel Systems.

32. **Blamey, J, et al.** The calcium looping cycle for large-scale CO2 capture. *Progress in Energy and Combustion Science.* 2010, 35, pp. 260–279.

33. **Nguyen, Tuong-Van.** *System Analysis of Chemical and Carbonate Looping Processes in IGCC Power Plants for CO2 separation.* Division of Energy Technology, Department of Energy and Environment, Chalmers University of Technology. 2011. Master's Thesis.

34. **Kim, Young-Seok and Yang, Seung-Man.** Absorption of carbon dioxide through hollow fiber membranes using various aqueous absorbents. *Separation and Purification Technology.* 2000, Vol. 21, pp. 101–109.

35. **Powell, Clem E. and Qiao, Greg G.** Polymeric CO2/N2 gas separation membranes for the capture of carbon dioxide from power plant flue gases. *Journal of Membrane Science.* August 2006, Vol. 279, 1-2, pp. 1-49.

36. **Zhao, Li, et al.** A parametric study of CO2/N2 gas separation membrane processes for post-combustion capture. *Journal of Membrane Science.* 2008, Vol. 325, pp. 284–294.

37. **Hussain, Arshad and Hägg, May-Britt.** A feasibility study of CO2 capture from flue gas by a facilitated transport membrane. *Journal of Membrane Science.* September 1, 2010, Vol. 359, 1-2, pp. 140-148.

38. **Lee, Hong-Joo, Suda, Hiroyuki and Haraya, Kenji.** Gas Permeation Properties in a Composite Mesoporous Alumina Ceramic Membrane. *Korean Journal of Chemical Engineering.* 2005, Vol. 22, pp. 721-728.

39. **Kloeppel, James E.** Synthetic molecular sieve binds water better than zeolites. *Xiinyuan Molecular Sieve.* [Online] Xinyuan Technology Co. Ltd. [Cited: 31 Mars 2011.] http://www.molecularsieve.org/Synthetic_molecular_sieve_binds_water_better_than_zeolites.htm.

40. **Casale, Dominico.** *Developing a multi-stage membrane system for CO2 separation in post-combustion processes.* Facoltà di Ingegneria, Università dell’Aquila, L'Aquila, and Institute of Energy and Climate Research, Fuel Cells (IEK-3), Forschungszentrum Jülich, Germany. 2011. Master Thesis.

41. **Brunetti, A, et al.** Membrane technologies for CO2 separation. *Journal of Membrane Science.* 2010, 359, pp. 115–125.

42. **Freeman, Benny D.** Basis of Permeability/Selectivity Tradeoff Relations in Polymeric Gas Separation Membranes. *Macromolecules.* 1999, Vol. 32, pp. 375-380.

43. **Van der Sluijs, J.P., Hendriks, C.A. and Blok, K.** Feasibilty of Polymer Membranes for Carbon Dioxide Recovery from Flue Gases. *Energy Conv.* 1992, Vol. 33, pp. 429-436.

44. **Bloch, Heinz P. and Budris, Allan R.** *Pump User's Handbook: Life Extension.* s.l. : Fairmont Press, 2010. ISBN-10: 1439837406.

45. **Boge Compressed Air Systems.** Product Range. *Boge Compressed Air Systems.* [Online] [Cited: 30 Mars 2011.] http://www.boge.com/ae/artikel/download/Brochure305_EN_Controls.pdf. 305-GB-3.5-05.2009/T.

46. **Javed, Saqib.** *Refrigeration and Heat Pump Hardware.* Göteborg, Sweden : Division of Building Services Engineering, Department of Energy and Environment, Chalmers University of Technology, 30 November 2010. Presentation in the course Air-conditioning, refrigeration and heat pump technology.

47. **Bloch, Heinz P.** *A Practical Guide to Compressor Technology.* 2nd Edition. Wes Des Moines : John Wiley & Sons Inc., 2006. ISBN-13: 978-0-471-72793-4.

48. **Silla, Harry.** *Chemical Process Engineering - Design and Economics.* Stevens Institute of Technology. Hoboken, New Jersey, U.S.A. : Markel Dekker Inc., 2003. ISBN 978-0-203-91245-4.

49. **Gresh, Theodore.** *Compressor performance: Aeodynamics for the user.* 2nd Edition. s.l. : Butterworth-Heinemann, 2001. ISBN 0 7506 7372 7.

50. **Pfeiffer Vacuum.** Classification of Vacuum Pumps. *Pfeiffer Vacuum.* [Online] Pfeiffer Vacuum GmbH. [Cited: April 28, 2011.] http://www.pfeiffer-vacuum.com/know-how/vacuum-generation/pump-principles-and-vacuum-pump-performance-data/classification-of-vacuum-pumps/technology.action?chapter=tec2.1.1.

51. **Holm, Jim.** Classification of Heat Exchangers. *Taking a big bite out of Global Warming . . . NOW !* [Online] [Cited: 29 April 2011.] http://www.coal2nuclear.com/Heat%20Exchangers%20-%20Classification%20of%20Heat%20Exchangers%20-%200471321710.pdf.

52. **Sinnott, R. K., Coulson, John Metcalfe and Richardson, John Francis.** *Chemical Engineering Design (Coulson and Richardson's Chemical Engineering Series).* Fourth Edition. s.l. : Elsevier Butterworth-Heinemann, 2005. Vol. 6. ISBN 0 7506 6538 6.

53. **Bartlet, Dean A.** The Fundamentals of Heat Exchangers. *The Industrial Physicist.* 1996, Vol. 2, 4, pp. 18-21.

54. **Rafferty, Kevin and Culver, Gene.** Heat Exchangers. *Geo-Heat Center Quarterly Bulletin.* 1998, Vol. 19, 1, pp. 20-26.

55. **Grundfos.** Plate Heat Exchanger. *Thinking Building Universe - Grundfos Commercial Building Services.* [Online] Grundfos. [Cited: 29 April 2011.] http://cbs.grundfos.com/GPO_Austria/lexica/AC_Plate_heat_exchanger.html#-.

56. **Herzog, Howard and Golomb, Dan.** Carbon Capture and Storage from Fossil Fuel Use. *Encyclopedia of Energy.* 2004, Vol. 1.

57. **VGB Power Tech e.V.** *Konzeptstudie: Referenzkraftwerk Nordrhein-Westfalen (RKW NRW).* Essen, Germany : s.n., February 2004.

58. **Hildebrand, Ashleigh N. and Herzog, Howard J.** Optimization of Carbon Capture Percentage for Technical and Economic Impact of Near-Term CCS Implementation at Coal-Fired Power Plants. *Energy Procedia.* February 2009, Vol. 1, 1, pp. 4135-4142.

59. **Zhao, Li, et al.** How gas separation membrane competes with chemical absorption in post-combustion capture. *Energy Procedia.* 2011, 4, pp. 629-636.

60. **Zhao, Li, et al.** Cascaded Membrane Processes for Post-Combustion CO2 Capture. 2011.

61. **Sijbesma, Hylke, et al.** Flue gas dehydration using polymer membranes. *Journal of Membrane Science.* 2008, 313, pp. 263-276.

62. **Kuhn, S., et al.** *Wärmetauscher zur Abwärmenutzung.* s.l. : Forchungszentrum Jülich, 1994. ISSN 0946-0012.

63. *Corrosion Aspects of Materials Selection for CO2 Transport and Storage.* **Bettge, Dirk, et al.** Frankfurt am Main : s.n., June 20-22, 2011. 2nd ICEPE.

64. Overall Heat Transfer Coefficient. *The Engineering Toolbox.* [Online] [Cited: July 28, 2011.] http://www.engineeringtoolbox.com/overall-heat-transfer-coefficient-d_434.html.

65. Valutaomvandlare. *OANDA.* [Online] OANDA Corporation. [Cited: July 15, 2011.] http://www.oanda.com/lang/sv/currency/converter/.

66. **Riensche, E., et al.** *Helmholtz Alliance MEM-BRAIN Progress report.* 2011.

67. **Point Carbon.** Carbon. *Point Carbon.* [Online] [Cited: July 18, 2011.] http://www.pointcarbon.com/productsandservices/carbon/.

68. **Tvinnereim, Endre and Røine, Kjetil.** *Carbon 2010 - Return of the sovereign.* s.l. : Point Carbon, 2010.

69. **Singh, D., et al.** Techno-economic study of CO2 capture from an existing coal-fired power plant: MEA scrubbing vs. O2/CO2 recycle combustion. *Energy conversion and management.* 2003, Vol. 44, 19, pp. 3073-3091.

70. **Abu-Zahra, Mohammad R. M., et al.** CO2 capture from power plants Part II. A parametric study of the economical performance based on mono-ethanolamine. *International journal of greenhouse gas control.* April 2007, Vol. 1, 2, pp. 135-142.

71. **Andersson, Klas, et al.** The CO2 avoidance cost of a large scale O2/CO2 power plant. *Proceedings of the 7th International Conference on Greenhouse Gas Control Technologies.* 2005, pp. 1787-1790.

72. *Carbon Dioxide Capture from Power Generation: Status of Cost and Performance.* **Finkenrath, Matthias.** Frankfurt am Main : International Energy Agency, June 20-22, 2011. 2nd ICEPE.

73. **Favre, Eric.** Carbon dioxide recovery from post-combustion processes: Can gas permeation membranes compete with absorption? *Journal of Membrane Science.* 2007, Vol. 294, pp. 50–59.

74. **Corti, Andrea, Fiaschi, Daniele and Lombardi, Lidia.** Carbon Dioxide Removal in Power Generation using Membrane Technology. *Energy.* 2004, Vol. 29, pp. 2025-2043.

75. **Lyngfelt, Anders.** *Capture and storage of carbon dioxide.* Göteborg : Division of Energy Technology, Department of Energy and Environment, Chalmers University of Technology, 24 November 2009. Presentation in the course Sustainable Energy Futures.

76. *Thermodynamical optimization of solvents for CO2 absorption.* **Artl, W.** Frankfurt am Main, Germany : s.n., 21-22 January 2008. Workshop CO2-Capture, -Utilization and -Sequestration, Status and Perspectives, PROCESSNET, DECHEMA-Haus.